PHD

The analysis of boxed microstrip

Railton, C. J.

Award date:
1987

Awarding institution:
University of Bath

THE ANALYSIS OF BOXED MICROSTRIP

submitted by C. J. Railton

for the degree of Ph.D.

of the University of Bath

1987

COPYRIGHT

C. J. Railton

ProQuest LLC
789 East Eisenhower Parkway
P.O. Box 1346
Ann Arbor, MI 48106-1346

TO ANGELA

ACKNOWLEDGMENTS

I would like to thank my supervisor, Professor T. E. Rozzi, for his help and guidance during the course of this work. I would also like to thank my colleagues for helpful discussions. Finally I would like to thank RSRE as a part of whose research contract this work was carried out.

SYNOPSIS

The purpose of the work described in this thesis is to investigate new techniques for the analysis of boxed microstrip discontinuities. This is aimed at improving the methods currently used in the computer aided design of boxed microstrip circuits. The culmination of the work described herein is the presentation of a new technique for the characterisation of cascades of strongly coupled step discontinuities in microstrip. In addition, an efficient method of calculating the complete mode spectrum of uniform planar transmission lines is presented together with many results. These include "complex modes" in microstrip first reported as a result of this work. Computer programs of general application have been written and are described.

CONTENTS

3. Application to Uniform Microstrip

PUBLICATIONS

"The Efficient Calculation of high order microstrip modes for use in discontinuity problems" Proc. Eu M.C. 1986 pp 529-534.
Co-authors T. E. Rozzi and J. Kot.

"The Rigorous analysis of strongly coupled step discontinuities in microstrip" Proc. Eu M.C. 1987
Co-author. T.E. Rozzi

"Complex Modes in Boxed Microstrip" IEEE Trans MTT May 1988

CHAPTER 1

INTRODUCTION

Origins of Microstrip

The origins of microstrip, as a transmission line, can be traced back to the years following the second world war when people began to look for alternatives to the then ubiquitous rectangular waveguide. This search was motivated largely by the requirement to design components with a wider bandwidth than was possible in waveguide. A step in this direction was the development of ridged waveguide [1] which had a lower cut off frequency for the dominant mode, but this was not the complete answer.

Coaxial transmission line had the advantages of a wide bandwidth, due to the zero frequency cut-off of the dominant TEM mode. It also had the potential of being miniaturised. There were, however, difficulties in the fabrication of components using it. Ways of overcoming these difficulties led first to replacing the central cylindrical core of the coaxial line with a thin strip and the outer cylinder with a rectangular box.

Subsequent development led to the removal of the side walls and extending the top and bottom walls of the box. Thus "stripline" was developed. At about the same time, the early 1950's, the structure was modified in that the top plate was omitted, and the strip was supported by a dielectric layer placed on the bottom plate forming a "microstripline". The waveguiding mechanism of microstrip was now complicated by the fact that the fields were shared between layers of different dielectric constants and was thus no longer TEM. This meant that the transmission line parameters were frequency dependent thereby complicating design procedures. For this reason microstrip was not popular and was to remain so for another decade.

Stripline and Microstripline remained in competition for some years with much progress being made in both leading to a symposium on "Microwave Strip Circuits" being held in 1954 and a special issue of IRE Microwave Theory and Techniques in March 1955.

Sometime in the mid 1960's microstrip returned to the scene in a modified form. The cross-section was substantially reduced and the term "micro" was stressed. This modification greatly reduced both the resistive and reactive aspects of discontinuities thereby removing one of the main objections for prefering stripline.

Moreover the resulting miniaturation offered a more compact circuitry and paved the way to microwave integrated circuits in which microstrip is used today.

Other "planar" waveguiding structures have also been developed, each with their own advantages and disadvantages, largely with the aim of using higher frequencies and of easing the problem of fabricating microwave integrated circuits. Microstrip can be used from very low frequencies to many tens of GHz. At higher frequencies, particularly into the millimetre wave region, losses, including radiation losses, increase greatly, higher order modes become a problem and fabrication tolerances become difficult to meet. It is thought that a normal practical frequency limit for microstrip is 60GHz [2].

Inverted microstrip, is a variant on microstrip in which the electric field is concentrated in the air region rather than the dielectric layer. Thus the effective permittivity is lower and a wider strip can be used for a specified characteristic impedance. This relaxes fabrication tolerance problems. In addition higher frequencies can be used. Manufacturing problems for this structure, and its variant trapped inverted microstrip are, however, severe.

Coplanar waveguide is becoming of increasing importance as a means of constructing microwave integrated circuits. This structure can be used at somewhat lower frequencies than those at which microstrip is generally useful. In addition the earthed "side-planes" reduce the effects of coupling between neighbouring lines, and they facilitate the connection of active components such as diodes across the line without having to drill the substrate. A detailed treatment of coplanar waveguide is given by Gupta [3].

Finline or "E-plane" transmission line is used at higher frequencies and exhibits low loss, about three times better than microstrip. In addition fabrication is comparitively simple. Unlike the previous "planar" structures the dominant mode of finline is not quasi-TEM and has no propagating mode at zero frequency. It is similar in some respects to ridged waveguide.

For high frequency applications, into the optical region, structures such as Slotline and Imageline have been developed. Whilst having some properties in common with the structures described above, they are, being dielectric waveguides, not considered in this thesis. It is interesting to note that the "rods" in the eye which convey optical signals are a form of dielectric waveguide.

Theoretical Research on Microstrip prior to 1984

During the 1950's when stripline dominated over microstrip, work was carried out to calculate the transmission line parameters, in particular the characteristic impedance. Being a pure TEM mode, the exact result could be derived using conformal mapping. Although exact, the result involved the calculation of elliptic functions, and prior to the advent of high speed computers, this was laborious. A simple approximation was subsequently produced [4] for use in design. At this stage, the reactive effects associated with stripline discontinuities tended to be ignored either as being of little importance or purely because noone knew how to characterise them. Discontinuities in stripline began to be treated by means of equivalent circuit models, the rigorous Green's function analysis being avoided as being too formidable a problem.

After the rebirth of microstrip, the equivalent circuits developed for stripline were applied thereto. This, however, met with only limited success and in the late 1960's and early 1970's much work was undertaken to produce new techniques which would be applicable to microstrip.

In this latter period, work on microstrip split mainly into three approaches. First there was the Quasi-static approximation in which the dominant mode was considered to be TEM or an approximation thereto. This work followed on from the work on stripline and made use both of exact conformal mapping techniques, or of numerical techniques to calculate the capacitance of various microstrip structures. Hence their static parameters such as the characteristic impedance and propagation constant of uniform microstrip, and the capacitance and inductance associated with discontinuities could be derived. A selection of references dealing with this approach is [7]-[33] and [89]-[106].

It soon became clear that the quasi-static approximation was inadequate at high frequencies and that a better model was needed. Various "equivalent waveguide" models were developed which were more amenable to exact analysis than the real thing. The most notable of these were the planar waveguide model [36] and the waveguide model of Getsinger [37]. The non-hybrid nature of the modes in the model could not, however, give an accurate representation of the real microstrip modes. This is especially noticeable in the phase of the scattering parameters of a microstrip step discontinuity, some of which are of the wrong sign. As a result, empirical shifts in reference plane were introduced into the model.

Using this method a large amount of data has been produced concerning various microstrip structures, including diverse filter configurations. A thorough treatment of this method is given in a book by Mehran [6]. A selection of references showing the development of the planar model is given below [36]-[42] and [107]-[125].

The third approach is that of attempting to analyse the actual structure, rather than an approximation to it, and taking account of the actual field patterns associated therewith, instead of making a non-hybrid approximation. Clearly this approach is more difficult and more demanding of computer power, but is capable, in principle, of producing an answer to any desired degree of accuracy. As time went on, the limitations of approximate methods became more apparent and the cheapness of computer power increased. Both these trends made the rigorous approach more attractive.

Rigorous analysis has been attempted using a number of methods including Finite Difference methods [43], Finite Element methods [47], Singular Integral Equation methods [48], Transmission Line Matrix methods [55] and Spectral Domain methods [59]. The latter has recently become the most popular for microstrip. A selection of references making use of the rigorous approach is given in [43]-[88].

The treatment of microstrip discontinuities has followed similar methods to those used for uniform microstrip. Due to the added difficulty in dealing with a structure with an extra dimension of inhomogeneity, however, the movement from quasi-static to waveguide model to rigorous analysis has lagged behind the corresponding movement in uniform lines. By 1984 we see relatively few treatments of the microstrip discontinuity by rigorous methods compared with either the planar waveguide model treatments or with the rigorous treatments of uniform microstrip. A selection of references is given [126]-[129].

Progress in microstrip research during 1984-1987

During this period, in which the work described in this thesis was carried out, research has continued mainly on the rigorous approach both to uniform microstrip and to various discontinuities therein. The former has moved into the area of unified treatments of generalised planar transmission lines with the inclusion in various forms of Itoh's method of calculating the Green's functions [73]. In the latter various approaches can be identified.

Jansen [125] and Sorrentino [128] enclose the structure containing the discontinuity within metal walls to form a resonator. The resonant frequency of the structure is then calculated using variational methods leading to the characterisation of the discontinuity. In [125] the strip currents are expanded in a suitable, but unspecified, set of basis functions. Many results for the microstrip step discontinuity are given in [132] showing the success of the method. Much computer power is required, however, to obtain these accurate results.

Jackson and Pozar [131] also use a current expansion, but apply the method to open microstrip. Their basis functions consist of incident and reflected travelling waves and a set of piecewise sinusoidal functions near the discontinuity. Again the method is successful but requires much computer time.

Omar and Schunemann [130] and Uhde [133] have applied mode matching to the modes on each side of the discontinuity. This has the advantage over the above methods that cascades of discontinuities can easily be handled. This is because the amplitudes of the scattered higher modes are available during the course of calculation.

The disadvantages of the method are that it is susceptable to the "relative convergence" phenomenon by which the solution may converge to the wrong answer, and that a large set of simultaneous equations must be solved.

Johns [135] has applied the Transmission Line Matrix method to the microstrip step discontinuity and obtained its dispersion characteristic. The strength of this method, however, appears to lie in more complex structures such as the helicopter shown at the end of [135].

Also during this period the phenomenon of "complex modes" was first reported in finline [129] and in microstrip [136]. The existence of these modes has implications in the treatment of discontinuities.

In this thesis the uniform microstrip, the microstrip step discontinuity and cascades of strongly coupled step discontinuities are treated using rigorous methods. The former is treated as a special case of a more general planar structure. The high order modes of microstrip are efficiently and accurately calculated for use in the step discontinuity problem. The method used to analyse the step attempts to maintain the ease of extension to the cascade of steps exhibited by [130] and [131], but without the disadvantages.

This is achieved by expanding the transverse E field at the discontinuity in a suitable set of vector basis functions and applying a variational method. By this means the "relative convergence" phenomenon is removed and the size of the set of simultaneous equations is reduced. The amplitude of as many scattered higher order modes as are required are available from this formulation.

Structure of this Thesis

Chapter 2 considers the analysis of the general planar structure including microstrip, finline and coplanar line. Resonators and antennas are also briefly considered. The Green's functions for these structures are derived, together with their assymptotic limits and the location of their poles. The suitability of different basis functions for various cases of the general structure is discussed, and a set of basis functions for microstrip is derived.

In Chapter 3 the preceeding results are applied specifically to boxed microstrip and results for the mode spectrum thereof are presented. A discussion of the nature of these modes, including the recently reported "complex modes" is given. In addition some results for the characteristic impedance of boxed microstrip are presented.

All these results are in agreement with other published results where they are available.

Chapter 4 describes the formulation of the single step and multiple step discontinuity in microstrip. Various practical aspects of the formulation are discussed including the convergence of the Green's function, the number and the nature of the basis functions required. The network formulation of the multiple step is described including the concept of "accessible" and "localised" modes, and results for the single and the double step are presented.

In chapter 5 the results of chapter 2 are applied to a boxed microstrip resonator. The main aim of this, is to provide a comparison between the method of chapter 4 for the analysis of step discontinuities in microstrip, and the methods used in [126] and [132]. It is shown that while these are capable of producing accurate and stable numerical results, the computational effort is large. In addition, if strongly coupled steps are to be analysed, the amount of computation required becomes prohibitive.

Chapter 6 presents a description of the computer programs developed during the course of this work.

Finally there is a summary of the progress resulting from the work described herein and suggestions for future research.

References

1. S. B. Cohn "Properties of Ridge Waveguide"
Proc. IRE Vol 35 pp 783-788 Aug 1947.

2. T. C. Edwards "Foundations for Microwave Circuit Design"
Wiley 1981

3. K. C. Gupta et al. "Microstrip lines and slotlines"
Artech 1979

4. S. B. Cohn "Problems in strip transmission lines"
IRE Trans. MTT Vol MTT-3 pp 119-126 March 1955

5. IEEE Trans MTT-32 No. 9 September 1984

6. R. Mehran "Grundelemente des Rechnergestutzten Entwurfs von Mikrostreifleitungs-schaltungen" Verlag H. Wolff. Aachen

7 F. Assadourian et al. "Simplified Theory of Microstrip Transmission System"
Proc IRE 40(1952) pp1651-1657

8 M. Arditi "Characteristics and Applications of Microstrip for Microwave Wiring"
IRE Trans MTT-3 1955 No. 2 pp 31-56

9 K.G. Black and T.J. Higgins "Rigorous determination of the parameters of Microstrip Transmission Lines"
IRE Trans MTT-3 1955 No. 2 pp 93-113

10 H. A. Wheeler " Transmission Line properties of parallel wide strips by conformal mapping approximation"
IEEE Trans MTT-12 1964 pp 280-289

11 H. A. Wheeler "Transmission line properties of parallel strips separated by dielectric sheet"
IEEE Trans MTT-13 1965 pp 172-185

12 H. F. Green "The Numerical solution of some important transmission line problems"
IEEE Trans MTT-13 1965 pp676-692

13 M. V. Schneider "Computation of impedance and attenuation of TEM lines by finite difference methods"
IEEE Trans MTT-13 1965 pp793-800

14 H. Kaden "Leitungs- und Kopplungskonstanten bei Streifenleitungen"
AEU 21 1967 pp 109-111

15 P. Silvester "TEM wave properties of microstrip transmission lines"
Proc IEEE 115 1968 pp 43-48

16 E. Yamashita and R. Mittra "Variational method for the analysis of microstrip lines"
IEEE Trans MTT-16 1968 pp 251-256

17 H. E. Stinehelfer "An accurate calculation of uniform microstrip transmission lines"
IEEE Trans MTT-16 1968 pp 439-444

18 E. Yamashita "Variational method for the analysis of microstrip like transmission lines"
IEEE Trans MTT-16 1968 pp 529-535

19 T.G. Bryant and J. A. Weiss "Parameters of Microstrip Transmission lines and of coupled pairs of microstrip lines"
IEEE Trans MTT-16 1968 pp 529-535

20 H. L. Clemm "Kapazitatsbelag und Wellenwiederstand von Unsymmetrischen Streifenleitungen"
Frequenz 22 1968 pp 196-201

21 H.L. Clemm "Berechnung von Kapazitat und Wellenwiederstand der Streifenleitungen auf einem Dielektrischen Trager mit Hilfe der Teilflachen Methode"
Frequenz 23 1969 pp 143-151

22 M.V. Schneider "Microstrip lines for Microwave Integrated Circuits"
Bell Syst. Techn. J. 1969 pp 1421-1444

23 A. Farrar and A.T. Adams "Characteristic impedance of microstrip by method of moments"
IEEE Trans MTT-18 1970 pp 65-66

24 S.V. Judd et al. "An analytical method for calculating microstrip transmission line parameters"
IEEE Trans MTT-18 1970 pp 78-87

25 D.L. Gish and O. Graham "Characteristic Impedance and Phase Velocity of a Dielectric Supported air strip transmission line with side walls"
IEEE Trans MTT-18 1970 pp131-148

26 R. Mittra and T. Itoh "Charge and Potential Distributions in Shielded Striplines"
IEEE Trans MTT-18 1970 pp149-156

27 E. Yamashita and K. Atsuki " Analysis of Thick-strip transmission lines"
IEEE Trans MTT-19 1971 pp120-122

28 P. Silvester and P. Benedek "Electrostatics of the Microstrip - Revisited"
IEEE Trans MTT-20 1972 pp756-758

29 A. Farrar and A.T. Adams "A potential theory for covered microsrtrip"
IEEE Trans MTT-21 1973 pp 494-496

30 B.N. Das and K.V.S.V.R. Prasad "A Generalised Formulation of Electromagnetically Coupled Striplines"
IEEE Trans MTT-32 1984 pp 1427-1433

31 V. Postoyalko "Green's Function treatment of edge singularities in the quasi-TEM analysis of Microstrip"
IEEE Trans MTT-34 1986 pp 1092-1095

32 Z. Pantic and R. Mittra "Quasi-TEM analysis of Microwave Transmission lines by the finite element method"
IEEE Trans MTT-34 1986 pp 1096-1103

33 E. Yamashita et al. "Analysis method for Generalised suspended striplines"
IEEE Trans MTT-34 1986 pp 1457-1463

Microstrip dispersion models

34 C.P. Hartwig et al. "Frequency dependent behaviour of Microstrip"
1968 G-MTT International Symposium, Detroit, Digest pp110-119

35 R.E. Eves "Guided waves in limit cases of microstrip"
IEEE Trans MTT-18 1970 pp 231-232

36 G. Kompa and R. Mehren "Planar Waveguide model for calculating microstrip components"
Electronics Letters 11 1975 pp 459-460

37 M.V. Schneider "Microstrip Dispersion"
Proc IEEE 60 1972 pp 144-146

38 W.J. Getsinger "Microstrip Dispersion Model"
IEEE Trans MTT-21 1973 pp 34-39

39 H.J. Carlin "A simplified circuit model for Microstrip"
IEEE Trans MTT-21 1973 pp 589-591

40 B. Bianco et al. "Frequency dependence of microstrip parameters"
Alta Frequenza 43 1974 pp 413-416

41 R.P. Owens "Predicted Frequency dependence of microstrip characteristic impedance using the planar waveguide model"
Electronics Letters 12 1976 pp 269-270

42 E. Yamashita et al. "An approximate dispersion formula of microstrip lines for CAD of MIC's"
IEEE Trans MTT-27 1979 pp 1036-1038

Field Theoretical analysis of uniform microstrip

43 J.S. Hornsby and A. Gopinath "Numerical Analysis of a dielectric loaded waveguide with a microstrip line - finite diference methods"
IEEE Trans MTT-17 1969 pp 684-690

44 J.S. Hornsby and A. Gopinath "Fourier analysis of a dielectric loaded waveguide with a microstrip line"
Electronics Letters 5 1969 pp 265-267

45 J.B. Davies and D.G. Corr "Computer analysis of the fundamental and higher order modes in single and coupled microstrip"
Electronics Letters 6 1970 pp 683-685

46 D. Gelder "Numerical determination of microstrip properties using the transverse field components"
Proc IEEE 117 1970 pp 699-703

47 P. Daly "Hybrid mode analysis of microstrip by finite element methods"
IEEE Trans on MTT-19 1971 pp 19-25

48 R. Mittra and T. Itoh "A new technique for the analysis of the dispersion characteristics of microstrip lines"
IEEE Trans on MTT-19 1971 pp 47-56

49 G. Kowalski and R. Pregla "Dispersion characteristics of shielded microstrips with finite thickness"
AEU 25 1971 pp 193-196

50 G. Kowalski and R. Pregla "Dispersion Characteristics of single and coupled microstrips"
AEU 26 1972 pp 276-280

51 R.P. Wharton and G.P. Rodrigue "A dominant mode analysis of Microstrip"
IEEE Trans MTT-20 1972 pp 552-555

52 D.G. Corr and J.B. Davies "Computer analysis of the fundamental and higher order modes in single and coupled microstrip"
IEEE Trans on MTT-20 1972 pp 669-678

53 M.K. Krage and G.I. Haddad "Frequency dependent characteristics of microstrip transmission lines"
IEEE Trans on MTT-20 1972 pp 678-688

54 R. Jansen "A modified least squares boundary residual (LSBR) method and its application to the problem of shielded microstrip dispersion"
AEU 28 1974 pp 275-277

55 S. Akhtarzad and P. Johns "Three-dimensional transmission line matrix computer analysis of microstrip resonators"
IEEE Trans MTT-23 1975 pp990-997

56 E. Yamashita and K. Atsuki "Analysis of Microstrip-like transmisssion lines by the non-uniform discretisation of integral equations"
IEEE Trans on MTT-24 1976 pp 195-200

57 Mirshekar-Syahkal and B. Davies "Accurate solution of microstrip and coplanar structures for dispersion and for dielectric and conductor losses"
IEEE Trans on MTT-27 1979 pp 694-699

58 F. Arndt and G.U. Paul "The reflection definition of the characteristic impedance of microstrip"
IEEE Trans on MTT-27 1979 pp 694-699

59 E.J. Denlinger "A frequency dependent solution for microstrip transmission lines"
IEEE Trans MTT-19 1971 pp 30-39

60 T. Itoh and T. Mittra "Spectral Domain approach for calculating the dispersion characteristics of microstrip lines"
IEEE Trans MTT-21 1973 pp 496-499

61 Van de Capelle and P.J. Luypert "Fundamental and Higher order modes in open microstrip lines"
Electronics Letters 9 1973 pp 345-346

62 T. Itoh. and R. Mittra "A technique for computing dispersion characteristics of shielded microstrip lines"
IEEE Trans MTT-22 1974 pp 896-898

63 T. Itoh "Analysis of microstrip resonators"
IEEE Trans MTT-22 1974 pp 946-952

64 R. Jansen "A Moment method for covered microstrip dispersion"
AEU 29 1975 No. 1 pp 17-20

65 R.H. Jansen "Unified user orientated computation of shielded covered and open planar microwave and millimetre wave transmission line characteristics"
IEEE J MOA 3 1974 pp 14-22

66 J.B. Knorr and Tufekcioglu "Spectral domain calculation of microstrip characteristic impedance"
IEEE Trans MTT-23 1975 pp 725-728

67 A. Farrar and A.T. Adams "Computation of propagation constants for the fundamental and higher order modes in microstrip"
IEEE Trans MTT-24 1976 pp 456 460

68 R. Jansen "High speed computation of single and coupled microstrip parameters including dispersion, higher order modes loss and finite strip thickness"
IEEE Trans MTT-26 1978 pp 75-82

69 R. Jansen "Unified user-orientated computation of shielded covered and open planar microwave and millimetre wave transmission line characteristics"
IEEE Trans MOA 3 1979 pp 14-22

70 H. Ermert "Guiding and radiation characteristics of planar waveguides"
IEEE Trans MOA-3 1979 pp 59-62

71 E. F. Kuster and D. C. Chang "An appraisal of methods for computation of the dispersion characteristic of open microstrip"
IEEE Trans MTT-27 1979 pp 691-694

72 D. Mirshekar and J. Davies "Accurate solution of microstrip and coplanar structures for dispersion and for dielectric and conductor losses"
IEEE Trans MTT-27 1979 pp 694-699

73 T. Itoh "Spectral domain Imittance Approach for Dispersion Characteristics of Generalised printed transmission lines"
IEEE Trans MTT-28 1980 pp 733-736

74 J. Knorr and P. Shayda "Millimetre wave finline characteristics"
IEEE Trans MTT-28 1980 pp 737-743

75 L. Schmidt and T. Itoh "Spectral domain analysis of dominant and higher order modes in fin-lines"
IEEE Trans MTT-28 1980 pp 981-985

76 Y. Shih and W. Hoefer "Dominant and second order mode cutoff frequencies in finlines calculated with a two dimensional TLM program"
IEEE Trans MTT-28 1980 pp 1443-1448

77 A. El-Sherbiny "Exact analysis of shielded microstrip lines and bilateral finlines"
IEEE Trans MTT-29 1981 pp 669-675

78 J. S. Hornsby "Full wave analysis of microstrip resonator and open circuit end effect"
Proc IEE Vol 129 H 1982 pp 338-341

79 R. Vahldieck "Accurate hybrid mode analysis of various finline configurations including multilayered dielectrics, finite metallization thickness and substrate holding grooves"
IEEE Trans MTT-32 1984 pp 1454-1460

80 T. Kitazawa and R. Mittra "Analysis of Finline with finite metallization thickness"
IEEE Trans MTT-32 1984 pp 1484-1487

81 A. Omar and K. Schunemann "Space Domain decoupling of LSE and LSM fields in generalised planar guiding structures"
IEEE Trans MTT-32 1984 pp 1626-1632

82 J. Bornemann "Rigorous field theory analysis of quasiplanar waveguides"
Proc IEE Vol. 132 H 1985 pp 1-6

83 G. Mariki and C. Yeh "Dynamic three-dimensional TLM analysis of microstriplines on anisotropic substrate"
IEEE Trans MTT-33 1985 pp 789-799

84 M. Hashimoto "A rigorous solution for dispersive microstrip"
IEEE Trans MTT-33 1985 pp 1131-1137

85 A. Omar and K. Schunemann "Formulation of the singular integral equation technique for planar transmission lines"
IEEE Trans MTT-33 1985 pp 1313-1321

86 C. Olley and T. Rozzi "Systematic characterisation of the spectrum of unilateral finline"
IEEE Trans MTT-34 1986 pp 1147-1156

87 H. Yee and K. Wu "Printed circuit transmission line characteristic impedance by transverse modal analysis"
IEEE Trans MTT-34 1986 pp 1157-1163

88 J. Dekleva and V. Roje "Accurate numerical solution of coupled integral equations for microstrip transmission line"
Proc IEE Vol. 134 H 1987 pp163-168

Quasi static treatment of Discontinuities

89 H.M. Altschuler and A.A. Gliner. "Discontinuities in the centre conductor of symmetric strip transmission line"
IRE Trans MTT-8 1960 pp 328-339

90 I.M. Stephenson and B. Easter "Resonant techniques for establishing the equivalent circuits of small discontinuities in microstrip"
Electronics letters 7 1971

91 A. Farrar and A.T. Adams "Matrix methods for microstrip three dimensional problems"
IEEE Trans MTT-20 1972 pp 497-504

92 M. Maeda "An analysis of gap in microstrip transmission lines"
IEEE Trans MTT-20 1972 pp 390-396

93 T. Itoh R. Mittra and R. D. Ward "A new method for solving discontinuity problems in microstrip lines"
1972 IEEE-GMTT Int. Microwave Symp. Digest pp 68-70

94 T. Itoh, R. Mittra and R.D. Ward "A method for computing edge capacitance of finite and semi-finite microstrip lines"
IEEE Trans MTT-20 1972 pp 847-849

95 P. Silvester and P. Benedek "Equivalent capacitance of microstrip open circuits"
IEEE Trans MTT-20 1972 pp511-516

96 P. Benedek and P. Silvester "Equivalent capacitance for microstrip gaps and steps"
IEEE Trans MTT-20 1972 pp 729-733

97 P. Silvester and P. Benedek " Microstrip discontinuity capacitances for right angle bends, T junctions and crossings"
IEEE MTT-21 1973 pp 341-346 correction in IEEE MTT-23 1975 p 456

98 R. Horton "Equivalent representation of an abrupt impedance step in microstrip line"
IEEE MTT-21 1973 pp 562-564

99 Y. Rahmat-Samii, T. Itoh and R. Mittra "A Spectral domain Analysis for solving Microstrip Discontinuity Problems"
IEEE Trans MTT-22 pp372-378

100 A. F. Thompson and A. Gopinath "Calculation of microstrip discontinuity inductances"
IEEE Trans MTT-23 1975 pp 648-655

101 B. Easter "The equivalent circuit of some microstrip discontinuities"
IEEE Trans MTT-23 1975 pp 665-660

102 A. Gopinath et. al. "Equivalent circuit parameters of microstrip step change in widthand cross junctions"
IEEE Trans MTT-24 1976 pp 142-144

103 C. Gupta and A. Gopinath "Equivalent circuit capacitance of microstrip step change in width"
IEEE Trans MTT-25 1977 pp 819-822

104 B.M. Neale and A. Gopinath "Microstrip discontinuity inductances"
IEEE Trans MTT-26 1978 pp 827-830

105 A. Gopinath and C. Gupta "Capacitance parameters of discontinuities in microstriplines"
IEEE Trans MTT-26 1978 pp 831-836

106 Garg Ramesh and Bahl "Microstrip discontinuities"
Int. J. Electronics 45 1978

107 I. Wolff, G. Kompa and R. Mehren "Calculation method for microstrip discontinuities and T-junctions"
Electronics Letters, 8 1972 pp 177-179

108 I. Wolff "Computer aided design of microstrip power dividers"
Proc. 3rd Eu MC 1973 Paper A. 12.5

109 G. Kompa and R. Mehran "Planar waveguide model for calculating microstrip components"
Electronics letters 11 1975 pp459-460

110 R. Mehran "The frequency dependent scattering matrix of microstrip right angle bends, T-junctions and crossings"
AEU 29 1975 pp 454-460

111 G. Kompa "Frequency dependent behaviour of microstrip offset junctions"
Electronics Letters 11 1975 pp 537-538

112 R. Mehran "Frequency dependent equivalent circuits for microstrip right angle bends, T-junctions and crossings"
AEU 30 1976 pp80-82

113 G. Kompa "S matrix computation of microstrip discontinuities with a planar waveguide model"
AEU 30 1976 pp 58-64

114 W. Menzel and I. Wolff "A method for calculating the frequency dependent properties of microstrip discontinuities"
IEEE Trans MTT-25 1977 pp 107-112

115 W. Menzel "Calculation of inhomogeneous microstrip lines"
Electronics Letters 13 1977 pp 183-184

116 R. Mehran "Calculation of microstrip bends and Y-junctions with arbitrary angle"
IEEE Trans MTT-26 1978 pp 400-405

117 G. Kompa "Design of stepped microstrip components"
Radio and Electronics Engineer 48 1978 pp 53-63

118 W. Menzel "The frequency dependent transmission properties of microstrip Y-junctions and 120 degree bends"
IEEE J. MOA 2 1978 pp 55-59

119 R. Mehran "Computer aided design of microstrip filters considering dispersion, loss and discontinuity effects"
IEEE Trans MTT-26 1979 pp 239-245

120 G. Kompa and R. Mehren "Microstrip filter analysis using a waveguide model"
Radio and Electronic Engineer 50 1980 pp 54-58

121 F. Giannini, R. Sorrentino and J. Vrba "Planar circuit analysis of microstrip radial stub"
IEEE Trans MTT-32 1984 pp 1652-1655

122 M. Helard et. al. "Theoretical and experimental investigation of finline discontinuities"
IEEE Trans MTT-33 1985 pp 994-1003

123 T. S. Chu, T. Itoh and Y. Shih "Comparitive study of mode-matching formulations for microstrip discontinuity problems"
IEEE Trans MTT-33 1985 pp 1018-1023

124 T.S. Chu and T. Itoh "Analysis of microstrip step discontinuity by the modified residue calculus technique"
IEEE Trans MTT-33 1985 pp 1024-1028

125 T.S. Chu and T. Itoh "Generalised scattering matrix method for analysis of cascaded and offset microstrip step discontinuities"
IEEE Trans MTT-34 1986 pp 280-284

Field Theoretical treatment of discontinuities

126 R.H. Jansen "Hybrid mode analysis of end effects of planar microwave and millimetrewave transmission lines"
Proc. IEE Vol. 128 part H 1981 pp 77-86

127 H. El Hennawy and K. Schunemann "Impedance Transformation in Fin-lines"
Proc IEE Vol. 129 H 1982 pp 342-350

128 T. Kitazawa and R. Mittra "An investigation of striplines and finlines with periodic stubs"
IEEE Trans MTT-32 1984 pp 684-688

129 R. Sorrentino and T. Itoh "Transverse Resonance Analysis of Finline Discontinuities"
IEEE Trans MTT-32 1984 pp 1633-1638

130 A. Omar and K. Schunemann "Transmission matrix representation of Finline discontinuities"
IEEE Trans MTT-33 1985 pp 765-770

131 R. Jackson and D. Pozar "Full-wave analysis of microstrip open end and gap discontinuities"
IEEE Trans MTT-33 1985 pp 1036-1046

132 N. Koster and R. Jansen "The Microstrip Step Discontinuity: A Revised Description"
IEEE Trans MTT-34 1986 pp 213-223

133 K. Uhde "Discontinuities in finlines on semiconductor substrate"
IEEE Trans MTT-34 1986 pp 1499-1507

134 A. Omar and K. Schunemann "The effect of complex modes at finline discontinuities"
IEEE Trans MTT-34 1986 pp 1508-1514

135 P. Johns "Use of condensed and symmetrical TLM nodes in computer aided electromagnetic design"
Proc. IEE Vol. 133 H 1986 pp 368-374

136 C.J. Railton, T. Rozzi and J. Kot "The Efficient Calculation of high order Microstrip modes for use in discontinuity problems"
Proc. Eu M.C. 1986 pp 529-534

137 C.J. Railton and T. Rozzi "The Rigorous analysis of strongly coupled step discontinuities in microstrip"
Proc. Eu. M. C. 1987

CHAPTER 2

THE ANALYSIS OF PLANAR WAVEGUIDE STRUCTURES

2.1. Introduction

The purpose of this chapter is to develop the theory for the analysis of general planar waveguide. Although mainly concerned with boxed microstrip, much of the theory is so readily generalised that, with little extra effort, it is possible to produce formulae and computer programs with much wider application.

After a brief resumé of previous work of this nature, the general method of analysis is described. After deriving the Green's function for the general slab loaded waveguide, and expanding the currents on the strips in terms of suitable known sets of basis functions, Galerkin's method is applied. This transforms the problem to a set of algebraic simultaneous equations which can be solved to yield the solution to the problem. In the case of bound waveguide modes, these equations are homogeneous and the problem becomes that of finding the zeros of the characteristic determinant. In the case of an open structure we can also calculate its response to an incident field.

In an appendix to this chapter is provided the PASCAL procedure for calculating the Green's functions for a general planar structure. It is small and efficient enough to be used on a computer as small as the Sinclair Spectrum.

2.2. Background

The problem of characterising microstrip has been receiving attention fairly continuously since the second world war. Much of the early work treated the microstrip as a TEM transmission line and the methods used for calculating the propagation constants and characteristic impedances were those of calculating the capacitance of the structure. As recently as 1984 we see such a solution [1] using a conformal mapping technique. This reference also contains a brief review of previous attempts at the problem.

The most well known example of this approach is that of Wheeler [2], whose approximate analysis and synthesis formulae are quoted in the majority of books on microstrip circuit design. They still form the basis of much engineering calculation especially at low frequencies.

As the frequencies at which microstrip was to be used rose, however, it became apparant that the TEM approximation was no longer adequate. Due to the magnitude of the computation required for a rigourous analysis, and the limited amount of computer power available at the time, various "quasi-static" approximations made their appearance. The more successful of these were based on replacing the microstrip with simpler structures which were more readily analysed. Examples of this are the equivalent structures used by Getsinger [3] and Mehran [4].

Rigorous treatments of microstrip and finline were carried out using various methods by Yamashita [5], Itoh and Mittra [6,7] , Jansen [8] and others. In particular, with the introduction of the equivalent transmission line model of planar transmission lines by Itoh [9], it became a computationally simple matter to derive the Green's function for a planar transmission line with any number of layers. With a suitable choice of basis functions for the unknown fields or currents laminar structures with any metallisation pattern can be dealt with.

2.3. General Theory

Consider a laminar structure consisting of layers of dielectric whose interfaces are normal to the y direction and which extend to infinity in the x-z plane. Initially we assume no current sources. In this case Maxwell's equations dictate that:

$$\nabla \cdot \underline{H} = 0 \tag{2.1}$$

$$\nabla \cdot \underline{E} = 0 \tag{2.2}$$

This means that we may express $\underline{H}$ and $\underline{E}$ as curls of vectors giving:

$$\underline{E} = j\omega\mu_o \nabla \times \underline{\Pi}_H \tag{2.3}$$

$$\underline{H} = \nabla \times \nabla \times \underline{\Pi}_H$$

or

$$\underline{H} = j\omega\epsilon \nabla \times \underline{\Pi}_E \tag{2.4}$$

$$\underline{E} = \nabla \times \nabla \times \underline{\Pi}_E$$

$\underline{\Pi}_e$ and $\underline{\Pi}_m$ are referred to as the electric and magnetic Hertzian potentials. Each of these satisfies the Helmholz equation. Solving this equation for the structure under consideration leads to two sets of solutions. In one set the y component of $\underline{E}$ is zero (TE-to-y), in the other the y component of $\underline{H}$ is zero (TM-to-y). Examination of the above equations shows that these solutions can be derived from the y components of the Hertzian potentials, the other components being set to zero. The field components for each set of modes is given as follows [13]:

for TM-to-y modes:

$$\underline{E} = -j\omega\mu_o \left\{ \underline{\hat{x}}.\frac{\partial \Pi_m}{\partial z} - \underline{\hat{z}}.\frac{\partial \Pi_m}{\partial x} \right\} \qquad (2.5)$$

$$\underline{H} = \underline{\hat{x}}.\frac{\partial^2 \Pi_m}{\partial y \partial x} - \underline{\hat{y}}.\left\{ \frac{\partial^2}{\partial x^2} + \frac{\partial^2}{\partial z^2} \right\} \Pi_m - \underline{\hat{z}}.\frac{\partial^2 \Pi_m}{\partial y \partial z}$$

for TE-to-y modes:

$$\underline{H} = -j\omega\epsilon \left\{ \underline{\hat{x}}.\frac{\partial \Pi_e}{\partial z} - \underline{\hat{z}}.\frac{\partial \Pi_e}{\partial x} \right\} \qquad (2.6)$$

$$\underline{E} = \underline{\hat{x}}.\frac{\partial^2 \Pi_e}{\partial y \partial x} - \underline{\hat{y}}.\left\{ \frac{\partial^2}{\partial x^2} + \frac{\partial^2}{\partial z^2} \right\} \Pi_e - \underline{\hat{z}}.\frac{\partial^2 \Pi_e}{\partial y \partial z}$$

The form of the Hertzian potentials will depend on the boundary conditions of the structure. For a boxed planar waveguide it will have the following form in each layer:

$$\sum_n A_n \, T(\alpha_n x) \, T(k_y y) \, \exp(-j\beta z) \qquad (2.7)$$

where A_n are arbitrary constants and T(x) stands for Cos(x) or Sin(x) as applicable.

We now wish to ascertain the fields in the structure due to current sources located at any of the interfaces. We can derive a formula for the fields at the interfaces having the following form:

$$\underline{E}_i(x,z) = \sum_j \; < \; \underline{\underline{g}}_{ij}(x,z|x',z'), \; \underline{I}_j(x',z') > \qquad (2.8)$$

where i,j=1..number of layers-1

$\alpha_n = n\pi/a$

a is the box width

and the inner product is defined as:

$$< \underline{A} \, , \, \underline{B} > = \int\int \underline{A} \, . \, \underline{B} \; dx' \; dz'$$

In general since the E field produced by a source current will not just be parallel to that source current, the Green's function $\underline{\underline{g}}_{ij}$ will be a dyadic (tensor of rank 2) quantity.

The derivation of the Green's dyadic will be given in the next section. In that section, use is made of the fact that, for a special choice of coordinates in the x-z plane, $\underline{\underline{g}}_{i,j}$ is diagonal and a current directed along one of these special coordinate axes results in a E field in that same direction.

We may also derive a formula for the currents at the interfaces resulting from source fields at any of the interfaces.

$$\underline{J}_i(x,z) = \sum_j \; < \; \underline{\underline{f}}_{i,j}(x,z|x',z'),\ \underline{E}_j(x',z') > \qquad (2.9)$$

As will be seen later, it will be advantagous to use one or other of the above formulae depending on the geometry of the structure under consideration.

We now turn our attention to the question of including conductors in the basic structure. We will restrict ourselves to infinitely thin strips located at the dielectric interfaces and with edges parallel to the x or to the z direction.

This is consistent with microstrip and other planar waveguiding structures. We seek solutions to Maxwell's equations for this type of structure.

Essentially we use Galerkin's method with either the fields or the currents at each interface as the unknown functions. Taking the case of unknown currents as an example, we start by expanding the currents at each interface in terms of suitable basis functions and substituting in equation 2.9.

$$\underline{I}_j(x,z) = \sum_q a_{jq}\, \underline{I}_{jq}(x,z) \qquad (2.10)$$

$$\underline{E}_i(x,z) = \sum_j \left\langle \underline{\underline{g}}_{ij} \cdot \sum_q a_{jq}\, \underline{I}_{jq} \right\rangle \qquad (2.11)$$

Now multiply by each of the basis functions in turn and take the inner product. By noting that the inner product of current and total E field is zero for a perfect conductor we get the following:

$$\sum_j \sum_q a_{jq} \left\langle \underline{I}_{kl}(x,z) \cdot \underline{\underline{g}}_{ij}(x,z|x',z') \cdot \underline{I}_{jq}(x',z') \right\rangle$$

$$= \left\langle \underline{E}^i, \underline{I}_{kl} \right\rangle \qquad (2.12)$$

where E^i is the incident field.

This is a set of simultaneous equations from which the coefficients $a_{j,q}$ may be obtained. Substitution in equations 2.10 and 2.11 then gives the currents on the metal and the fields in the aperture.

Equation 2.12 is quite general, and is applicable to a large number of problems. The following gives some examples of this.

1. Boxed microstrip.

Here we place metal planes at x=a/2, x=-a/2, y=-d, y=h to form a box. There are two layers whose interface is at y=0, and there is one strip of width w running in the z direction. Because of the closed nature of the structure, only bound modes exist therefore we seek solutions to equation 2.12 with zero incident field.

Thus

$$\sum_q a_q < \underline{I}_o(x,z) \, . \, \underline{\underline{G}}(x,z|x',z') \, . \, \underline{I}_q(x',z') > = 0 \qquad (2.13)$$

Due to the fact that the structure is uniform in the z direction, we can set the z dependence of the currents and of the Green's function to $\exp(-j\beta z)$. This leads to the following set of homogeneous equations:

$$\sum_{q} a_q \langle \underline{I}_p(x) \cdot \underline{\underline{G}}(x|x') \cdot \underline{I}_q(x') \rangle = 0 \qquad (2.14)$$

Solutions are found by setting the determinant of the quadratic form equal to zero.

ii. Unilateral Fin-line and coplanar waveguide.

Here we have a situation similar to that of microstrip but with two differences. Firstly there are three layers although only one interface has metallisation. Secondly there is normally greater than 50% metallisation on this interface. The latter makes it computationally more efficient to use aperture fields as the unknowns, the former affects only the calculation of the Green's function.

If we have metal only on interface 2 then the appropriate form of the equation is as follows:

$$\sum_q a_q < \underline{E}_{zt}(x) \, , \, \underline{\underline{f}}_{zz}(x|x') \, , \, \underline{E}_{zq}(x') > = 0 \qquad (2.15)$$

iii. Microstrip resonator

In this case we have a rectangular strip placed on the interface between the two dielectric layers. Since the structure is non-uniform in the z direction as well as the x and y directions, we must retain the unknown z dependence of the currents. The basis functions in which the unknown currents are to be expanded must be complete sets in (x,z).

For resonance we require a finite response for zero incident field, therefore the appropriate form of equation 2.12 is:

$$\sum_q a_q < \underline{I}_t(x,z) \, , \, \underline{\underline{g}}(x,z|x',z') \, , \, \underline{I}_q(x',z') > = 0 \qquad (2.16)$$

iv. Microstrip antenna

Consider a microstrip antenna consisting of an array of rectangular patches placed at the interface between two dielectric layers. There may be several layers in the complete structure, the uppermost one being air.

The antenna is analysed as a receiving antenna. By the principle of reciprocity this will also give information about the antenna used as a transmitter. The antenna is illuminated by an incident field $\underline{E}^i$.

The appropriate form of equation 2.12 in this case is:

$$\sum_q a_{sq} < \underline{I}_{sq}(x,z) \cdot \underline{\underline{G}}_{ss}(x,z|x',z') \cdot \underline{I}_{sq}(x',z') > = < \underline{E}^i, \underline{I}_{sq} > \qquad (2.17)$$

From this one can calculate the currents in the patches for any incident field, this information together with suitable feed modelling will give information about antenna directivity.

2.4. Green's Functions for a generalised planar waveguide

In this section is presented a systematic method of deriving the Green's functions for a planar structure with an arbitrary number of layers and with metallisation on any of the dielectric boundaries. The method is equally applicable to boxed or open structures, to waveguide, resonators or antennas. General impedance type boundary conditions may be specified at the ground plane and other boundaries to the structure if they exist.

Recently, the computation of the generalised Green's functions for a planar structure has been reported [10] using a different method. In that case, however, only one metallised interface is catered for. The method described here is completely general, and simple to program.

The method is based on the equivalent transmission line formulation described in [9] by Itoh. Here we consider the multilayer structure to be an inhomogeneous transmission line in the y direction which is capable of supporting TE and TM modes with respect to y.

First, by means of the network theory of transmission lines, the relationship between the equivalent voltages and currents at each dielectric interface is established. The actual hybrid modes are then resolved into their TE-to-y and TM-to-y components, the above relationships are applied to each component. Finally the components are recombined to form the hybrid mode.

The following describes this process in more detail.

The characteristic impedances of the equivalent transmission lines formed by the i^{th} dielectric layer for TE-to-y and TM-to- y modes are given by:

$$Y_{TM_i} = \frac{\omega \epsilon_o \epsilon_i}{k_i} \qquad (2.18)$$

$$Y_{TE_i} = \frac{k_i}{\omega \mu} \qquad (2.19)$$

where k_i is the wave number in the y direction in layer i and is given by:

$$k_i = (\epsilon_i k_o^2 - \alpha^2 - \beta^2)^{1/2} \qquad (2.20)$$

and

α is the propagation coefficient in the x direction

β is the propagation coefficient in the z direction

Transmission line theory gives the admittances looking up from the i^{th} dielectric interface, in other words from the boundary between layer i+1 and layer i as follows:

$$Y^{H}_{i-1} = Y_{TE_i} \frac{j\, Y_{TE_i} \operatorname{Tan} k_i d_i + Y^{u}_{H_i}}{j\, Y^{u}_{H_i} \operatorname{Tan} k_i d_i + Y_{TE_i}} \qquad i = 2..N \qquad (2.21)$$

$$Y^{E}_{i-1} = Y_{TM_i} \frac{j\, Y_{TM_i} \operatorname{Tan} k_i d_i + Y^{u}_{E_i}}{j\, Y^{u}_{E_i} \operatorname{Tan} k_i d_i + Y_{TM_i}} \qquad i = 2..N \qquad (2.22)$$

Similarly for the admittances looking down from the i^{th} interface are given by:

$$Y^{H}_{i} = Y_{TE_i} \frac{j\, Y_{TE_i} \operatorname{Tan} k_i d_i + Y^{d}_{H_{i-1}}}{j\, Y^{d}_{H_{i-1}} \operatorname{Tan} k_i d_i + Y_{TE_i}} \qquad (2.23)$$

$$Y^{E}_{i} = Y_{TM_i} \frac{j\, Y_{TM_i} \operatorname{Tan} k_i d_i + Y^{d}_{E_{i-1}}}{j\, Y^{d}_{E_{i-1}} \operatorname{Tan} k_i d_i + Y_{TM_i}} \qquad (2.24)$$

$$i = 1..N-1$$

The quantities Y_{TEN}, Y_{TEO}, Y_{TMN} and Y_{TMO} are the admittances at the upper and lower boundaries. For an open boundary they would be zero, for a metal boundary they would be infinite.

The total admittance seen at the i^{th} dielectric interface is the sum of the admittances looking up and looking down:

$$Y_{Eii} = Y_{Ei}^{u} + Y_{Ei}^{d} \qquad (2.25)$$

$$Y_{Hii} = Y_{Hi}^{u} + Y_{Hi}^{d}$$

The transfer admittances between boundaries is:

$$Y_{Eij} = Y_{Ej}^{u} \,/\, Y_{Ejj}\, Y_{Ei}^{u} \qquad i > j \qquad (2.26)$$

$$Y_{Eij} = Y_{Ej}^{d} \,/\, Y_{Ejj}\, Y_{Ei}^{d} \qquad i < j$$

Denoting Z_{xij} as $1/Y_{xij}$ etc. we have for the components of the generalised Greens impedance matrix relating E_u, E_v on interface i to J_u, J_v on interface j the following dyadic quantities:

$$\underline{\underline{Z}}_{ij} = \begin{pmatrix} Z_{xij} & 0 \\ 0 & Z_{yij} \end{pmatrix} \qquad (2.27)$$

where u and v are the directions of the transverse-to-y E field for TE-to-y and TM-to-y modes respectively.

The zeros in the off diagonal positions of the dyadic imply that a current in the u (or v) direction gives rise to an E field in the u (or v) direction. In general, as stated above, this is the case only for this particular choice of directions.

In order to represent the hybrid modes of the actual transmission line we use the forms of equation 2.5 and 2.6. leading to expressions such as the following:

For the case of boxed waveguide we have:

$$\underline{E}\ (x,0,z) = \sum_{n=0}^{\infty} \underline{E}_n\ T\ (\alpha_n x)\ \exp(-j\beta z) \qquad (2.28)$$

For the case of a totally enclosed resonator we have:

$$\underline{E}\ (x,0,z) = \sum_{n=0}^{\infty} \sum_{m=0}^{\infty} \underline{E}_n\ T\ (\alpha_n x)\ T\ (\beta_m z) \qquad (2.29)$$

where T(x) represents Sin(x) or Cos(x) depending on the boundary conditions.

The corresponding Green's functions are also expressed as a single sum and double sum respectively. eg.

$$\underline{\underline{g}}(x,z|x',z') =$$

$$\sum_{n=0}^{\infty}\sum_{m=0}^{\infty} \underline{\underline{g}}_{nm}(\alpha,\beta \mid \alpha',\beta')\ T(\alpha_n x)T(\beta_m z)T(\alpha'_n x')T(\beta'_m z') \qquad (2.30)$$

For open structures the summations would be replaced by integrals.

For each component of equations 2.28 and 2.29 the directions u and v are at an angle T to the x and z axes where:

$$\text{Sin } T = \frac{\alpha}{\sqrt{(\alpha^2 + \beta^2)}} \qquad (2.31)$$

In order to apply expression 2.27 fields expressed in x and z coordinates we to must post-multiply $\underline{\underline{Z}}_{i,j}$ by:

$$\begin{pmatrix} \text{Sin } T & -\text{Cos } T \\ \text{Cos } T & \text{Sin } T \end{pmatrix}$$

and pre-multiply by its inverse, (equal to its transpose). These are equivalent to rotations through the angles +/- T.

Each component of the dyadic Green's matrix expressed in terms of x and z is therefore:

$$\underline{\underline{g}}_{nm} = \frac{1}{\alpha^2 + \beta^2} \begin{pmatrix} \alpha^2 Z_E + \beta^2 Z_H & \alpha\beta\,(Z_H - Z_E) \\ \alpha\beta\,(Z_H - Z_E) & \alpha^2 Z_H + \beta^2 Z_E \end{pmatrix} \qquad (2.32)$$

Thus we have the Green's matrix which relates Ex and Ez at any dielectric interface to the currents Jx and Jz at each dielectric interface.

Given the waveguide geometry, the Green's matrix is computed in a systematic manner with the following steps:

1. For each layer calculate k, k Tan kd, Y_E and Y_H
2. For the top interface calculate the admittances looking up
3. For the bottom interface calculate the admittances looking down
4. For intermediate interfaces calculate the admittances using the recurrance formulae.
5. Calculate the matrix Y_E and Y_H and form the matrix of dyadics Z.
6. For each element of Z pre and post-multiply by the rotation matrix and its inverse.

By this means the Green's function can be calculated for planar structures of arbitrary complexity with no increase in the complexity of the method. The appendix to this chapter describes a simple PASCAL procedure utilising this method.

2.5. Assymptotic values of the Green's function

As α becomes large compared with β the elements of the Green's matrix can be accurately approximated by much simpler expressions. By judicious use of the derivatives of some field and current components, the assymptotic limit of the elements of the characteristic determinant can be made to contain an inverse square dependence on α. This lends itself to an accurate evaluation of the infinite series, or integral to infinity, which is required for evaluating the characteristic determinant.

In the limit we can make the following simplifications to the formulae presented above.

$$Y_{TM_z} = \frac{-j\omega\epsilon_o\epsilon_z}{\alpha} \tag{2.33}$$

$$Y_{TE_z} = \frac{j\alpha}{\omega\mu} \tag{2.34}$$

$$Y^H_{z_z} = Y^H_{z_z} = -j\alpha \,/\, \omega\mu \tag{2.35}$$

$$Y^H_{z_z} = -\omega\epsilon_o\epsilon_{z+z} \,/\, j\alpha \tag{2.36}$$

$$Y^H_{z_z} = -\omega\epsilon_o\epsilon_z \,/\, j\alpha \tag{2.37}$$

We can see that for large α, the admittances depend only on the layers immediately adjacent to the appropriate interface. This is expected since the y directed wave is highly evanescent in this case and has neglegible amplitude at the next interface.

2.6. Poles in the Green's impedance functions

For computational reasons it is necessary to be able to locate the poles of the Green's function. These are, in fact, located at the positions of the modes of the dielectrically loaded waveguide. In a boxed structure these are the box modes and in an open structure they are the surface wave modes. That this should be so can be seen if the Green's function is expressed in terms of the eigenvectors of the structure [11,page 821].

$$\underline{\underline{g}}(x,x') = \sum_m \frac{\underline{E}_m(x)\ \underline{E}_m(x')}{\lambda_m - \lambda} \qquad (2.38)$$

where E_m is the m_{th} eigenvector and λ_m is the corresponding eigenvalue. Clearly the Green's function has a simple pole at $\lambda = \lambda_m$.

Again we can consider a bound mode to be a resonance of the transverse equivalent circuit. In the resonant condition an infinite response will be produced from any finite source, provided the structure is lossless. This corresponds to a pole for the Green's function.

Poles in the diagonal terms of the Green's matrix occur when:

$$Y_{E\,i\,u} = Y_{E\,i\,d} \quad \text{or} \quad Y_{H\,i\,u} = Y_{H\,i\,d} \tag{2.39}$$

To evaluate these requires the solution of another, albeit simpler, transcendental equation. We can, however, take the process one step further and look for the poles in equation 2.39. These are given as follows:

$$\text{Tan}\ k_i d_i = 0 \qquad \text{Tan}\ k_{i-1} d_{i-1} = 0 \tag{2.40}$$

$$\text{Cot}\ k_i d_i = 0 \qquad \text{Cot}\ k_{i-1} d_{i-1} = 0 \tag{2.41}$$

in other words when:

$$k_i d_i = n\pi/2 \quad \text{or} \quad k_{i-1} d_{i-1} = n\pi/2 \tag{2.42}$$

for any integer value of n.

Thus we may find the roots of equation 2.40 and 2.41, search between these for the roots of equations 2.39, these being the poles of the Green's function elements.

2.7. Special cases of the Green's matrix

The Green's matrices applicable to various planar transmission lines are now recovered from the general derivation.

For the case of boxed microstrip the Green's matrix consists of one dyadic element.

$$G_{zz} = \frac{-j\left((\epsilon_1 k_o^2 - \beta^2)\, k_{zn} \tan k_{zn} d_2 \right)}{\det} + \frac{\left(\epsilon_2 k_o^2 - \beta^2 \right) k_{1n} \tan k_{1n} d_1)}{\det} \qquad (2.43)$$

$$G_{zx} = G_{xz} = - \frac{\beta \alpha_n k_{zn} \tan k_{zn} d_2}{\det} - \frac{\beta \alpha_n k_{1n} \tan k_{1n} d_1}{\det} \qquad (2.44)$$

$$G_{xx} = \frac{j\left((\epsilon_1 k_o^2 - \alpha_n^2)\, k_{zn} \tan k_{zn} d_2 \right)}{\det} + \frac{\left(\epsilon_2 k_o^2 - \alpha_n^2 \right) k_{1n} \tan k_{1n} d_1)}{\det} \qquad (2.45)$$

where

$\det = \Psi \epsilon_o (X)(Y)$

$X = \epsilon_1 k_{zn} \tan k_{zn} d_2 + \epsilon_2 k_{1n} \tan k_{1n} d_1$

$Y = k_{1n} \cot k_{1n} d_1 + k_{zn} \cot k_{zn} d_2$

As $\alpha \rightarrow \infty$ the assymptotic forms are given by:

$$g_{zz} = j\beta^2 / (\epsilon_1 + \epsilon_2) \qquad (2.46)$$

$$g_{zx} / \alpha = g_{xz} / \alpha = -\beta / 2(\epsilon_1 + \epsilon_2)$$

$$g_{xx} / \alpha^2 = -j/2(\epsilon_1 + \epsilon_2)$$

The poles of the function are given by XY = 0

The corresponding expressions for the Green's functions, for use where the microstrip is to be analysed using the aperture fields as the unknown, are as follows:

$$f_{xx} = \frac{(\epsilon_1 k_o^2 - \beta^2)}{k_{1n} \mathrm{Tan}\ k_{1n} d_1} + \frac{(\epsilon_2 k_o^2 - \beta^2)}{k_{2n}\ \mathrm{Tan}\ k_{2n} d_2} \qquad (2.47)$$

$$f_{xz} = f_{zx} = \beta \alpha_n \left\{ \frac{1}{k_{1n} \mathrm{Tan}\ k_{1n} d_1} + \frac{1}{k_{2n}\ \mathrm{Tank}_{2n} d_2} \right\} \qquad (2.48)$$

$$f_{zz} = \frac{(\epsilon_1 k_o^2 - \alpha_n^2)}{k_{1n} \mathrm{Tan}\ k_{1n} d_1} + \frac{(\epsilon_2\ k_o^2 - \alpha_n^2)}{k_{2n}\ \mathrm{Tan}\ k_{2n} d_2} \qquad (2.49)$$

$k_{2n}\ \mathrm{Tank}_{2n} d_2$

For the case of a three layer structure consisting of a substrate layer between two air layers with metal on one of its interfaces such as unilateral finline or suspended microstrip, the functions are given as follows.

$$f_{xx} = \frac{\alpha_n^2 Y_1 + \beta^2 Y_2}{\alpha_n^2 + \beta^2} \qquad (2.50)$$

$$f_{xz} = \frac{\alpha_n \beta \ (Y_2 - Y_1)}{\alpha_n^2 + \beta^2} \qquad (2.51)$$

$$f_{zx} = f_{xz}$$

$$f_{zz} = \frac{\alpha_n^2 Y_2 + \beta^2 Y_1}{\alpha_n^2 + \beta^2} \qquad (2.52)$$

where:

$$Y_1 = j\omega\epsilon_o \left\{ \frac{1}{T3} + \frac{\epsilon_r + \epsilon_r^2 \, T1/C2}{T2 + \epsilon_r \, T1} \right\}$$

$$Y_2 = \frac{1}{j\omega\mu} \left\{ C3 + \frac{1 + T2/C1}{1/C2 + 1/C1} \right\}$$

$$Ti = k_{in} \, Tan \, k_{in} \, d_i$$

$$Ci = k_{in} \, Cot \, k_{in} \, d_i$$

2.8. Basis functions for the unknown currents

In the following, the basis functions for the unknown currents are discussed. For the case where the fields are taken as the unknown functions the following theory is immediately applicable if for currents, strips, and microstrip read fields, apertures and finline and vice versa. Also for I_x, I_z, E_x, E_z read E_z, E_x, I_z and I_x respectively.

In order to solve equation 2.12 for the structure under investigation, it is necessary to select a suitable set of basis functions. There are several constraints on this choice.

i. Each function must be non-zero only on the metal. ii. The set of functions must form a complete and minimal set in the space of functions which are non-zero only on the metal.

The first condition is a consequence of the fact that the current only exists where there is a conductor. The second condition ensures that the solution to equation 2.12 converges as the number of basis functions increases [12]. In addition to these conditions it is desirable that the basis functions should be as similar as possible to the actual current existing in the structure.

This means that the higher order basis functions can be neglected without losing significant accuracy, thus leading to a small set of equations and low computational effort. To this end we make use of the edge condition [13]. Namely that, in the vicinity of a metal edge, the current normal to the 180 degree edge varies as the square root of the distance from the edge and the transverse current varies as the reciprocal of this. If these conditions are incorporated into the basis functions, it has been shown that good results can be achieved using only a single term [14].

The Green's function for the structure has been derived in the form of an infinite series or integral of trigonometric terms. ie. as a Fourier series or Fourier transform depending on whether the structure is boxed or open. The evaluation of the quadratic form of equation 2.12 is facilitated if the Fourier transform of the basis functions is available in a manageable form.

For a planar transmission line which is uniform in the z direction, we need consider only the cross-section normal to z and define a set of bases for each strip which are functions of x, and are non-zero only on that strip.

We calculate the appropriate Fourier transforms for generalised boxed microstrip

$$\tilde{I}_x(n) = \int I_x(x) \, \text{Sin}\, \alpha_n(x + a/2)\, dx \qquad (2.53)$$

$$\tilde{I}_w(n) = \int I_w(x) \, \text{Cos}\, \alpha_n(x + a/2)\, dx \qquad (2.54)$$

in the following manner:

Suppose that there are r strips and let the r^{th} strip stretch from c_r to d_r on one of the dielectric interfaces.

Let

$$y_r = x - (c_r + d_r) / 2 \qquad (2.55)$$

So that:

$$- \frac{w_r}{2} < y_r < \frac{w_r}{2}$$

Thus:

$$\tilde{I}_x(n) = \sum_r \int_{-w_r/2}^{w_r/2} I_x(y_r) \text{Sin}\, \alpha_n(y_r + (c_r + d_r)/2 + a/2)\, dy_r$$

$$= \sum_r \text{Sin}\, \alpha_n\left(\frac{c_r + d_r + a}{2} \right) \int I_x(y) \, \text{Cos}\, \alpha_n y \, dy$$

$$+ \sum_r \text{Cos}\, \alpha_n\left(\frac{c_r + d_r + a}{2} \right) \int I_x(y) \, \text{Sin}\, \alpha_n y \, dy \qquad (2.56)$$

And:

$$\bar{I}_m(n) = \sum_r \int_{-w_r/2}^{w_r/2} I_m(y_r)\cos \alpha_n(y_r + (c_r + d_r)/2 + a/2\ )\ dy_r$$

$$= \sum_r \sin \alpha_n\left(\frac{c_r + d_r + a}{2}\right) \int I_m(y) \sin \alpha_n y\ dy$$

$$- \sum_r \cos \alpha_n\left(\frac{c_r + d_r + a}{2}\right) \int I_m(y) \cos \alpha_n y\ dy \qquad (2.57)$$

It can be seen that if $I_m(y)$ is an even function then the second term on the right hand side of equation 2.56 vanishes, likewise if $I_m(y)$ is an odd function then the first term vanishes.

In a similar manner one or other of the terms on the right hand side of equation 2.57 vanish depending on the parity of I_m.

We expand I_{mr} and I_{nr} , the currents on the r^{th} strip, in terms of known basis functions thus:

$$I_{mr}(y_r) = \sum_p Z_{pr}\ I_{mpr} \qquad (2.58)$$

$$I_{nr}(y_r) = \sum_p X_{pr}\ I_{npr} \qquad (2.59)$$

By integrating the second equation by parts and making use of the fact that I_{mpr} is zero at the edges of the strip we can show:

$$\int I_{mpr}(y) \cos \alpha_n y \, dy = - \int \frac{I'_{mpr}(y)}{\alpha_n} \sin \alpha_n y \, dy \quad n > 0$$

$$= -\int y I'_{mpr}(y) \, dy \qquad n = 0$$

(2.60)

$$\int I_{mpr}(y) \sin \alpha_n y \, dy = \int \frac{I'_{mpr}(y)}{\alpha_n} \cos \alpha_n y \, dy \qquad n > 0$$

$$= 0 \qquad\qquad n = 0$$

(2.61)

The advantage of this procedure is that the edge singularity for Iz is the same as that for the derivative of Ix, thus the same basis functions can be used to expand both.

It is noted that the convergence of the summation in the Green's functions as n increases is improved because of the factor of α_n appearing in the denominator as a result of the integration. This is, in fact, offset by the fact that the basis functions for Ix diminish more rapidly than those for the derivative of Ix by a similar factor of α_n.

A set of functions satisfying the edge condition is the following:

$$I_{zmr} = I'_{zmr} = \frac{T_m(2x_r/w_r)}{\sqrt{(1 - (2x_r/w_r)^2)}} \qquad (2.62)$$

where:

x_r=0 is the position of the centre of the r^{th} strip

w_r is the width of the r_{th} strip

$T_m(x)$ are Tchebychev polynomials

These functions are appropriate for strips placed anywhere on the dielectric interfaces and have the correct edge singularity. Their Fourier transforms are easily expressed in terms of Bessel functions. In addition only the first term contributes to the total longitudinal current.

The transforms defined by equations 2.56 and 2.57 can now be expressed as Bessel functions.

$$\bar{I}_z(n) = \sum_p \sum_r Z_{zpr} Q_{zprn} + Z_{(zp+1)r} R_{(zp+1)rn} \qquad (2.63)$$

And:

$$\tilde{I}^{\circ}_{m}(n) = \sum_{p}\sum_{r} X_{zpr}Q_{zprm} + X_{(zp+1)r}R_{(zp+1)rm} \qquad n > 0$$

$$= \sum_{r} w_r/4 \qquad m = 1\ ,\ n = 0$$

$$= 0 \qquad \text{otherwise}$$

(2.64)

where:

$$Q_{rm} = \text{Sin}\ \alpha_n\left\{ \frac{c_r + d_r + a}{2} \right\} J_{zp}(\alpha_n w/2)$$

$$R_{rm} = \text{Cos}\ \alpha_n\left\{ \frac{c_r + d_r + a}{2} \right\} J_{zp+1}(\alpha_n w/2)$$

and we have made use of the fact that I_{zpr} and I°_{mpr} are even or odd functions according to whether p is an even or an odd number. Note that m starts at 1 for I°_{m} rather than 0 because the zero'th term is not zero at the edge as the boundary conditions require. Indeed the assumption made when carrying out the integration by parts above is not valid if the zero'th term is included.

For the case of finline or coplanar line, the first and last strips are effectively bisected by an electric wall. The appropriate transform for the first strip is the following:

$$I_x(n) = \int_{-a/2}^{c_1} I_x(x) \cos \alpha_n (x + a/2)\, dx \qquad (2.65)$$

$$= \int_{0}^{c_1 + a/2} I_x(y_1) \cos \alpha_n (y_1 + a)\, dx$$

$$= (-1)^n J_p(\alpha_n w_1) \qquad p \text{ even}$$

similarly for the last strip:

$$I_x(n) = \int_{d_R}^{a/2} I_x(x) \cos \alpha_n (x + a/2)\, dx \qquad (2.66)$$

$$= \int_{d_R - a/2}^{0} I_x(y_R) \cos \alpha_n (y_R + a)\, dx$$

$$= +/- J_p(\alpha_n w_1) \qquad p \text{ even}$$

The sign depending on the sign of $E_x(y)$.

Note that if the strips adjacent to the walls of the box are of the same width ie. $a/2-d_x = c_1$, then the terms with even values of n will vanish if E_x is an odd function of x. Similarly the terms with odd values of n will vanish if E_x is an even function of x.

We can now substitute into the equation for the fields 2.11 thus:

$$E_i(x,z) = \sum_j \sum_q \sum_n \bar{g}_{ij}(n).\bar{I}_{jq}(n) \quad T(\alpha_n x)T(\beta_m z) \qquad (2.67)$$

where

i,j = 1.. number of layers-1

q = 1.. number of basis functions on each interface

n = 1.. ∞

For microstrip this reduces to:

$$E_z(x) = \sum_n \left(\bar{g}_{zz}\,\bar{I}_z + \frac{\bar{g}_{zx}}{\alpha_n}\,\bar{I}_x^* \right) \text{Sin}\ \alpha_n \left(x + a/2 \right) \qquad (2.68)$$

$$E_x(x) = \sum_n \left(\bar{g}_{xz}\,\bar{I}_z + \frac{\bar{g}_{xx}}{\alpha_n}\,\bar{I}_x^* \right) \text{Cos}\ \alpha_n \left(x + a/2 \right) \qquad (2.69)$$

where the components of g are given by equations 2.43 - 2.45.

In order to confirm that the singularity incorporated into the basis functions is the best one, it is useful to be able to try basis functions containing any specified singularity. This is done as follows: Let the basis functions for I_{α} and I_{α}' be:

$$I_{\alpha mr} = I'_{\alpha mr} = \frac{K_m C_m^{\lambda}(2x_r/w_r)}{(1 - (2x_r/w_r)^2)^{\alpha-\beta-\lambda}} \qquad (2.70)$$

where $C_m^{\lambda}(x)$ is the Gegenbauer polynomial

$$K_m = \frac{4\Gamma(\lambda)2^{2\lambda}}{w_r^{1+\lambda}\pi\Gamma(2\lambda+1)}$$

and $\lambda > 0$.

The Sine and Cosine transforms are then given by:

$$\bar{I}_m(n) = \sum_p \sum_r Z_{2pr} Q_{2prn} + Z_{(2p+1)r} R_{(2p+1)rn} \qquad (2.71)$$

And:

$$\bar{I}'_m(n) = \sum_p \sum_r X_{2pr} Q_{2prm} + X_{(2p+1)r} R_{(2p+1)rm}$$

$$n > 0$$

$$= \sum_r \frac{w_r^{1-\lambda}}{4(1+\lambda)\Gamma(\lambda+1)} \qquad m = 1 \ , \ n = 0$$

$$= 0 \qquad \text{otherwise}$$

$$(2.72)$$

where:

$$Q_{rn} = \text{Sin } \alpha_n \left\{ \frac{c_r + d_r + a}{2} \right\} \frac{J_{2p+\lambda}(\alpha_n w/2)}{(\alpha_n w/2)^\lambda}$$

$$R_{rn} = \text{Cos } \alpha_n \left\{ \frac{c_r + d_r + a}{2} \right\} \frac{J_{2p+1+\lambda}(\alpha_n w/2)}{(\alpha_n w/2)^\lambda}$$

Note that if we set $\lambda = 0$ in the above, we recover the original singularity.

Note also that when n=0 we need the following limit:

$$\lim_{x \to 0} \frac{J_\lambda(x)}{x^\lambda} = \frac{1}{2^\lambda \Gamma(1+\lambda)}$$

By this means it is possible to examine the convergence of the method as the number of basis functions is increased with various singularities. The results of doing this on microstrip are presented in the next chapter.

2.9 Conclusion

The theory presented in this chapter makes possible the analysis of general planar structures including planar waveguide, resonators and antennas. By making use of variational methods, and basis functions incorporating the singularities of the currents and fields in the vicinity of the metal edges, good numerical efficiency is achieved.

List of Figures

References

1. R Callarotti and A. Gallo "On the solution of a Microstripline with two dielectrics"
IEEE Trans MTT-32 1984 pp 333-339

2 H. A. Wheeler " Transmission Line properties of parallel wide strips by conformal mapping approximation"
IEEE Trans MTT-12 1964 pp 280-289

3 W.J. Getsinger "Microstrip Dispersion Model"
IEEE Trans MTT-21 1973 pp 34-39

4 G. Kompa and R. Mehren "Planar Waveguide model for Calculating microstrip components"
Electronics Letters 11 1975 pp 459-460

5 E. Yamashita and K. Atsuki "Analysis of Microstrip-like transmission lines by the non-uniform discretisation of integral equations"
IEEE Trans on MTT-24 1976 pp 195-200

6 R. Mittra and T. Itoh "A new technique for the analysis of the dispersion characteristics of microstrip lines"
IEEE Trans on MTT-19 1971 pp 47-56

7 T. Itoh and T. Mittra "Spectral Domain approach for calculating the dispersion characteristics of microstrip lines"
IEEE Trans MTT-21 1973 pp 496-499

8 R.H. Jansen "Unified user orientated computation of shielded covered and open planar microwave and millimetre wave transmission line characteristics"
IEEE J MOA 3 1974 pp 14-22

9 T. Itoh "Spectral domain Imittance Approach for Dispersion Characteristics of Generalised printed transmission lines"
IEEE Trans MTT-28 1980 pp 733-736

10 N. Das and D Pozar "A Generalised Spectral Domain Green's function for Multi-layer dielectric substrates with application to Multilayer transmission lines"
IEEE Trans MTT-35 1987 pp 326-335

11 Morse and Feshbach "Methods of Theoretical Physics"
Prentice-Hall 1973

12 Jones "Methods in Electromagnetic Wave Propagation"
Clarenden Press 1979

13 R.E. Collin "Field Theory of Guided Waves"
McGraw-Hill 1960

14 C. Olley and T. Rozzi "Systematic characterisation of the spectrum of unilateral finline"
IEEE Trans MTT-34 1986 pp 1147-1156

Appendix - PASCAL procedure for calculating the Green's functions of general planar structures

```
PROCEDURE SETN (G : GEOMTYPE ; BYCURRENT:BOOLEAN;
      ALPHA2,BETA2:REAL) ;
 {Note that since all the impedence functions
are pure real or pure imaginary, the j's have
 been supressed. Thus:
 GYZ, GXZ and GZX are real if BETA is real
 GZZ , GXX and GYX are imaginary.
 }
VAR
KO2,DETX, DETY, T1, T2 : REAL ;
YFN, YGN : REAL;
KNSQ,TN,YHU,YHD,YEU,YED:ARRAY[1..MAXLAYER] OF REAL;
YE,YH:ARRAY[1..MAXLAYER,1..MAXLAYER] OF REAL;
KN:ARRAY[1..MAXLAYER] OF COMP;
I,J:1..MAXLAYER;
BEGIN
KO2:=SQR(KO);
WITH G DO BEGIN
FOR I:=1 TO LAYERS DO BEGIN
KNSQ[I] := ALPHA2 + BETA2 - EPSR[I] * SQR (KO) ;
IF KNSQ[I] >= 0 THEN KN[I].ARG := 0
ELSE KN[I].ARG := PI2;
KN[I].V := SQRT (ABS (KNSQ[I])) ;
```

```
TN[I]:=C1(KN[I],THICK[I]);
{ C1(Z,X) = Z * TAN ( Z * X )  }
END;
IF MAG[2] THEN BEGIN
{ True if the upper boundary is a magnetic wall}
YHU[LAYERS-1]:=-TN[LAYERS];
YEU[LAYERS-1]:=-EPSR[LAYERS]*KO2*TN[LAYERS]
/KNSQ[LAYERS];
END ELSE BEGIN
YHU[LAYERS-1]:=-KNSQ[LAYERS]/TN[LAYERS];
YEU[LAYERS-1]:=-EPSR[LAYERS]*KO2/TN[LAYERS];
END;
IF MAG[1] THEN BEGIN
{ True if the lower boundary is a magnetic wall }
YHD[1]:=-TN[1];
YED[1]:=-EPSR[1]*KO2*TN[1]/KNSQ[1];
END ELSE BEGIN
YHD[1]:=-KNSQ[1]/TN[1];
YED[1]:=-EPSR[1]*KO2/TN[1];
END;
```

```
IF LAYERS>2 THEN
FOR I:=2 TO LAYERS-1 DO BEGIN
YHD[I]:=(-TN[I]+YHD[I-1])/(1-TN[I]*YHD[I-1]/KNSQ[I]);
YED[I]:=(-TN[I]*EPSR[I]*KO2/KNSQ[I]+YED[I-1])
       /(1-TN[I]*YED[I-1]/(EPSR[I]*KO2));
YHU[I-1]:=(-TN[I]+YHU[I])/(1-TN[I]*YHU[I]/KNSQ[I]);
YEU[I-1]:=(-TN[I]*EPSR[I]*KO2/KNSQ[I]+YEU[I])
       /(1-TN[I]*YEU[I]/(EPSR[I]*KO2));
END;
IF BYCURRENT THEN
FOR I:=1 TO LAYERS-1 DO BEGIN
YE[I,I]:=KO2/(YEU[I]+YED[I]);
YH[I,I]:=KO2/(YHU[I]+YHD[I]);
END
ELSE
FOR I:=1 TO LAYERS-1 DO BEGIN
YE[I,I]:=YEU[I]+YED[I];
YH[I,I]:=YHU[I]+YHD[I];
END;
```

```
FOR I:=1 TO LAYERS-1 DO FOR J:=1 TO LAYERS-1 DO
IF I>J THEN BEGIN
YE[I,J]:=YEU[J]/(YE[J,J]*YEU[I]);
YH[I,J]:=YHU[J]/(YH[J,J]*YHU[I]);
END ELSE
IF J>I THEN BEGIN
YE[I,J]:=YED[J]/(YE[J,J]*YED[I]);
YH[I,J]:=YHD[J]/(YH[J,J]*YHD[I]);
 END;
 IF BYCURRENT THEN BEGIN
 GXZ := SQRT(ABS(BETA2*ALPHA2))
      * (YE[1,1] + YH[1,1])/(ALPHA2+BETA2) ;
 GZZ := (ALPHA2 * YH[1,1] - BETA2
      * YE[1,1])/(ALPHA2+BETA2) ;
 GXX := (-BETA2 * YH[1,1] + YE[1,1]
      * ALPHA2)/(ALPHA2+BETA2) ;
 END ELSE BEGIN
 GXZ := -SQRT(ABS(BETA2*ALPHA2))
      * (YE[1,1] + YH[1,1])/(ALPHA2+BETA2) ;
 GZZ := (ALPHA2 * YE[1,1] - BETA2
      * YH[1,1])/(ALPHA2+BETA2) ;
 GXX := (-BETA2 * YE[1,1] + YH[1,1]
      * ALPHA2)/(ALPHA2+BETA2) ;
 END;
 END;
 END ;
```

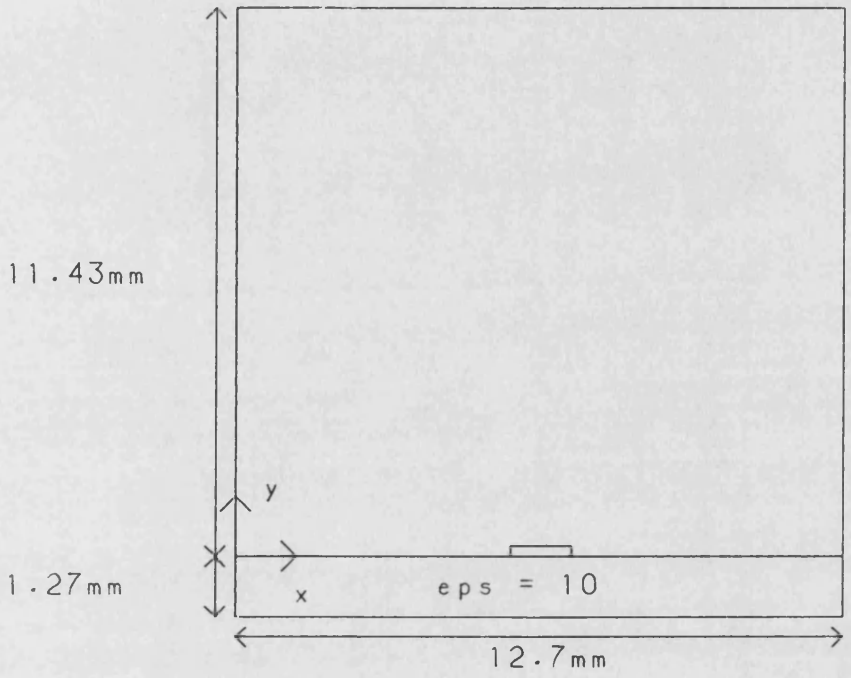

Fig. 2.1 - Microstrip cross section

CHAPTER 3

APPLICATION TO UNIFORM MICROSTRIP

3.1. Introduction

In this chapter the theory which has been developed for general planar structures is applied to boxed microstrip. The mode spectrum, characteristic impedance and field patterns are calculated and discussed.

The dispersion characteristics of the first 20 non-complex modes of a microstrip are shown, and it is shown by direct evaluation of the overlap integrals that the calculated field patterns are orthogonal, as theory requires [10].

The field patterns of various modes are shown as contour plots and as isometric projections showing clearly the singularity at the strip edge, and the concentration of field around the air-dielectric interface.

The behaviour of the propagation constant with strip width is shown, revealing the existence of "complex modes" at certain strip widths.

All of these results are required for the treatment of discontinuities in boxed microstrip described in chapter 4.

Finally the characteristic impedance is calculated as a function of frequency for various strip widths and some properties of the dependance highlighted. It is seen that there is considerable disagreement with the quasi-static formulae at other than low frequencies.

3.2. Calculation of the Boxed Microstrip mode spectrum

In Chapter 2 it was shown that the field patterns existing in a layered structure could be found by solving the general equation (2.12). For the case of boxed microstrip which is uniform in the z direction and for which it is required to find only bound modes, equation (2.14) was derived.

All the modes for a uniform microstrip are given by finding roots of equations (2.14). To facilitate its solution, we substitute equations (2.43)-(2.45) and (2.63)-(2.64) to give explicitly:

$$\det \begin{pmatrix} A^{xx} & A^{xz} \\ A^{zx} & A^{zz} \end{pmatrix} = 0 \qquad (3.1)$$

where the matrices A^{ij}_{pq} are given by:

$$\sum_{n} \bar{I}_{iq} \bar{g}_{ij} \bar{I}_{jp} \qquad (3.2)$$

The Greens impedances as calculated using the equivalent transmission line method are given in equation (2.43)-(2.45). The same functions have been calculated directly using the boundary conditions at the interface in Appendix 1. Expressions for all the field components are also given in the appendix. Comparison of the appendix with the formulation presented in chapter 2 clearly demonstrates the elegance of the transmission line method, even for a comparitively simple structure such as microstrip.

At a given frequency there will be an infinite number of values for the propagation constant, beta, which will satisfy condition 3.1. Because equation 2.70 is at least a quadratic in β^2, there can be roots for which β^2 is complex. This gives rise to the phenomenon of "complex modes" which have previously been found in other waveguiding structures [1] and which have recently been reported for the first time in microstrip [2]. In practice, however, by far the majority of the solutions are, either pure real or pure imaginary.

A real propagation constant represents a lossless propagating mode, an imaginary propagation constant represents a lossless evanescent mode.

A complex propagation coefficient represents a propagating wave which either decays or grows depending on the sign of the imaginary part. It would appear at first sight that, in a lossless medium with no energy sources, neither of the latter cases is possible. Indeed they are not possible in isolation. The possibility remains, however, that a pair of modes may exist having complex conjugate propagation coefficients.

The energy lost from one is exactly balanced by the energy gained by the other. The total effect being that of a single evanescent mode. Such solutions have been found and are described in more detail in section 3.4. Such modes can be excited by discontinuities and the energy stored therein must be taken into account in discontinuity analysis.

The energy stored by an evanescent mode can be either capacitive or inductive. In other words the integral of the Poynting vector over the microstrip cross section can be negative imaginary or positive imaginary. For a pair of complex modes, the energy stored changes from being inductive to capacitive in a cyclic manner with distance from the source of excitation.

This is in accordance with the fact that by changing the strip width, the complex modes can be resolved into two modes with pure imaginary propagation coefficients, one inductive and one capacitive.

We now proceed to find the modes of boxed microstrip by finding the zeros of the characteristic determinants of equation 3.1. In finding these zeros, care must be taken to make sure none of the zeros are missed on the one hand, or to necessitate large amounts of computation on the other. A straight forward search is impractible due to the fact that the determinant contains a large number of poles, many of which are close to the searched for zeros. The method used in this work makes use of the fact that the poles of the characteristic equation can be found without difficulty using the technique described in section 2.6. By carrying out the search between the poles, the computational efficiency is greatly increased.

The search is facilitated by the following property of the characteristic equation, namely that between any two poles there can be none, one or two roots. That this is the case can be seen by examining the form of the characteristic determinant. For the formulation in terms of unknown aperture fields this can be expressed as follows:

$$\det(\beta^2) = \sum \bar{E}_x^2 \, \bar{E}_z^2 \, (\alpha^2 + \beta^2) \, Y_E \, Y_H$$

where $\bar{E}_x$ and $\bar{E}_z$ are the Fourier transforms of the x and z components of the E field in the aperture.

$$Y_E = \frac{\epsilon_2 \, \text{Tan} \, k_1 d_1}{k_1} + \frac{\epsilon_1 \, \text{Tan} \, k_2 d_2}{k_2}$$

$$Y_H = k_1 \, \text{Tan} \, k_1 d_1 + k_2 \, \text{Tan} \, k_2 d_2$$

$$k_1^2 = \epsilon_1 k_o^2 - \alpha^2 - \beta^2$$

By expanding the tangents as infinite series we get the following:

$$\det(\beta^2) = \sum_n R_n^2 \, (\alpha^2 + \beta^2)$$

$$* \left\{ K1 \sum_k \frac{1}{(2k-1)^2 - (2k_1 d_1/\pi)^2} + K2 \sum \frac{1}{(2k-1)^2 - (2k_2 d_2/\pi)^2} \right\}$$

where R is a real number

K1 and K2 are linear functions of β^2

The denominators can be rearranged as follows:

$$f_{nk} - \beta^2$$

where f_{nk} is independent of β and the poles of $\det(\beta^2)$ are located at $\beta^2 = f_{nk}$.

Now consider the behaviour of $\det(\beta^2)$ in the interval between two consecutive poles at $\beta^2 = f_{n_1k_1}$ and $\beta^2 = f_{n_2k_2}$. This behaviour will be dominated by the terms in the summation which give rise to the poles. Thus we express $\det(\beta^2)$ as follows:

$$\det(\beta^2) = \frac{M1}{f_{n_1k_1} - \beta^2} + \frac{M2}{f_{n_2k_2} - \beta^2} + F(\beta^2)$$

where M1 and M2 are linear functions of β^2

$F(\beta^2)$ is made up of the remaining terms of the summation.

All of the terms in $F(\beta^2)$ are either monotonically increasing or monotonically decreasing in the interval under investigation. This term cannot introduce zeros into the derivative of $\det(\beta^2)$, thus for the purpose of investigating the number of possible zeros within the interval, this term can be neglected.

The two terms which are left form a quadratic in β^2 and will, therefore, have two roots. Any or none of these may fall inside the interval between the poles.

Where there is a single root between the poles a bisection algorithm will find it. Otherwise the minimum of the function is searched for. If roots are present they can be quickly located. In addition, since there is a one to one correspondence between the modes of the slab loaded guide and the quasi TE and quasi TM modes of the microstrip, the total number of roots will be one greater than the total number of poles. The extra root corresponds to the quasi TEM mode of microstrip. If during a search of the real axis of the complex plane it is found that there are more poles than roots, then the existence of complex roots is indicated. Their approximate location can be ascertained by keeping a count of the number of poles minus the number of roots found as the search along the real axis proceeds. The exact positions of the roots can then be located by performing a search of the upper half of the complex plane. Once a root is found, it is known that its complex conjugate is also a root.

3.3. Computation of Inner Products

In order to normalise the field patterns of the microstrip modes, to verify that the calculated modes are orthogonal as they theoretically should be, to calculate characteristic impedance and to calculate the overlap integrals of modes either side of a discontinuity, it is necessary to calculate the inner product of two microstrip modes. An efficient method of so doing is described here.

$$< E \mid H > = \int\int (E \times H) \cdot \hat{z} \; dxdy$$

$$= \int\int (E_x H_y - E_y H_x) \; dxdy \qquad (3.3)$$

From the results of the previous analysis we have for each side of the step discontinuity, expressions for the E and H fields in the following form.

$$E_{xr} = \sum_n \bar{\bar{E}}^{+}_{xr}(n) \cos \alpha_n (x + a/2) \frac{\sin k_n^{+} (h - y)}{\sin k_n^{+} h} \qquad (3.4)$$

$$y > 0$$

$$E_{xr} = \sum_n \bar{\bar{E}}^{-}_{xr}(n) \cos \alpha_n (x + a/2) \frac{\sin k_n (d + y)}{\sin k_n d} \qquad (3.5)$$

$$y < 0$$

and similarly for the other components.

It is noted that Hx and Ky are discontinuous at the interface between air and substrate. Thus we must use the coefficients appropriate to the region. The superscript + on the coefficients indicates they apply to the air region ($y > 0$) whilst the superscript - indicates that they apply to the substrate region ($y < 0$).

If we split the inner product into two parts thus:

$$< E \mid H > = < E \mid H >_x - < E \mid H >_y \qquad (3.6)$$

where

$$< E \mid H >_x = \int \int E_x H_y \, dxdy$$

$$< E \mid H >_y = \int \int E_y H_x \, dxdy$$

we get for each part an expression of the following form

$$< E \mid H >_x = \qquad (3.7)$$

$$\sum_n \sum_m A_n^+ B_m^+ \int_0^a T(\alpha_n x)\, T(\alpha_m x)\, dx \int_0^h \frac{U(k_n^+(h-y))\, U(k_m^+(h-y))\, dy}{U(k_n^+ h)\, U(k_m^+ h)}$$

$$+ \sum_n \sum_m A_n^- B_m^- \int_0^a T(\alpha_n x) T(\alpha_m x)\, dx \int_{-d}^0 \frac{U(k_n(d+y))\, U(k_m(d+y))\, dy}{U(k_n d)\, U(k_m d)}$$

where T and U are either Sin or Cos depending on which field components are being used and A and B are the appropriate field coefficients.

This becomes:

$$\sum_n \varepsilon_n \left\{ \frac{A_n^- B_n^- \quad I_1}{U(k_{n1}d)U(k_{n2}d)} + \frac{A_n^+ B_n^+ \quad I_2}{U(k_{n1}'h)U(k_{n2}'h)} \right\} \quad (3.8)$$

where

$$I_1 = \int_{-d}^{0} \text{Cos}\,(k_{n1} - k_{n2})(d+y) \; -/+ \; \text{Cos}(k_{n1} + k_{n2})(d+y)\, dy$$

$$I_2 = \int_{0}^{h} \text{Cos}\,(k_{n1}' - k_{n2}')(h-y) \; -/+ \; \text{Cos}(k_{n1}' + k_{n2}')(h-y)\, dy$$

where ε_n = a if n=0

= a/2 if n>0

and the first signs are taken if U is Sin, the second signs are taken if U is Cos.

The results of doing the integrals is:

$$I_1 = \frac{\sin (k_{n1} - k_{n2})d}{k_{n1} - k_{n2}} -/+ \frac{\sin (k_{n1} + k_{n2})d}{k_{n1} + k_{n2}} \quad (3.9)$$

$$I_2 = \frac{\sin (k_{n1}' - k_{n2}')h}{k_{n1}' - k_{n2}'} -/+ \frac{\sin (k_{n1}' + k_{n2}')h}{k_{n1}' + k_{n2}'}$$

By expanding the Sin terms and substituting into 3.8 we find that the inner product is:

If U is Sin:

$$\sum A_n^- B_n^- \gamma_n \frac{k_{n2}\cot k_{n2}d - k_{n1}\cot k_{n1}d}{k_{n1}^2 - k_{n2}^2} \quad (3.10)$$

$$+ \sum A_n^+ B_n^+ \gamma_n \frac{k_{n2}'\cot k_{n2}'h - k_{n1}'\cot k_{n1}'h}{k_{n1}'^2 - k_{n2}'^2}$$

If U is Cos:

$$\sum A_n^- B_n^- \gamma_n \frac{k_{n2}\tan k_{n2}d - k_{n1}\tan k_{n1}d}{k_{n1}^2 - k_{n2}^2} \quad (3.11)$$

$$+ \sum A_n^+ B_n^+ \gamma_n \frac{k_{n2}'\tan k_{n2}'h - k_{n1}'\tan k_{n1}'h}{k_{n1}'^2 - k_{n2}'^2}$$

We define the functions P (Z1,Z2,X) and Q (Z1,Z2,X) as follows:

$$P(Z1,Z2,X) = \frac{Z2\ \mathrm{Cot}\ Z2.X \ - \ Z1\ \mathrm{Cot}\ Z1.X}{Z1^2 \ - \ Z2^2} \qquad (3.12)$$

$$Z1^2 \neq Z2^2$$

$$= \frac{1}{2}\left\{ \frac{X}{\mathrm{Sin}^2\ Z1.X} - \frac{1}{Z1\ \mathrm{Tan}\ Z1.X} \right\}$$

$$Z1^2 = Z2^2$$

$$Q(Z1,Z2,X) = \frac{Z1\ \mathrm{Tan}\ Z2.X \ - \ Z2\ \mathrm{Tan}\ Z1.X}{Z1^2 \ - \ Z2^2} \qquad (3.13)$$

$$Z1^2 \neq Z2^2$$

$$= \frac{1}{2}\left\{ \frac{X}{\mathrm{Cos}^2\ Z1.X} + \frac{1}{Z1\ \mathrm{Cot}\ Z1.X} \right\}$$

$$Z1^2 = Z2^2$$

Then the inner product < E | H > is equal to:

$$a\tau_n \sum_n E_{xn}^{+} H_{yn}^{+} \quad P\ (\ k_{n1}^{\circ}\ ,\ k_{n2}^{\circ}\ ,\ h\ )$$

$$+ \quad a\tau_n \sum_n E_{xn}^{-} H_{yn}^{-} \quad P\ (\ k_{n1}\ ,\ k_{n2}\ ,\ d\ )$$

$$- \quad a\tau_n \sum_n E_{yn}^{+} H_{xn}^{+} \quad Q\ (\ k_{n1}^{\circ}\ ,\ k_{n2}^{\circ}\ ,\ h\ )$$

$$- \quad a\tau_n \sum_n E_{yn}^{-} H_{xn}^{-} \quad Q\ (\ k_{n1}\ ,\ k_{n2}\ ,\ d\ ) \qquad (3.14)$$

3.4. CHARACTERISTIC IMPEDANCE OF MICROSTRIP

In the literature eg. [3 - 8] a great deal of discussion has taken place in regard to the definition of characteristic impedance for microstrip. Given the values of total transported power, total longitudinal current, and the potential difference between the box and the strip, three separate definitions of characteristic impedance are possible. In addition we have the "reflection definition" [9] where the reflection at a discontinuity of microstrip with a waveguide of known characteristic impedance is calculated and this is used to define the characteristic impedance of microstrip.

Unfortunately, except in the limit of zero frequency, all these methods give different answers. Moreover as a function of frequency, some of these answers increase and some decrease.

This ambiguity is the direct result of the hybrid nature of the microstrip mode and the attempt to apply concepts appropriate to TEM lines to a quasi-TEM microstrip. Thus for a microstrip the concept of characteristic impedance is an approximate one. It is generally accepted that the most physically meaningful definition is that based on total transported power and total longitudinal current.

This definition has been used in the following formulation.

Denoting the characteristic impedance by Z_o we have

$$Z_o = \frac{< E \mid H >}{\left\{ \int J_z \, dx \right\}^2} \qquad (3.15)$$

Because of the form of the basis functions chosen for the longitudinal current in equation (2.62), the integral in the denominator of equation (3.15) becomes simply:

$$a_o \int_{-w_r/2}^{w_r/2} \frac{dx_r}{\sqrt{(1 - (2x_r/w_r)^2)}} \qquad (3.16)$$

where a_o is the coefficient of the first term in the current eigenvector derived in the solution of equation 2.14. Due to the orthogonality properties of Tchebychev polynomials, this is the only term in the expansion of J_z to contribute to the integral.

The inner product in the numerator can be reduced, by applying Parseval's theorem, to a summation of the products of field terms, the derivation of which is given in section 3.3.

3.5 Computational Considerations

In calculating the parameters of microstrip, we are at liberty to choose the number of basis functions we wish to use and whether to use strip currents or aperture fields as the unknown functions in the formulation. Clearly there will be a trade off between accuracy and computer time. Trials have been carried out using various numbers of basis functions, using currents and fields, and containing the edge singularity and not containing this singularity. In the latter case the basis functions used were Gegenbaur polynomials with a singularity of zero. This is equivalent to using Legendre polynomials. The results are shown in Figs 3.1-3.2 for both a narrow strip and for a wide strip. It can be seen that two basis functions are required for accurate solutions when the singularity is included and currents are used. In the other cases about 5 functions are required. This again highlights the importance of a good choice of basis functions.

3.6 Results for The High order modes

The dispersion characteristics of the first 20 modes of the microstrip whose geometry is shown in Figure 3.3, is shown in Figure 3.4. These were calculated using a modest amount of computer power.

In Figs 3.5 and 3.6. we have a plot of the effective permittivity of the microstrip versus strip width. Also shown are the corresponding results for the slab loaded guide with no strip. It can be seen that, as would be expected, at very small strip widths, there is not much difference between the microstrip and the slab loaded guide. Some of the modes perturb the effective permittivity upwards while some perturb it downwards depending on whether the energy in the vicinity of the strip is predominantly magnetic or predominantly electric.

As the strip width is increased, the loci of the effective permittivity behave in several distinct ways depending on the mode. For some the locus remains very close to the corresponding slab guide mode, this is true for all the low order modes. For some the locus moves from being asymptotic to one slab guide mode at low strip widths to being asymptotic to the next slab guide mode at high strip widths, an example of this is between effective permittivities of -302 and -320. Here the variation of effective permittivity with strip width is considerable.

For a few modes this variation is so large that the locus approaches the next slab guide mode and appears to cross it and continue on the other side. In fact, as can be seen in the figure, this does not happen. Rather the locus reaches a maximum where the variation of effective permittity with strip width is zero, and then becomes negative. An example of this appears at effective permittivities between -332 and -345. Here we have the situation where, for strip widths between 0.5mm and 0.9mm there appears to be no microstrip mode corresponding to the slab guide modes with effective permittivities of -331.5, -338.5 and possibly -345. A closer examination reveals that for the strip widths where the modes appear to be missing, they in fact exist with complex conjugate propagation coefficients.

Figure 3.7. shows the locus of these modes as the strip width varies. Also shown are the adjacent modes, the 17th and 20th, and the modes of a slab loaded guide formed by removing the strip, the latter are the vertical lines. It can be seen that the phase of the propagation constant becomes large where the locus crosses the position of a slab guide mode. Higher order complex modes exhibit this same property. Since complex modes occur as low as the 18th, it is necessary to include them in a discontinuity calculation.

It can be said that where the dependence of the propagation coefficient of a mode on strip width is so strong so as to cause it to cross the neighbouring pole, the root splits into two and "straddles" the pole.

Another example of complex modes occurs at an effective permittivity of around -250. This time, however, the mode becomes complex for narrow strip widths.

The field patterns versus x at y=0 for an effective permittivity of around -335 are plotted in Figs 3.8 to 3.12. These show how the patterns change from looking like a perturbation of one slab guide mode to the perturbation of another slab guide mode as the strip width varies.

The same effect at an effective permittivity of around -265 is shown in Figs. 3.13 and 3.15. As the strip width is increased from very small to 2.75cm, the two distinct modes shown in 3.13 become more alike until they are indistinguishable as in Fig 3.15.

At even larger strip widths the modulus of the modes remain indistinguishable but the phase relationship between the field components is different. Eventually, when the modes have crossed the pole, they again become distinct.

The E field intensity over the box cross-section for the dominant mode and for mode 20 are shown in an isometric projection in Figure 3.16. It can be seen that the expected singularity exists at the strip edge. It can also be seen that the field is concentrated at the air-dielectric interface.

Figures 3.16 - 3.22 show isometric projections and contour plots of the transverse E field for various modes. These give a pictorial impression of the modes.

It is expected from theoretical considerations [10] that the microstrip modes will form a complete orthogonal set of functions whose domain is the guide cross section and which satisfy the boundary conditions. The following orthogonality condition applies:

$$< \underline{E_n}\ (x,y) \mid \underline{H_m}\ (x,y) > \ = K_n \delta_{nm}$$

where n and m are the mode numbers of the strip.

k_n is a complex number

The above inner product has been calculated using the method described in section 3 of chapter 3 for the first non-complex modes of a microstrip. The results, which show that the calculated modes are indeed orthogonal, are shown in Table 3.1.

This contrasts with the situation recently reported for Finline [11] where a large number of basis functions are required when using the spectral domain method to calculate accurate field patterns.

3.6 Results for the Characteristic Impedance of Microstrip

Figure 3.23 shows the calculated characteristic impedance of the microstrip whose geometry is given in Figure 3.3. It can be seen that after an initial reduction of impedance with frequency, the impedance steadily increases with frequency. This is in agreement with other published rigorous results [3] and does not agree with quasi-static formulas [12] except in the low frequency limit. Figure 3.24 shows the characteristic impedance for various strip widths, normalised to their values at zero frequency. It can be seen that the general shape is much the same, especially at low frequencies. It is also noted that the position of the minimum impedance appears to be independent of the strip width.

3.7 Variation of field pattern with frequency

Figures 3.25-3.28 show how the variation of the shape of the field pattern of the dominant mode of a microstrip as the frequency changes. It can be seen that the zero of the function moves closer to the strip as the frequency increases. This variation is a feature of the hybrid mode and contrasts with the situation in normal waveguide in which the modal function does not depend on frequency.

This feature has implications when modelling a discontinuity using an equivalent circuit. A waveguide discontinuity can be modelled by a transformer, representing the overlap between modes and by a reactance representing the stored energy in the mode. This has proved very successful in providing a frequency dependent model [13]. The fact that the microstrip modes are hybrid means that if this model were applied thereto, the transformer ratio would be frequency dependent. This severely complicates the application of this model to microstrip.

3.8 Conclusion

In this chapter the general Green's function method of analysis has been applied to boxed microstrip. By this means the complete mode spectrum of microstrip has been efficiently calculated. This includes "complex modes". By calculating the overlap integral between different modes it has been demonstrated that the calculated modes are genuinely orthogonal as theory requires. Also the characteristic impedance has been calculated for various microstrip geometries and shown to agree with other rigorous calculations but to disagree with quasi-static formulae.

References

1. P.J.B. Clarricoats and K.R. Slinn "Complex modes of propagation in dielectric loaded circular waveguide" Electronics Letters Vol 1 1965 pp 145-146

2. C.J. Railton, T. Rozzi and J Kot. "The efficient calculation of high order microstrip modes for use in discontinuity problems" Proc. Eu. M. C. 1986 pp 529-534

3. E.J. Denlinger "A Frequency Dependent Solution for Microstrip Transmission Lines" IEEE Trans on MTT. Vol. MTT-19. Jan 1971 pp30-39

4. R.H. Jansen and M. Kirschning "Arguments and an Acurate Model for the Power-Current Formulation on Microstrip Characteristic Impedance" Arch. Elek. Ubertragung. Vol 37 pp108-112 1983

5. W.J. Getsinger "Measurement and Modeling of the Apparent Characteristic Impedance of Microstrip" IEEE Trans on MTT. Vol MTT-31. Aug 1983 pp624-632.

6. E.F. Kuester et al. "Frequency Dependent definitions of Microstrip Characteristic Impedance" Dig. Int. URSI Symp. Electromagnetic Waves (Munich) 1980 pp 355B1-3

7. Yee and Wu. "Printed Circuit Transmission-Line Characteristic Impedance by Transverse Modal Analysis"
IEEE Trans on MTT. Vol MTT-34. Nov. 1986 pp1157-1163

8. M. Hashimoto. "A Rigorous Solution for Dispersive Microstrip"
IEEE Trans on MTT. Vol MTT-33. Nov. 1985 pp1131-1137

9. Arndt and Paul. "The Reflection Definition of the Characteristic Impedance of Microstrip"
IEEE Trans on MTT. Vol MTT-27. Aug 1979 pp724-731

10. R. Colin "Field Theory of Guided Waves"
McGraw-Hill 1960

11. A.S. Omar and K. Schunemann "Formulation of the Singular Integral Equation Technique for Planar Transmission Lines"
IEEE Trans MTT-33 Dec. 1985 pp 1313-1321

12. K.C. Gupta et. al. "Computer Aided Design of Microwave Circuits"
Artech 1981

13 T.E. Rozzi "A New Approach to the Network Modelling of Capacitive Irises and Steps in Wvaeguide"
Circuit Theory and Applications Vol 3 1979 pp 339-354

Appendix 3.1.

Derivation of the Microstrip Greens Impedance using the interface boundary conditions

We expand the fields in a shielded planar transmission line in terms of y directed Hertzian potentials as follows:

$$\underline{E} = -j\omega\mu\nabla \times \underline{\Pi}_H + k^2 \underline{\Pi}_E + \nabla\nabla . \underline{\Pi}_E \qquad \text{(A31.1)}$$

$$\underline{H} = k^2 \underline{\Pi}_H + \nabla\nabla . \underline{\Pi}_H + j\omega\epsilon\nabla \times \underline{\Pi}_E \qquad \text{(A31.2)}$$

where

$$\underline{\Pi}_H = \hat{y}\Psi_H(x,y)\, e^{-j\beta z}$$

$$\underline{\Pi}_E = \hat{y}\Psi_E(x,y)\, e^{-j\beta z}$$

$$\Psi_H = \sum_{n=0}^{n=\infty} C_n \frac{\sin k_n(h + y)}{\sin k_n h} \cos \alpha_n (x+a/2) \quad y<0 \qquad \text{(A31.3)}$$

$$\Psi_H = \sum_{n=0}^{n=\infty} D_n \frac{\sin k_n^*(h^* - y)}{\sin k_n^* h^*} \cos \alpha_n (x+a/2) \quad y>0 \qquad \text{(A31.4)}$$

$$\Psi_E = \sum_{n=0}^{n=\infty} A_n \frac{\text{Cos } k_n(h + y)}{\text{Cos } k_n h} \text{Sin } \alpha_n (x+a/2) \quad y<0 \quad (A31.5)$$

$$\Psi_E = \sum_{n=0}^{n=\infty} B_n \frac{\text{Cos } k_n^*(h^* - y)}{\text{Cos } k_n^* h^*} \text{Sin } \alpha_n (x+a/2) \quad y>0 \quad (A31.6)$$

$\alpha_n = n\pi/a$

and k_n, k_n^* are constrained by the relationship,

$k_n^2 = \epsilon_r k_0^2 - \beta^2 - \alpha_n^2$

$k_n^{*2} = k_0^2 - \beta^2 - \alpha_n^2$

We can write the fields in the substrate as follows:
(A1.7)

$$E_x(x) = \sum (-A_n k_n \alpha_n \tan k_n h + C_n \omega \mu_0 \beta) \text{Cos } \alpha_n (x + a/2)$$

$$E_y(x) = \sum A_n (\epsilon_r k_0^2 - k_n^2) \text{ Sin } \alpha_n (x + a/2)$$

$$E_z(x) = \sum (A_n k_n j\beta \tan k_n h + C_n j\omega \mu_0 \alpha_n) \text{Sin } \alpha_n (x + a/2)$$

$$H_x(x) = \sum (-A_n \omega \epsilon_0 \epsilon_r \beta - C_n k_n \alpha_n \cot k_n h) \text{Sin } \alpha_n (x + a/2)$$

$$H_y(x) = \sum C_n (\epsilon_r k_0^2 - k_n^2) \text{ Cos } \alpha_n (x + a/2)$$

$$H_z(x) = \sum (A_n j\omega \epsilon_0 \epsilon_r \alpha_n - C_n j\beta k_n \cot k_n h) \text{ Cos } \alpha_n (x + a/2)$$

Similarly in air: (A31.8)

$$E_x(x) = \sum (B_n k_n' \alpha_n \text{ Tan } k_n' h' + D_n \omega \mu_o \beta) \text{ Cos } \alpha_n (x + a/2)$$

$$E_y(x) = \sum B_n (k_o^2 - k_n'^2) \text{ Sin } \alpha_n (x + a/2)$$

$$E_z(x) = \sum (-B_n k_n' j\beta \text{ Tan } k_n' h' + D_n j\omega \mu_o \alpha_n) \text{Sin } \alpha_n (x + a/2)$$

$$H_x(x) = \sum (-B_n \omega \epsilon_o \beta + D_n k_n' \alpha_n \text{Cot } k_n' h') \text{Sin } \alpha_n (x + a/2)$$

$$H_y(x) = \sum D_n (k_o^2 - k_n'^2) \text{ Cos } \alpha_n (x + a/2)$$

$$H_z(x) = \sum (B_n j\omega \epsilon_o \alpha_n + D_n j\beta k_n' \text{Cot} k_n' h') \text{ Cos } \alpha_n (x + a/2)$$

Applying the boundary conditions at the air-dielectric interface we can obtain the following solutions for A B C and D.

$$C_n = D_n \quad \text{(A31.9)}$$

$$A_n = -B_n \frac{k_n' \tan k_n' h'}{k_n \tan k_n h} \quad \text{(A31.10)}$$

$$D_n = \frac{-\alpha_n \bar{J}_z + j\beta \bar{J}_x}{(\alpha_n^2 + \beta^2)(Y)} \quad \text{(A31.11)}$$

$$B_n = \frac{(\beta \bar{J}_z + j\alpha_n \bar{J}_x) k_n \tan k_n h}{(\alpha_n^2 + \beta^2)(X) \omega \epsilon_o} \quad \text{(A31.12)}$$

where

$$X = \epsilon_r k_n' \tan k_n' h' + k_n \tan k_n h \qquad \text{(A31.13)}$$

$$Y = k_n \cot k_n h + k_n' \cot k_n' h' \qquad \text{(A31.14)}$$

$$\bar{J}_x(n) = \int J_x(x) \operatorname{Sin} \alpha_n(x + a/2)\, dx \qquad \text{(A31.15)}$$

$$\bar{J}_z(n) = \int J_z(x) \operatorname{Cos} \alpha_n(x + a/2)\, dx$$

The integrals being taken over the strips since no current flows where there is no strip.

We now substitute into the equations for the x and z components of the fields and get an expanded version of (1) thus:

$$E_x(x) = \sum_n \left(g_{xx} \bar{J}_x + \frac{g_{xz}}{\alpha_n} \bar{J}_z' \right) \operatorname{Sin} \alpha_n (x + a/2) \qquad \text{(A31.16)}$$

$$E_z(x) = \sum_n \left(g_{zx} \bar{J}_x + \frac{g_{zz}}{\alpha_n} \bar{J}_z' \right) \operatorname{Cos} \alpha_n (x + a/2) \qquad \text{(A31.17)}$$

where

$$g_{zz} = \frac{-j\,(\,(\epsilon_r k_o^2 - \beta^2\,)\,k_n' \tan k_n' h}{\det} + \frac{(\,k_o^2 - \beta^2\,)\,k_n \tan k_n d)}{\det}$$

$$g_{zx} = g_{xz} = -\frac{\beta\alpha_n(k_n' \tan k_n' h + k_n \tan k_n d)}{\det}$$

$$g_{xx} = \frac{j\,(\,(\epsilon_r k_o^2 - \alpha_n^2\,)\,k_n' \tan k_n' h}{\det} + \frac{(\,k_o^2 - \alpha_n^2\,)\,k_n \tan k_n d)}{\det}$$

where

$$\det = \omega\epsilon_o(X)(Y)$$

$$X = \epsilon_r k_n' \tan k_n' h + k_n \tan k_n d$$

$$Y = k_n \cot k_n d + k_n' \cot k_n' h$$

As $\alpha \to \infty$ the assymptotic forms are given by:

$$g_{zz} = j\beta^2 / (\epsilon_1 + 1)$$

$$g_{zx} / \alpha = g_{xz} / \alpha = -\beta / 2(\epsilon_r + 1)$$

$$g_{xx} / \alpha^2 = -j/2(\epsilon_r + 1)$$

This is in agreement with the results obtained using the equivalent transmission line method.

Appendix 3.2 - Summations of the products of two basis functions - Application to uniform microstrip

In order to accurately calculate series such as that which appears in the characteristic equation of a microstrip eg. equations 2.14, an asymptotic function for the terms of the series as n goes to infinity is desirable. Together with an analytic expression for the sum to infinity of this function, this has the twofold benefit of reducing the number of terms which need be evaluated and of producing a more accurate answer.

This technique is used with great success in [2] for Schwinger functions as applied to microstrip with a centrally placed strip for even modes. In the following this technique is applied to the basis functions whose Fourier transforms contain Bessel functions for any microstrip or any pair of microstrips with no restriction of size or position of the strip.

The series in question is of the following form:

(A32.1).

$$\sum \frac{\mathrm{Sin}(nb_1+p_1\pi/2)J_{p1}(nx_1)\ \mathrm{Sin}(nb_2+p_2\pi/2)\ J_{p2}(nx_2)}{n}$$

where $J_p(x)$ is the p^{th} order Bessel function of x.

For large arguments the Bessel function has the following asymptotic form:

$$J_{p(x)} = \frac{2}{\sqrt{(\pi x)}} \left\{ \cos(u) + \frac{(1-4p^2)}{8x} \sin(u) \right\} \qquad (A32.2)$$

where $u = nx - e$

$e = (2p+1)\pi/4$

$\cos(u) = \cos(nx)\cos(e) + \sin(nx)\sin(e)$

$\sin(u) = \sin(nx)\cos(e) - \cos(nx)\sin(e)$

We can express A32.1 as:

$$\sum \frac{S - \bar{S}}{n} + \sum \frac{\bar{S}}{n} \qquad (A32.3)$$

where:

$$S = \sin(nb_1+p_1\pi/2) J_{p1}(nx_1) \sin(nb_2+p_2\pi/2) J_{p2}(nx_2)$$

$$\bar{S} = \sin(nb_1+p_1\pi/2) J_{p1}(nx_1) \sin(nb_2+p_2\pi/2) J_{p2}(nx_2)$$

The first term will converge in fewer terms than the original summation given by eqn. A32.1. The second term can be evaluated as follows:

$$
\begin{aligned}
S = & \\
\Big\{ & \cos(u1)\cos(u2)\sin(nb_1+p_1\pi/2)\sin(nb_2+p_2\pi/2) \\
+ & \frac{\sin(u1)\sin(u2)\sin(nb_1+p_1\pi/2)\sin(nb_2+p_2\pi/2)}{64\ n^2\ x_1\ x_2} \\
+ & \frac{\sin(u1)\cos(u2)\sin(nb_1+p_1\pi/2)\sin(nb_2+p_2\pi/2)}{8\ n\ x_1} \\
+ & \frac{\cos(u1)\sin(u2)\sin(nb_1+p_1\pi/2)\sin(nb_2+p_2\pi/2)}{8\ n\ x_2} \Big\}
\end{aligned}
$$

$$
* \frac{2}{n^2\pi\ \sqrt{(x_1\ x_2)}} \qquad \text{(A32.4)}
$$

We have:

$$
\begin{aligned}
2\ \sin(nb_1+p_1\pi/2)\sin(nb_2+p_2\pi/2) = & \\
& \sin((p_1+p_2)\pi/2)\ \sin(n(b_1+b_2) \\
+ & \cos((p_1-p_2)\pi/2)\ \cos(n(b_1-b_2) \\
- & \cos((p_1+p_2)\pi/2)\ \cos(n(b_1+b_2) \\
- & \sin((p_1-p_2)\pi/2)\ \sin(n(b_1-b_2) \qquad \text{(A32.5)}
\end{aligned}
$$

$$2\,\mathrm{Cos}(u_1)\,\mathrm{Cos}(u_2) =$$

$$\begin{aligned}
&\mathrm{Sin}(e_1 + e_2)\,\mathrm{Sin}(n(x_1 + x_2)\\
+\;&\mathrm{Cos}(e_1 - e_2)\,\mathrm{Cos}(n(x_1 - x_2)\\
+\;&\mathrm{Cos}(e_1 + e_2)\,\mathrm{Cos}(n(x_1 + x_2)\\
+\;&\mathrm{Sin}(e_1 - e_2)\,\mathrm{Sin}(n(x_1 - x_2)
\end{aligned} \qquad \text{(A32.6)}$$

$$2\,\mathrm{Sin}(u_1)\,\mathrm{Cos}(u_2) =$$

$$\begin{aligned}
&\mathrm{Sin}(e_1 + e_2)\,\mathrm{Cos}(n(x_1 + x_2)\\
+\;&\mathrm{Cos}(e_1 - e_2)\,\mathrm{Sin}(n(x_1 - x_2)\\
+\;&\mathrm{Cos}(e_1 + e_2)\,\mathrm{Sin}(n(x_1 + x_2)\\
-\;&\mathrm{Sin}(e_1 - e_2)\,\mathrm{Sin}(n(x_1 - x_2)
\end{aligned} \qquad \text{(A32.7)}$$

$$2\,\mathrm{Sin}(u_1)\,\mathrm{Sin}(u_2) =$$

$$\begin{aligned}
-\;&\mathrm{Sin}(e_1 + e_2)\,\mathrm{Sin}(n(x_1 + x_2)\\
+\;&\mathrm{Cos}(e_1 - e_2)\,\mathrm{Cos}(n(x_1 - x_2)\\
-\;&\mathrm{Cos}(e_1 + e_2)\,\mathrm{Cos}(n(x_1 + x_2)\\
+\;&\mathrm{Sin}(e_1 - e_2)\,\mathrm{Sin}(n(x_1 - x_2)
\end{aligned} \qquad \text{(A32.8)}$$

We now expand each term in the large bracket so as to cause all the terms to be of the form K Sin(nx) or K Cos(nx) where K is independent of n. For example the result for the first term is:

$$\begin{aligned}
S_1 = \;&\mathrm{Sin}((p_1 + p_2)\pi/2)\mathrm{Cos}(e_1 + e_2)\mathrm{Sin}(n(b_1 + b_2 + x_1 + x_2))\\
+\;&\mathrm{Sin}((p_1 + p_2)\pi/2)\mathrm{Cos}(e_1 + e_2)\mathrm{Sin}(n(b_1 + b_2 - x_1 - x_2))\\
+\;&\mathrm{Sin}((p_1 + p_2)\pi/2)\mathrm{Sin}(e_1 - e_2)\mathrm{Cos}(n(b_1 + b_2 - x_1 + x_2))\\
-\;&\mathrm{Sin}((p_1 + p_2)\pi/2)\mathrm{Sin}(e_1 - e_2)\mathrm{Cos}(n(b_1 + b_2 + x_1 - x_2))\\
-\;&\mathrm{Sin}((p_1 - p_2)\pi/2)\mathrm{Cos}(e_1 + e_2)\mathrm{Sin}(n(b_1 - b_2 + x_1 + x_2))\\
-\;&\mathrm{Sin}((p_1 - p_2)\pi/2)\mathrm{Cos}(e_1 + e_2)\mathrm{Sin}(n(b_1 - b_2 - x_1 - x_2))\\
-\;&\mathrm{Sin}((p_1 - p_2)\pi/2)\mathrm{Sin}(e_1 - e_2)\mathrm{Cos}(n(b_1 - b_2 - x_1 + x_2))\\
+\;&\mathrm{Sin}((p_1 - p_2)\pi/2)\mathrm{Sin}(e_1 - e_2)\mathrm{Cos}(n(b_1 - b_2 + x_1 - x_2))\\
-\;&\mathrm{Cos}((p_1 + p_2)\pi/2)\mathrm{Cos}(e_1 - e_2)\mathrm{Cos}(n(b_1 + b_2 + x_1 - x_2))\\
-\;&\mathrm{Cos}((p_1 + p_2)\pi/2)\mathrm{Cos}(e_1 - e_2)\mathrm{Cos}(n(b_1 + b_2 - x_1 + x_2))\\
-\;&\mathrm{Cos}((p_1 + p_2)\pi/2)\mathrm{Sin}(e_1 + e_2)\mathrm{Sin}(n(b_1 + b_2 + x_1 + x_2))\\
+\;&\mathrm{Cos}((p_1 + p_2)\pi/2)\mathrm{Sin}(e_1 + e_2)\mathrm{Sin}(n(b_1 + b_2 - x_1 - x_2))\\
+\;&\mathrm{Cos}((p_1 - p_2)\pi/2)\mathrm{Cos}(e_1 - e_2)\mathrm{Cos}(n(b_1 - b_2 + x_1 - x_2))\\
+\;&\mathrm{Cos}((p_1 - p_2)\pi/2)\mathrm{Cos}(e_1 - e_2)\mathrm{Cos}(n(b_1 - b_2 - x_1 + x_2))\\
+\;&\mathrm{Cos}((p_1 - p_2)\pi/2)\mathrm{Sin}(e_1 + e_2)\mathrm{Sin}(n(b_1 - b_2 + x_1 + x_2))\\
-\;&\mathrm{Cos}((p_1 - p_2)\pi/2)\mathrm{Sin}(e_1 + e_2)\mathrm{Sin}(n(b_1 + b_2 - x_1 - x_2))
\end{aligned} \qquad \text{(A32.9)}$$

In order to produce an analytical formula for the sum of the above function we require formulae for the following summations.

$$SUMS2 = \sum \frac{Sin\ (nx)}{n^2} \qquad (A32.10)$$

$$SUMC2 = \sum \frac{Cos\ (nx)}{n^2} \qquad (A32.11)$$

$$SUMS3 = \sum \frac{Sin\ (nx)}{n^3} \qquad (A32.12)$$

$$SUMC3 = \sum \frac{Cos\ (nx)}{n^3} \qquad (A32.13)$$

$$SUMS4 = \sum \frac{Sin\ (nx)}{n^4} \qquad (A32.14)$$

$$SUMC4 = \sum \frac{Cos\ (nx)}{n^4} \qquad (A32.15)$$

These summations can be found using the Geometric Series method as outlined in Collin [10].

We obtain:

$$SUMC2 = \frac{\pi^2}{6} - \frac{\pi x}{2} + \frac{x^2}{4} \qquad (A32.16)$$

By integration of both sides we get:

$$SUMS3 = \frac{\pi^2 x}{6} - \frac{\pi x^2}{4} + \frac{x^3}{12} \qquad (A32.17)$$

$$SUMC4 = \frac{(\pi x)^2}{12} - \frac{\pi x^3}{12} + \frac{x^4}{48} \qquad (A32.18)$$

Also we have

$$SUMS2 = x\,Ln(x) - x\left(1 + x^2\frac{B(2)}{12}\left(1 + x^2\frac{3B(4)}{5B(2).4.3.2}\left(1+ \ldots .\right.\right.\right.$$

$$\ldots\ x^2\,\frac{(2k-1)B(2k)(k-1)}{(2k+1)B(2k-2)2k(2k-1)k} \qquad (A32.19)$$

where B(k) is the k^{th} Bernouilli Number.

By integrating both sides of the above we can obtain expressions for SUMC3 and SUMS4. Note that it is necessary to take about 7 terms in the above infinite products to obtain sufficient accuracy.

For reference the Bernouilli numbers are:

B(0) = 1	B(10) = 5/66
B(2) = 1/6	B(12) = -691/2730
B(4) = -1/30	B(14) = 7/6
B(6) = 1/42	B(16) = -3617/510
B(8) = -1/30	B(18) = 43867/798

$$SUMS2 = xLn(x) - x\left\{ 1+\frac{x^2}{72} \left\{ 1 +\frac{x^2}{200} \left\{ 1 +\frac{5x^2}{441} \ldots \right.\right.\right. \qquad (A32.20)$$

$$SUMC3 = SN3 +\frac{x^2}{2} \left\{ Ln(x) - \frac{3}{2} \left\{ 1+ \frac{x^2}{216} \left\{1+ \frac{x^2}{300} \ldots \right.\right.\right. \qquad (A32.21)$$

$$SUMS4 = x \left\{SN3+\frac{x^2}{6} \left\{ Ln(x)- \frac{11}{6} - \frac{x^2}{240} \left\{1+ \frac{5x^2}{2100} \ldots \right.\right.\right. \qquad (A32.22)$$

The valus of the multipliers in the above series are as follows:

For SUMS2:

1/72 1/200 5/441 7/480 2/121 7601/425880

For SUMC3:

1/300 15/1764 7/600 10/726 7601/496860

For SUMS4:

5/2100 21/2200 5/429

Substituting back we obtain:

$$\sum \frac{\bar{S}_n}{n} = \text{Coeff} \left\{ S_1 + \frac{(1 - 4p\bar{x}^2)}{8x_1} S_2 \right. \qquad \text{(A32.23)}$$

$$\left. + \frac{(1 - 4p\bar{x}^2)}{8x_2} S_3 \frac{(1 - 4p\bar{x}^2)(1 - 4p\bar{x}^2)}{64\ x_1 x_2} S_4 \right\}$$

where coeff $= \dfrac{2}{\pi\sqrt{(x_1 x_2)}}$

We can use the above result for calculation the asymptotic sums for the expression 3.2 in the evaluation of uniform microstrip mode parameters. In this case we have from eqn 2.56:

$$x_1 = x_2 = \frac{\pi w}{2a} \qquad \text{(A32.24)}$$

$$b_1 = b_2 = \frac{\pi(a + 2 * offset)}{2a} \qquad \text{(A32.25)}$$

Asymptotic values for the inner products of fields

We use the result to improve the accuracy of the calculation of the inner products described in section 3.3. We restrict ourselves to the case of a microstrip step discontinuity of the type shown in Fig. 4.1 where the strips in regions (1) and (2) have widths and offsets of w_1 w_2 $offset_1$ and $offset_2$ respectively.

The results are valid for any real values of p and q. They are therefore applicable to the case where we are calculating overlap integrals between two microstrip modes such as the mode matching method and the variational method of Chapter 4 when the basis functions are chosen to be microstrip modes.

For the case of variational methods when we choose basis functions with a different singularity at the edge, since the Fourier transform of such a function contains fractional order Bessel functions, the required summation is obtained by replacing the denominator of equation A32.1 by $n^{2+s1+s2}$ where s1 and s2 are the edge singularities for the two sets of basis functions. p1 and p2 then take the values k+0.5-s1 k+0.5-s2 respectively where k is an integer.

This means that in place of A32.10 - A32.15 the powers of n will be fractional and closed form results corresponding to A32.16 etc. are not available. They can, however, easily be evaluated on the computer.

We have, from equations 3.13 and 3.14, for large values of n:

$$P = -1/2\alpha_n$$

$$Q = 1/2\alpha_n$$

In addition for microstrip we have for large n:

$$E_x(n) = SM_{xx}J_x(n) + SM_{xz}J_z(n)$$

$$H_y(n) = SM_{yz}J_z(n)$$

$$H_x^+(n) = H_x^-(n)$$

$$E_y^+(n) = E_y^-(n)$$

$$SM_{xz} = -\beta/(1+\epsilon_r)$$

$$SM_{xx} = -1/(1+\epsilon_r)$$

$$SM_{yz} = -1/2$$

J_{ij} is the i directed current in region j

The n^{th} term of 3.14 then becomes:

$$a^2 E_{xn} H_{yn}/n\pi$$

$$= a^2(SM_{xz}J_{z1}+SM_{xx}J_{x1})(SM_{yz}J_{z2})/n\pi$$

the error is of the order $1/n^2$

Also for large n the current basis functions can be approximated by making use of the asymptotic limit for Bessel functions given in equation A32.2.

$$\bar{I}_{i,j} = \mathrm{Sin}\left\{\alpha_n \frac{a + \mathrm{offset}}{2a} + \frac{p}{2}\right\}\sqrt{\frac{4a}{n\pi^2 w_1}}\,\mathrm{Cos}\left\{\frac{\alpha_n w_1}{2} - (2p+1)\frac{\pi}{4}\right\}$$

where p is the order of the Bessel function contained by the Fourier transform of the current $I_{i,j}$.

If we denote the sum given by equation A32.1 by:

$$SS(b_1, b_2, p_1, p_2, x_1, x_2)$$

then the asymptotic sum of equation 3.14 is given by:

$$SM_{x2}SM_{y2}\sum_{p}\sum_{q} Z_{p1}Z_{q2}SS(b_1, b_2, p, q, x_1, x_2)$$

$$+\ SM_{x1}SM_{y2}\sum_{p}\sum_{q} X_{p1}Z_{q2}SS(b_1, b_2, p+1, q, x_1, x_2)$$

where p and q range over the orders of the Bessel functions contained by the Fourier transform of the current I.

$$b_1 = \frac{\pi(a + offset_1)}{2a}$$

$$b_2 = \frac{\pi(a + offset_2)}{2a}$$

$$x_1 = \frac{\pi w_1}{2a}$$

$$x_2 = \frac{\pi w_2}{2a}$$

Z_{p1} is the p^{th} coefficient of the basis expansion of I_z in region i

X_{p1} is the p^{th} coefficient of the basis expansion of I_x in region i

The summations SS_{pq} depend on the geometry only and thus they can be calculated once at the start of the solution of a discontinuity problem and used for all the inner products which need to be evaluated.

The inner product becomes:

$$
\begin{aligned}
& a\Gamma \sum \Big\{ \quad E_{xn}H_{yn} \quad P(k_{n1}^{+}, k_{n2}^{+}, h) \\
& \qquad + E_{xn}H_{yn} \quad P(k_{n1}, k_{n2}, d) \\
& \qquad - \frac{SM_{xn}SM_{yn}}{\alpha_n} \\
& \qquad - E_{y\bar{n}}^{+}H_{x\bar{n}}^{+} \quad Q(k_{n1}^{+}, k_{n2}^{+}, h) \\
& \qquad - E_{y\bar{n}}^{-}H_{x\bar{n}}^{-} \quad Q(k_{n1}, k_{n2}, d) \Big\} \\
& + \quad SM_{x2}SM_{y2} \sum_{p} \sum_{q} Z_{p1}Z_{q2}SS(b_1, b_2, p, q, x_1, x_2) \\
& + \quad SM_{x1}SM_{y2} \sum_{p} \sum_{q} X_{p1}Z_{q2}SS(b_1, b_2, p+1, q, x_1, x_2)
\end{aligned}
$$

References

1. Boxed Microstrip Circuits - Annual Report 1983-1984
University of Bath

2. Collin "Field Theory of Guided Waves"
McGraw-Hill 1960

List of Figures

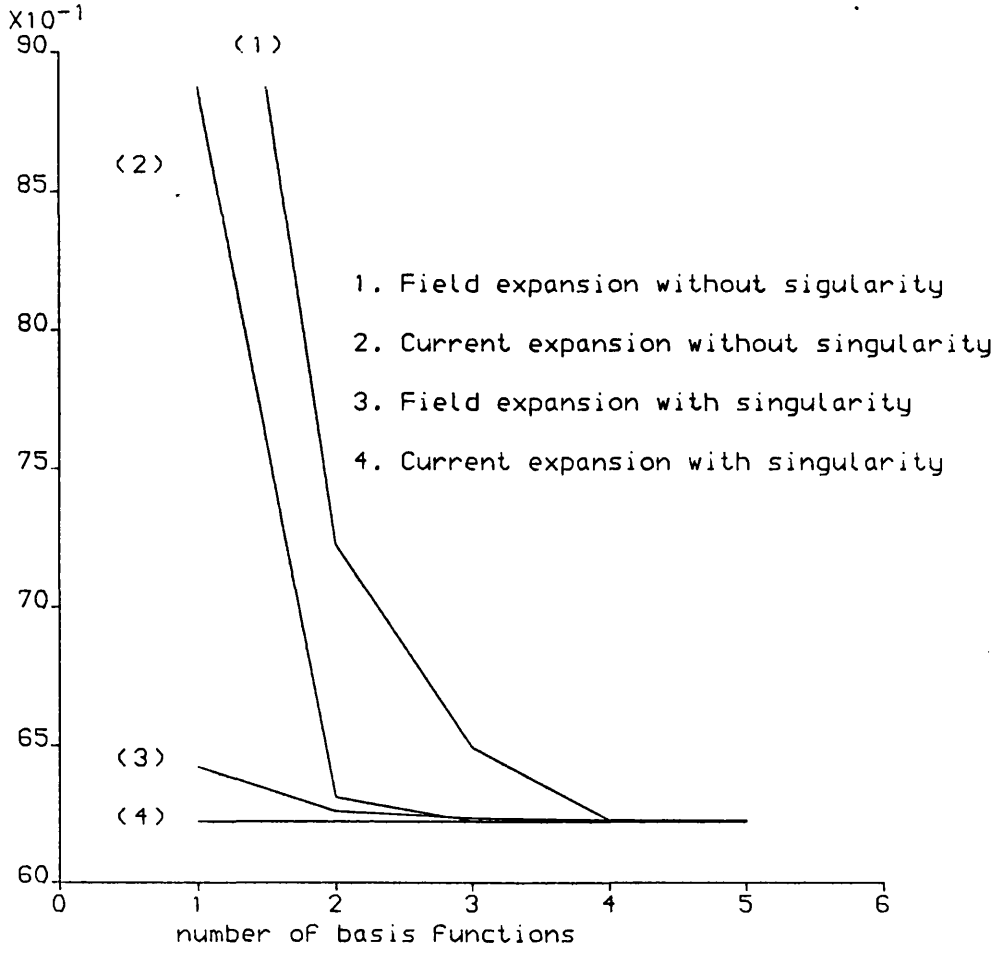

Fig. 3.1 - Convergence with various basis functions

Strip Width = 1.27mm

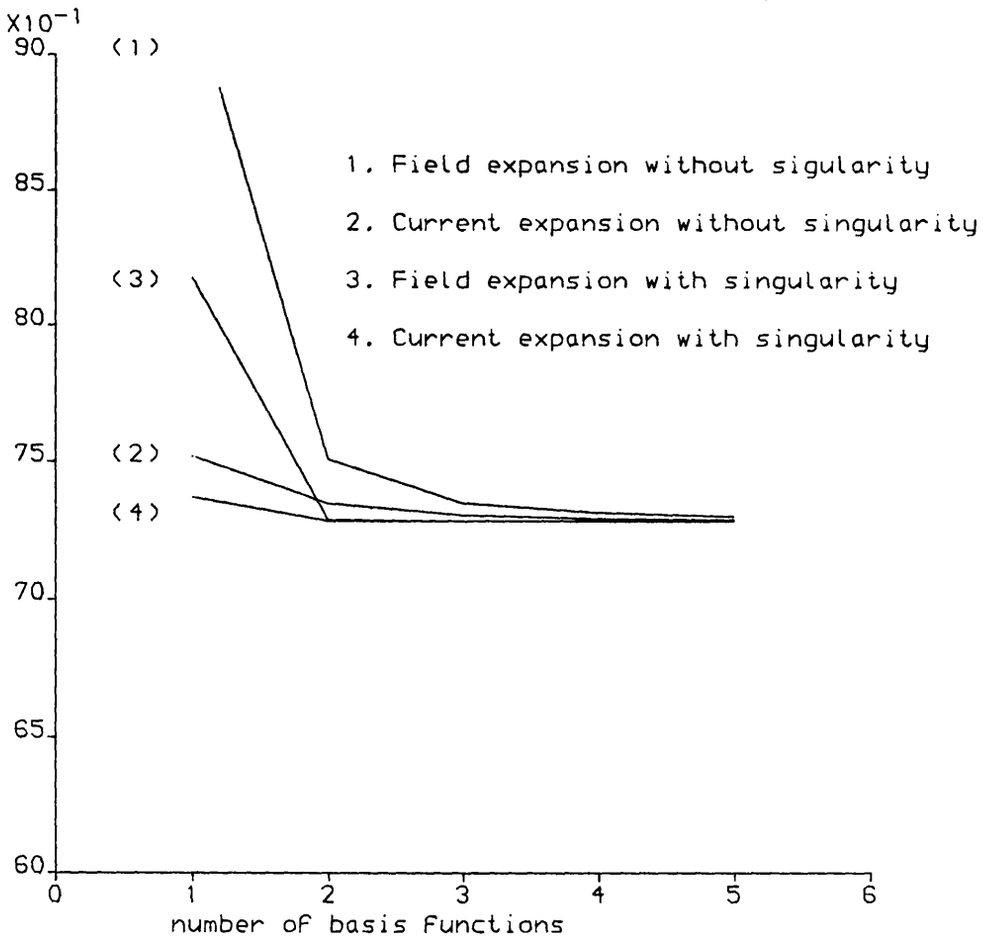

Fig. 3.2 - Convergence with various basis functions

Strip Width = 5.08mm

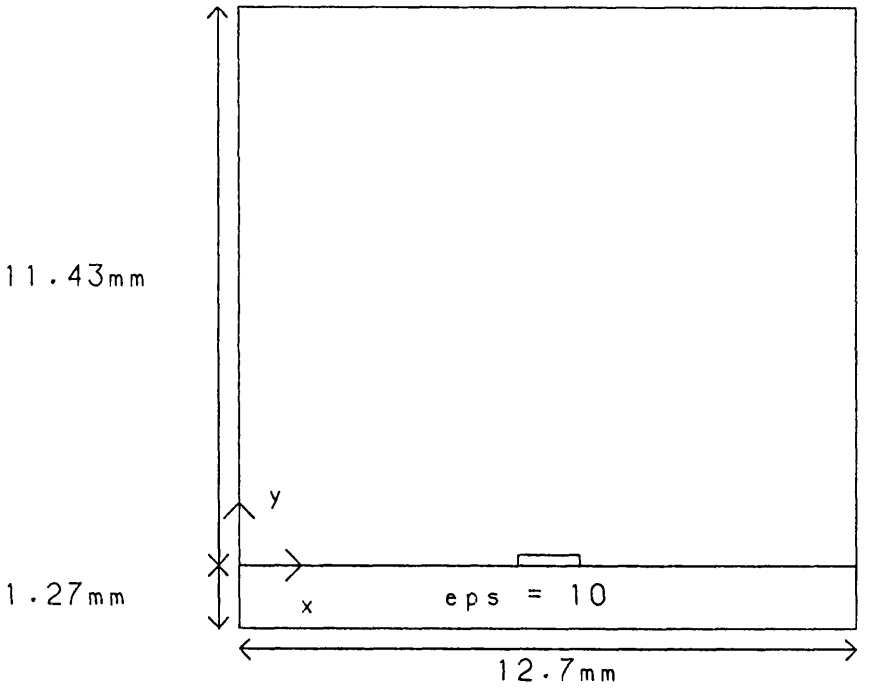

Fig. 3.3 - Microstrip cross section

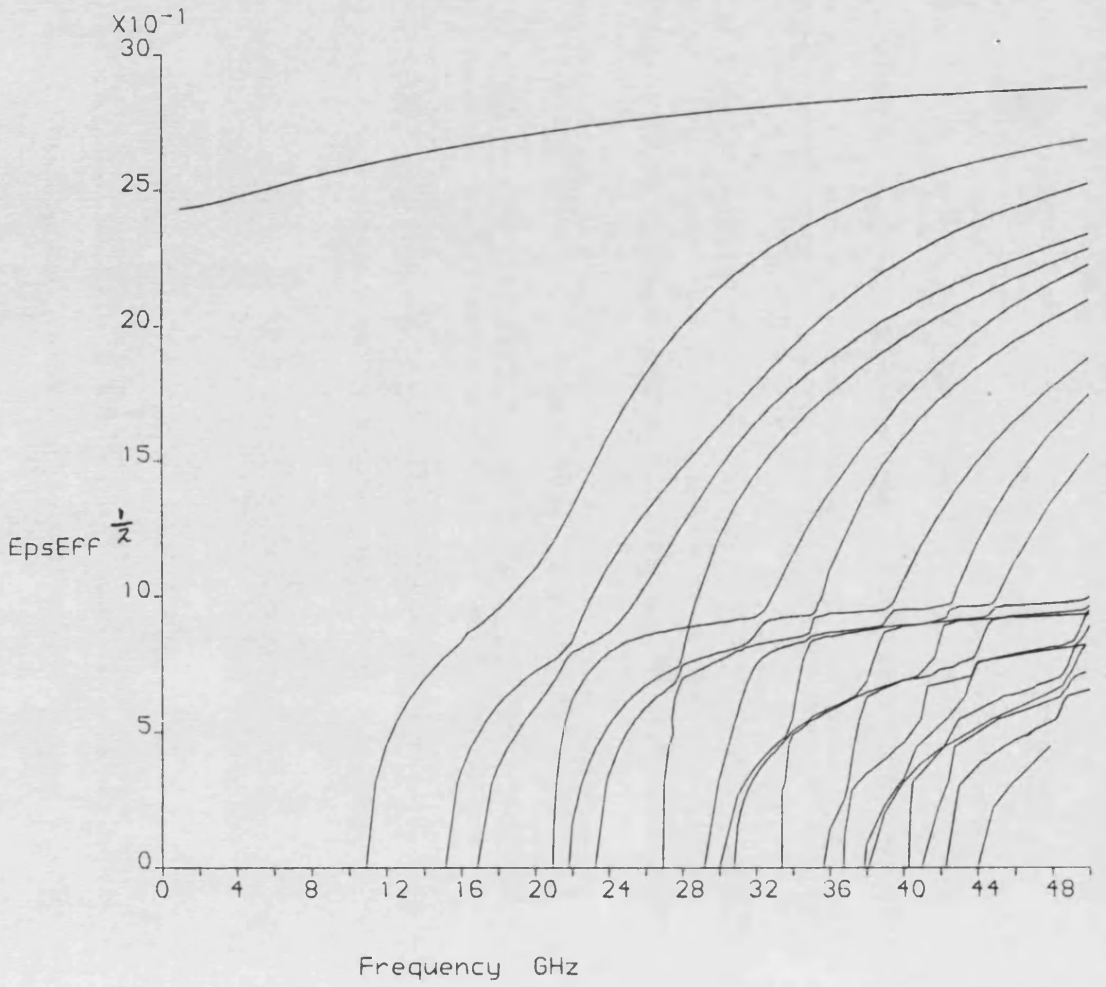

Fig. 3.4 - Higher order modes of microstrip
a=12.7mm d=1.27mm h=10.43mm w=1.27mm eps=8.875

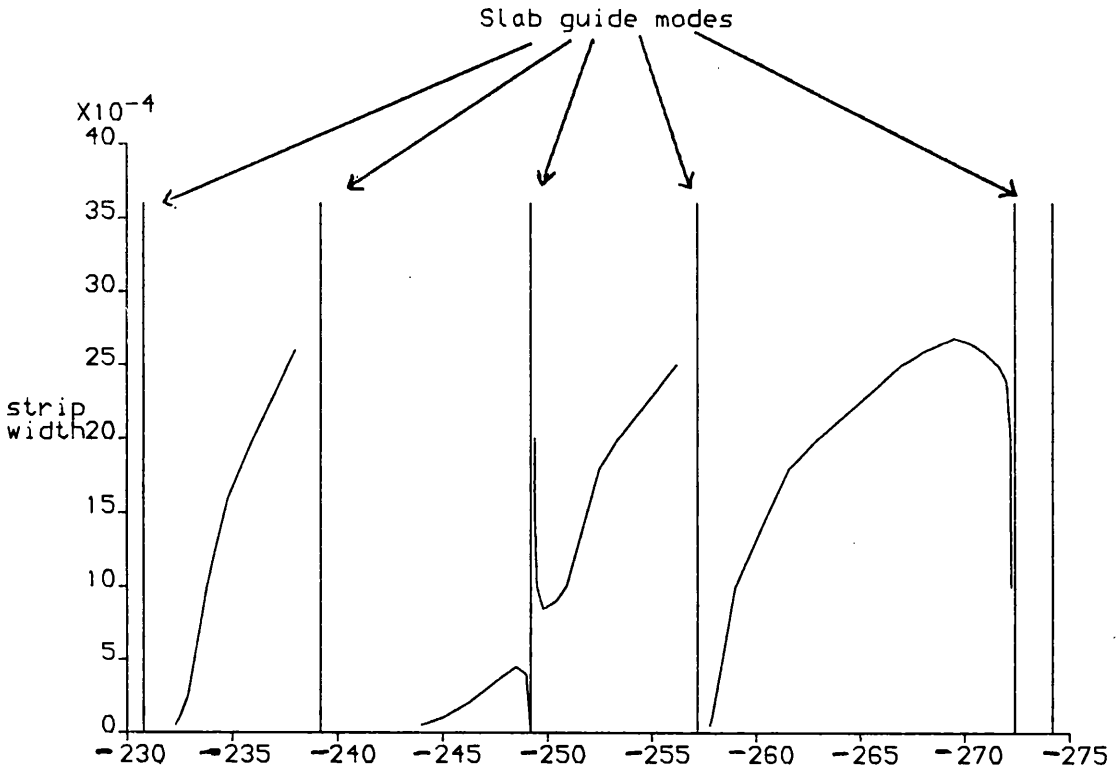

Fig. 3.5 - effective permittivity versus strip width

d=1.27mm h=11.43mm eps=8.875 a=12.7mm

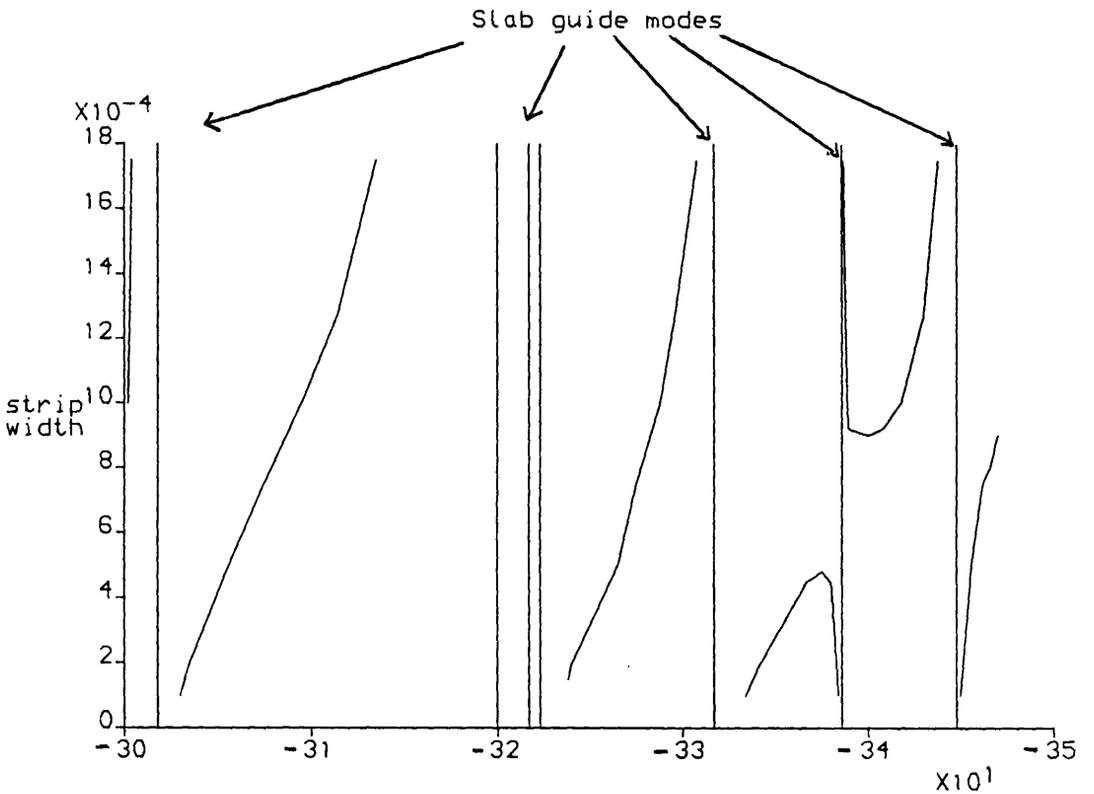

Fig. 3.6 - effective permittivity versus strip width

d=1.27mm h=11.43mm eps=8.875 a=12.7mm Freq = 6.5 - 8

Slab guide modes

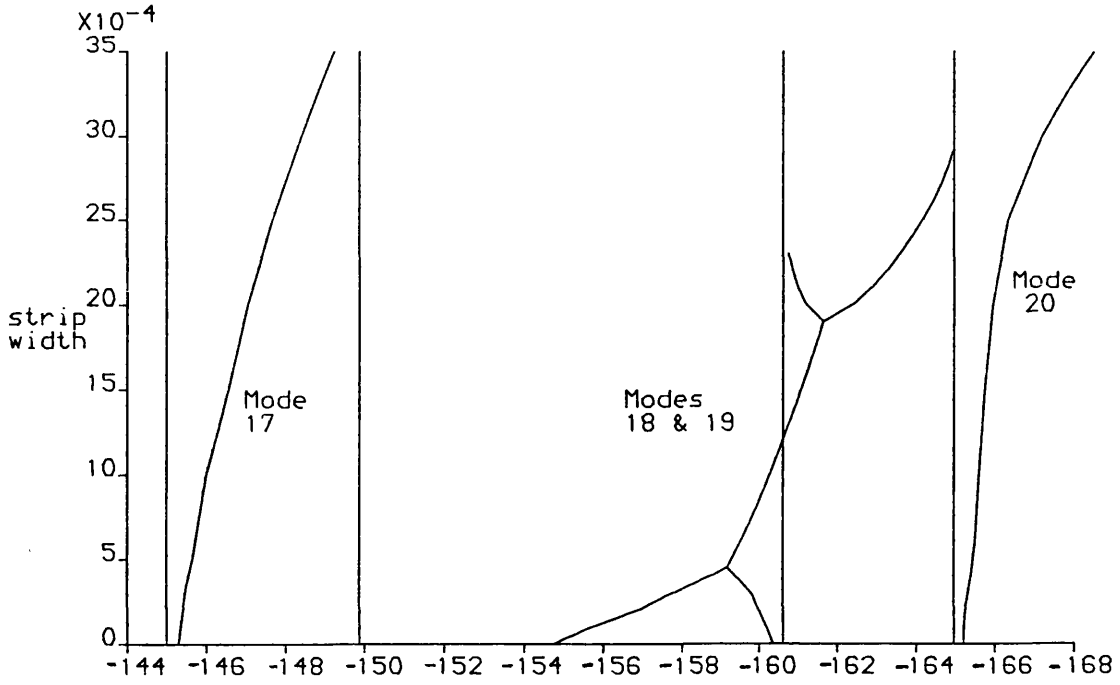

Fig. 3.7a - effective permittivity (real)

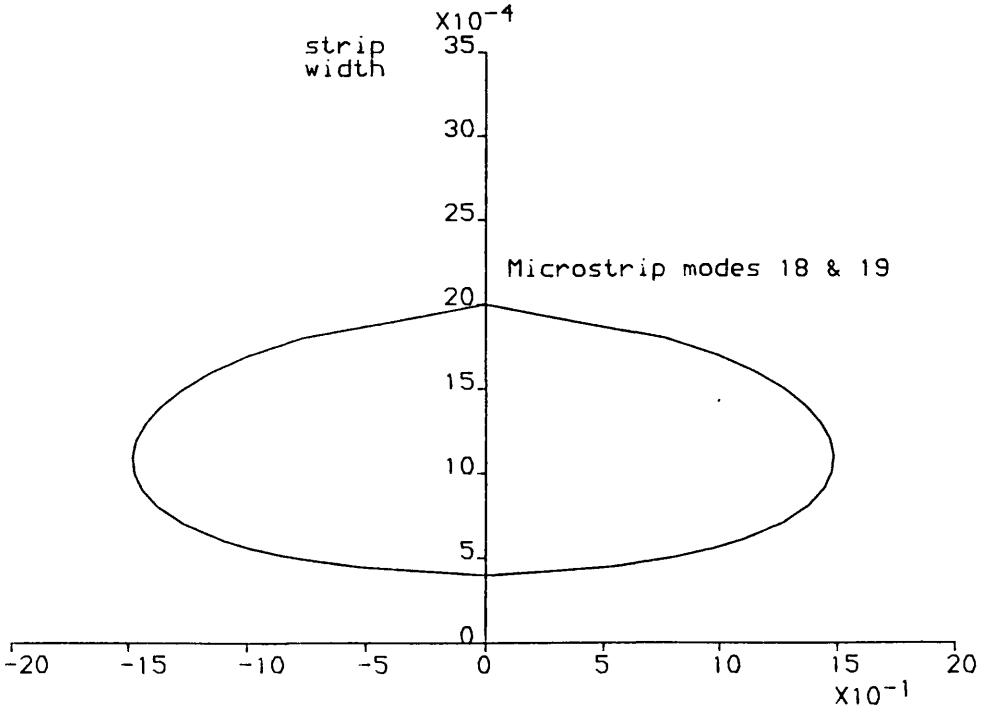

Fig. 3.7b - effective permittivity (imag)

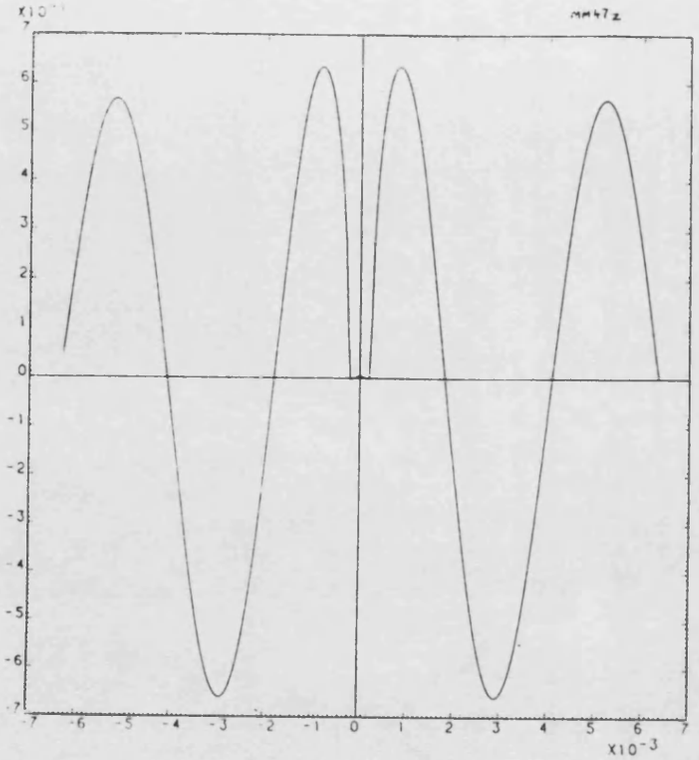

Box Width = 12.7 mm
Box Height = 12.7 mm
Strip Width = 0.47 mm
Strip Offset = 0
Dielectric Thickness = 1.27 mm
Dielectric Constant = 8.875
Frequency = 5 GHz
Effective Permittivity = -33?

PLOT of E_z versus X at Y = 0

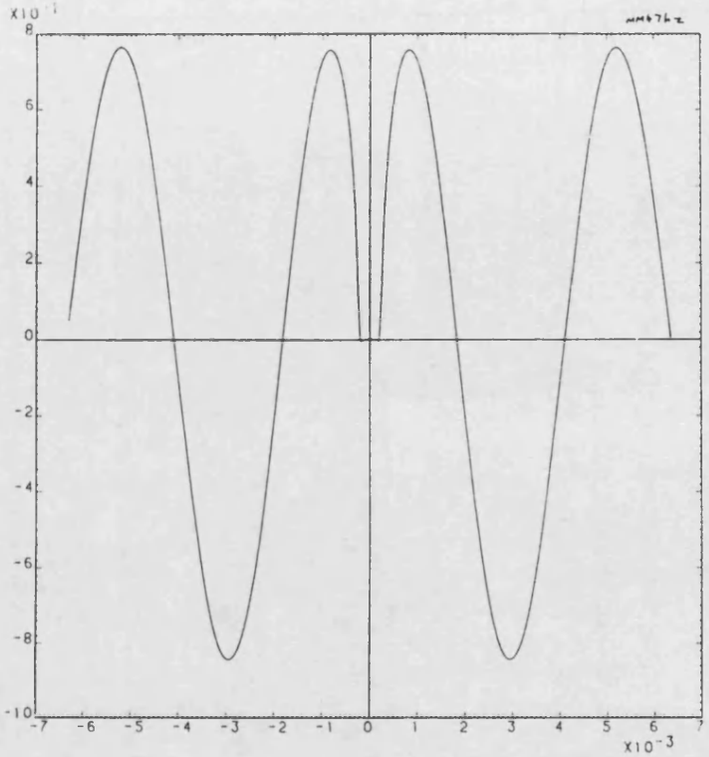

Box Width = 12.7 mm
Box Height = 12.7 mm
Strip Width = 0.47 mm
Strip Offset = 0
Dielectric Thickness = 1.27 mm
Dielectric Constant = 8.875
Frequency = 5 GHz
Effective Permittivity = -33?

PLOT of E_z versus X at Y = 0

Fig 3.8 - Plot of Ez versus x

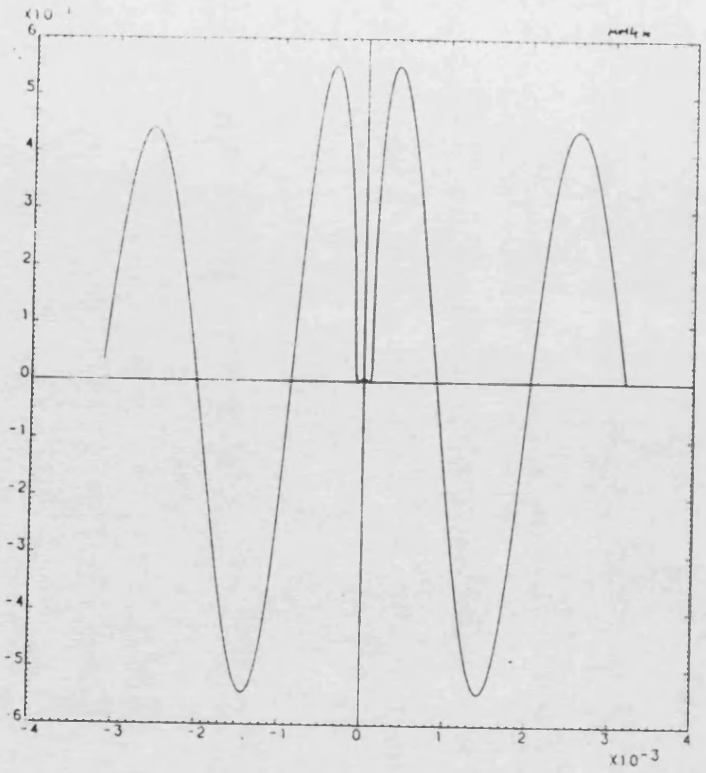

Box Width = 12.7 mm
Box Height = 12.7 mm
Strip Width = 0.4 mm
Strip Offset = 0
Dielectric Thickness = 1.27 mm
Dielectric Constant = 8.875
Frequency = 5 GHz
Effective Permittivity = -336.2

PLOT of E_z versus X at Y = 0

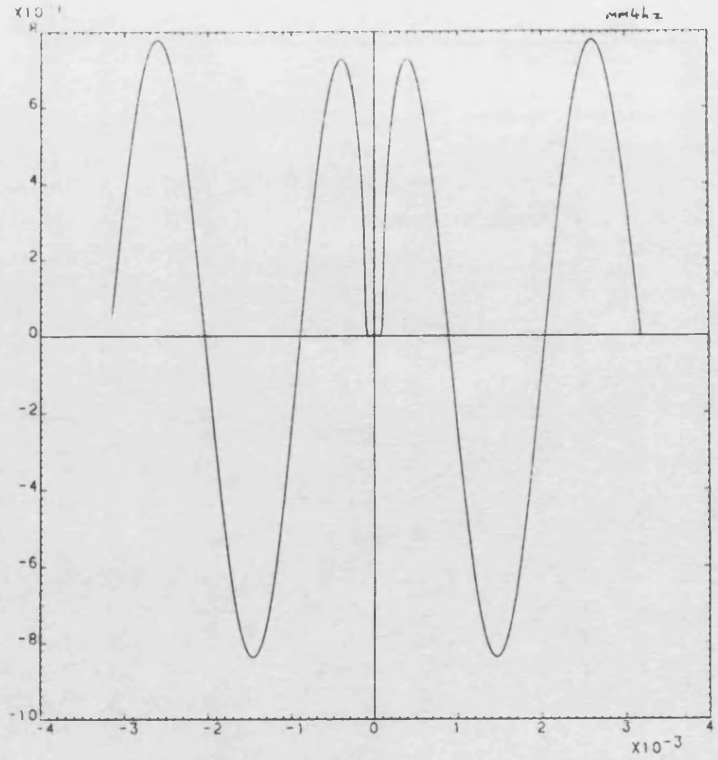

Box Width = 12.7 mm
Box Height = 12.7 mm
Strip Width = 0.4 mm
Strip Offset = 0
Dielectric Thickness = 1.27 mm
Dielectric Constant = 8.875
Frequency = 5 GHz
Effective Permittivity = -338.5

PLOT of E_z versus X at Y = 0

Fig 3.9 - Plot of Ez versus x

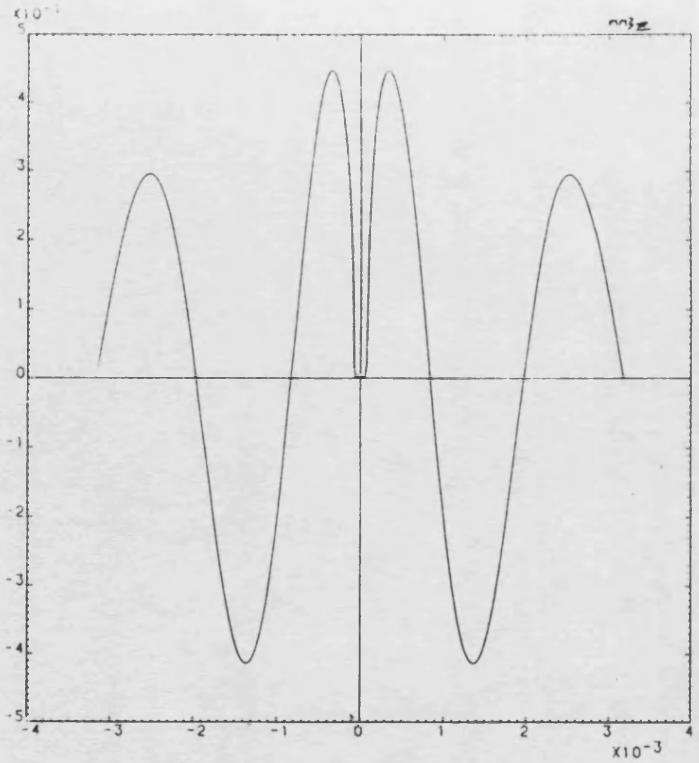

Box Width = 12.7 mm
Box Height = 12.7 mm
Strip Width = 0.3 mm
Strip Offset = 0
Dielectric Thickness = 1.27 mm
Dielectric Constant = 8.875
Frequency = 5 GHz
Effective Permittivity = -335.2

PLOT of E_z versus X at Y = 0

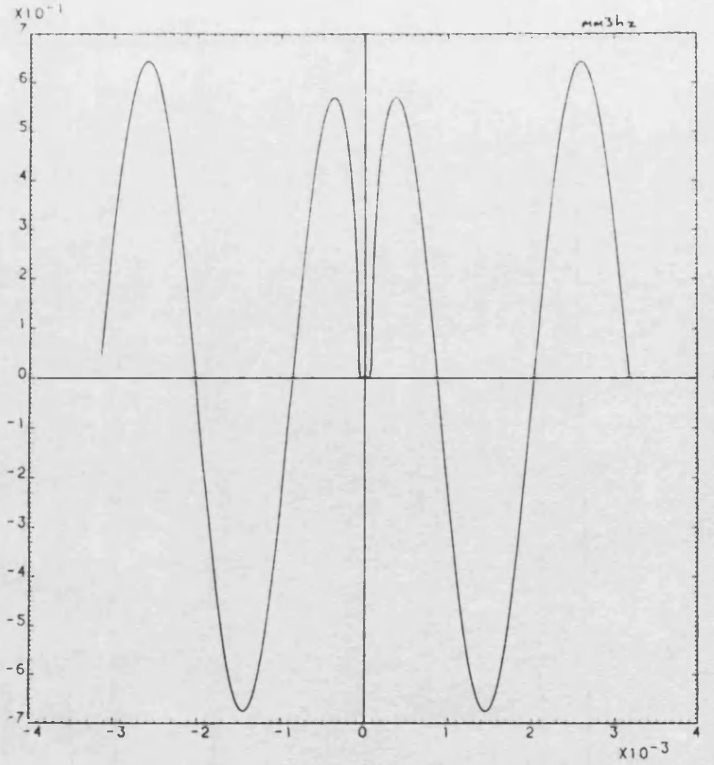

Box Width = 12.7 mm
Box Height = 12.7 mm
Strip Width = 0.3 mm
Strip Offset = 0
Dielectric Thickness = 1.27 mm
Dielectric Constant = 8.875
Frequency = 5 GHz
Effective Permittivity = -338.4

PLOT of E_z versus X at Y = 0

Fig 3.10 - Plot of Ez versus x

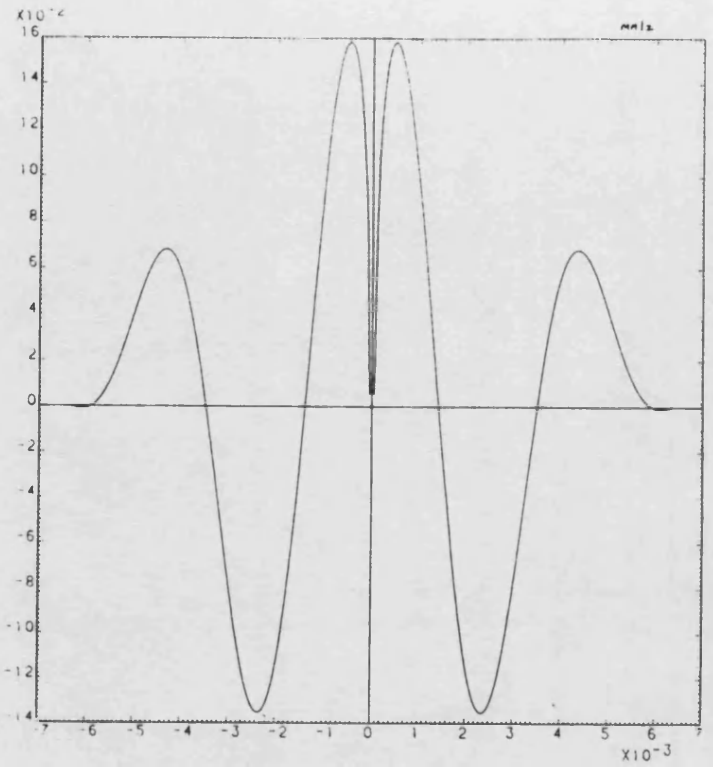

Box Width = 12.7 mm
Box Height = 12.7 mm
Strip Width = 0.1 mm
Strip Offset = 0
Dielectric Thickness = 1.27 mm
Dielectric Constant = 8.875
Frequency = 5 GHz
Effective Permittivity = -333.4

PLOT of E_z versus X at Y = 0

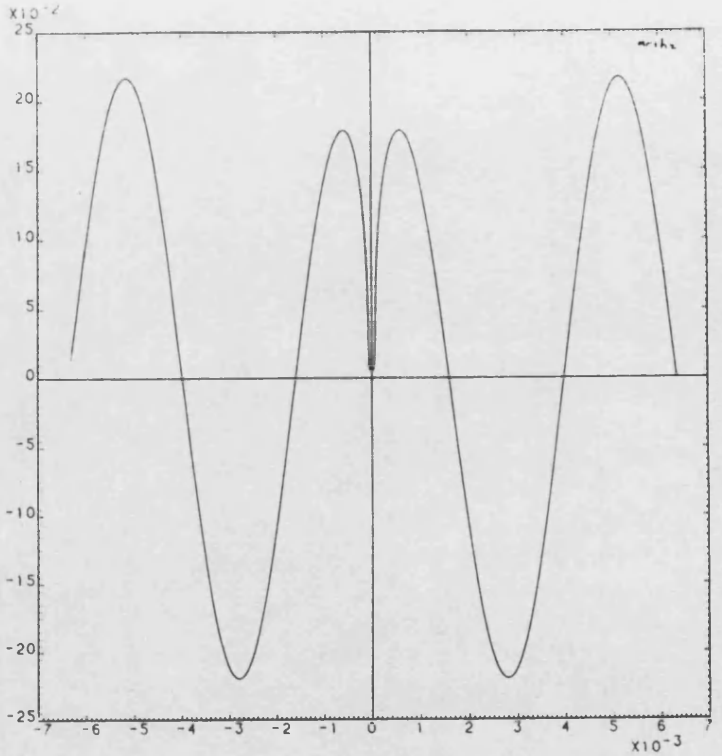

Box Width = 12.7 mm
Box Height = 12.7 mm
Strip Width = 0.1 mm
Strip Offset = 0
Dielectric Thickness = 1.27 mm
Dielectric Constant = 8.875
Frequency = 5 GHz
Effective Permittivity = -338.4

PLOT of E_z versus X at Y = 0

Fig 3.11 - Plot of Ez versus x

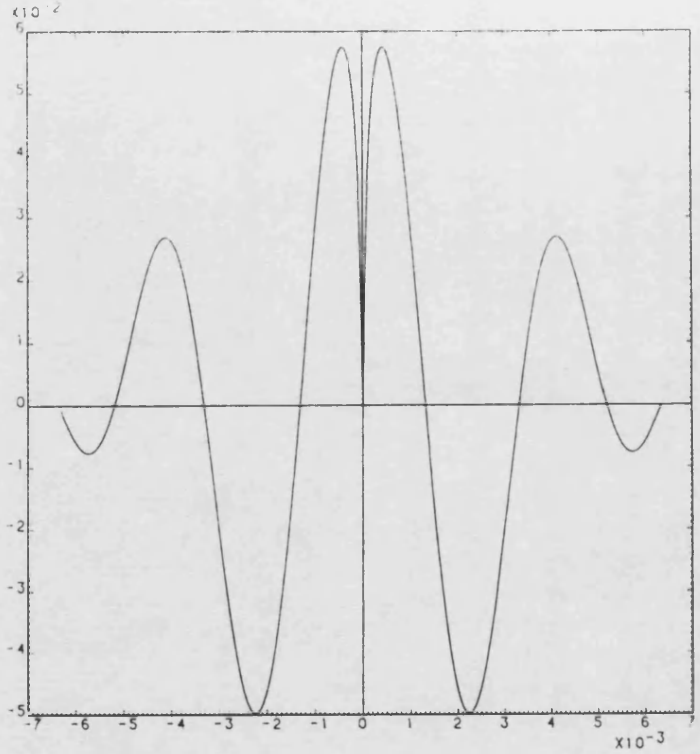

Box Width = 12.7 mm
Box Height = 12.7 mm
Strip Width = 0.05 mm
Strip Offset = 0
Dielectric Thickness = 1.27 mm
Dielectric Constant = 8.875
Frequency = 5 GHz
Effective Permittivity = -333

PLOT of E_z versus X at Y = 0

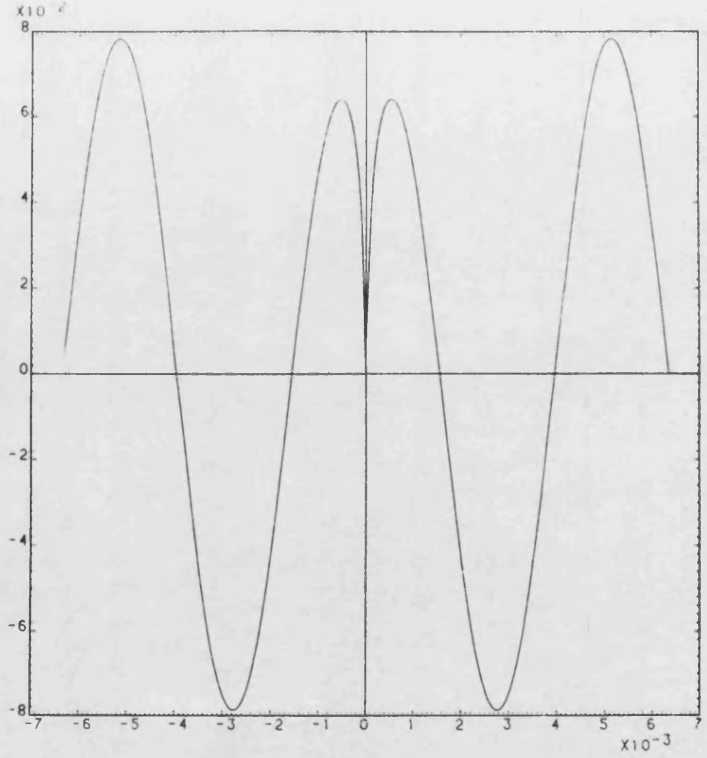

Box Width = 12.7 mm
Box Height = 12.7 mm
Strip Width = 0.05 mm
Strip Offset = 0
Dielectric Thickness = 1.27 mm
Dielectric Constant = 8.875
Frequency = 5 GHz
Effective Permittivity = -338.4

PLOT of E_z versus X at Y = 0

Fig 3.12 - Plot of Ez versus x

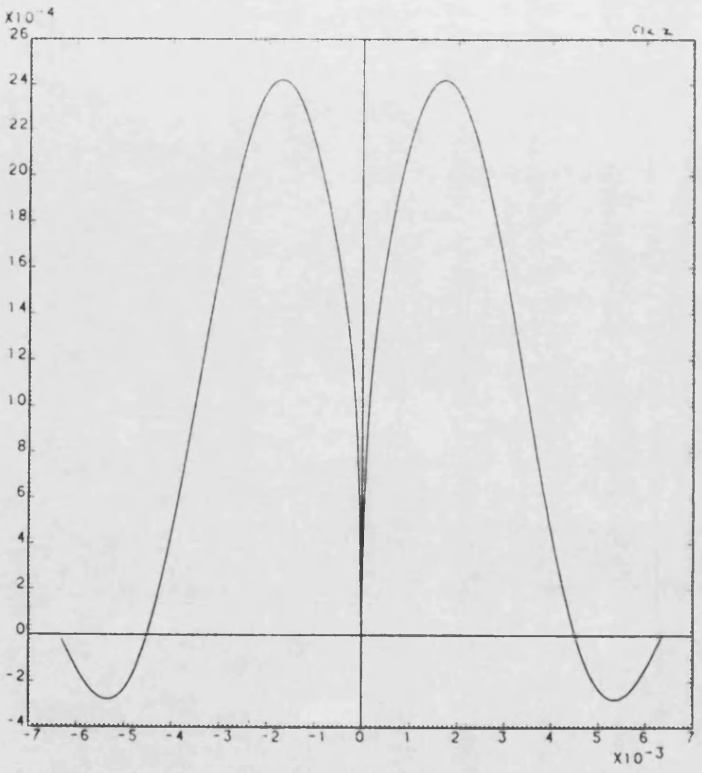

Box Width = 12.7mm
Box Height = 12.7mm
Strip Width = 0.05mm
Strip Offset = 0
Dielectric Thickness = 1.27mm
Dielectric Constant = 8.875
Frequency = 5GHz
Effective Permittivity = -257

Plot of Ez versus X at Y=0

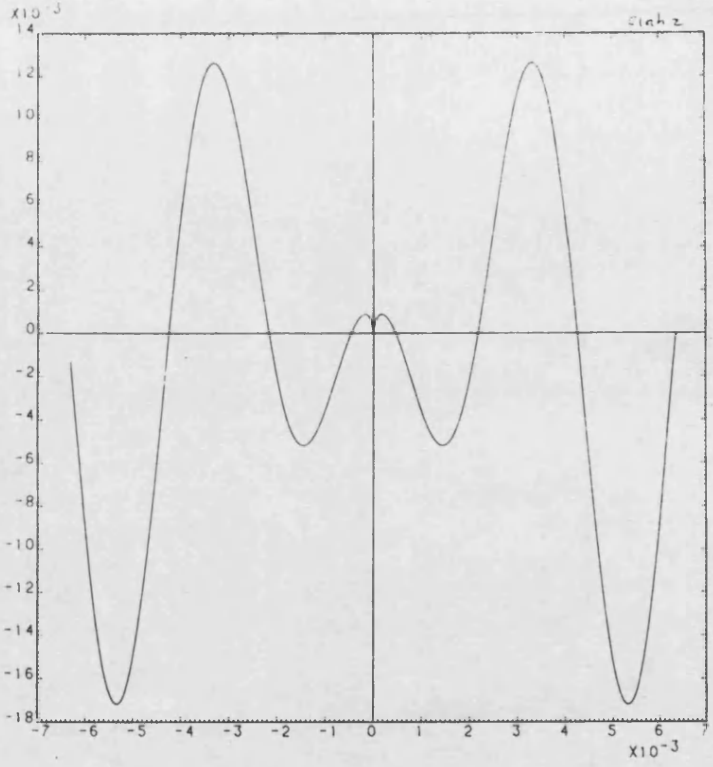

Box Width = 12.7mm
Box Height = 12.7mm
Strip Width = 0.05mm
Strip Offset = 0
Dielectric Thickness = 1.27mm
Dielectric Constant = 8.875
Frequency = 5GHz
Effective Permittivity = -273

Plot of Ez versus X at Y=0

Fig 3.13 - Plot of Ez versus x

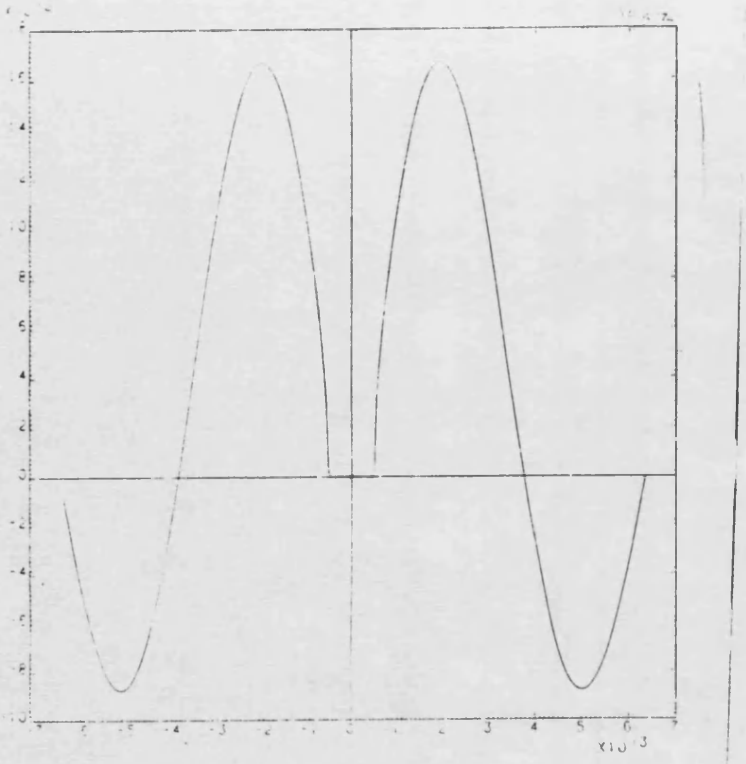

Box Width = 12.7mm
Box Height = 12.7mm
Strip Width = 1.27mm
Strip Offset = 0
Dielectric Thickness = 1.27mm
Dielectric Constant = 8.875
Frequency = 5GHz
Effective Permittivity = -260

Plot of Ez versus X at Y=0

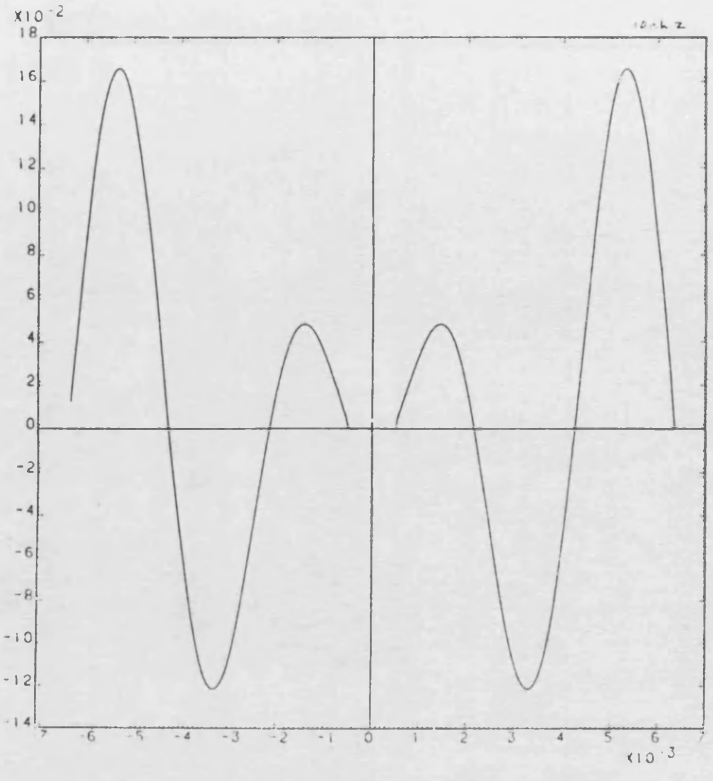

Box Width = 12.7mm
Box Height = 12.7mm
Strip Width = 1.27mm
Strip Offset = 0
Dielectric Thickness = 1.27mm
Dielectric Constant = 8.875
Frequency = 5GHz
Effective Permittivity = -273

Plot of Ez versus X at Y=0

Fig 3.14 - Plot of Ez versus x

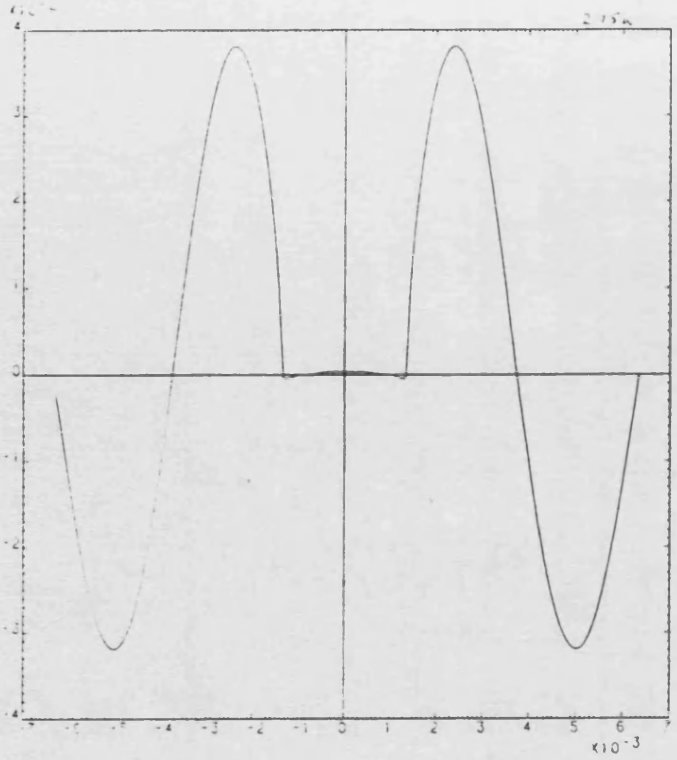

Box Width = 12.7mm
Box Height = 12.7mm
Strip Width = 2.7mm
Strip Offset = 0
Dielectric Thickness = 1.27mm
Dielectric Constant = 8.875
Frequency = 5GHz
Effective Permittivity = -270

Plot of Ez versus X at Y=0

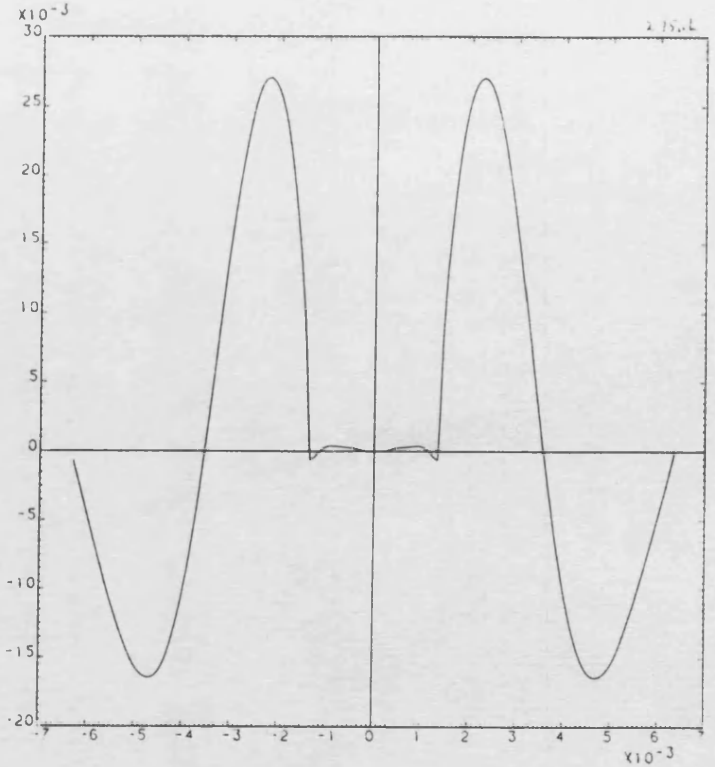

Box Width = 12.7mm
Box Height = 12.7mm
Strip Width = 2.7mm
Strip Offset = 0
Dielectric Thickness = 1.27mm
Dielectric Constant = 8.875
Frequency = 5GHz
Effective Permittivity = -270

Plot of Ez versus X at Y=0

Fig 3.15 - Plot of Ez versus x

Fig 3.16 - Isometric projection of E field in box cross-section

Fig 3.17 - Isometric projection of E field in box cross-section

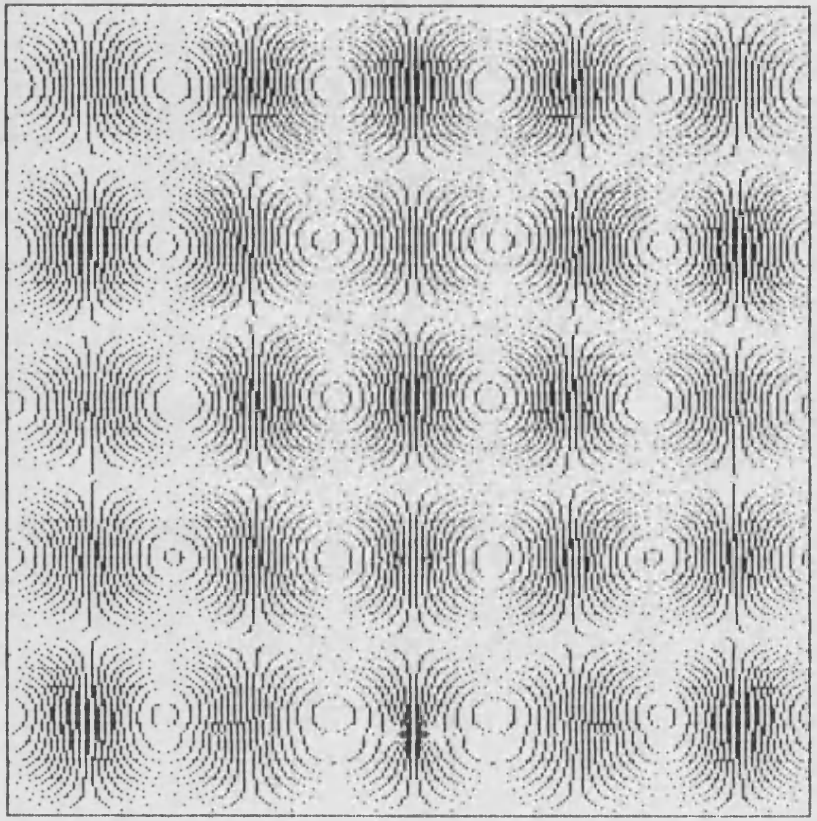

X directed E field
Frequency = 5.0 Strip width = 0.050 mm EpsEff = -277.22d397

Fig 3.18 - Contour plot of E field in box cross-section

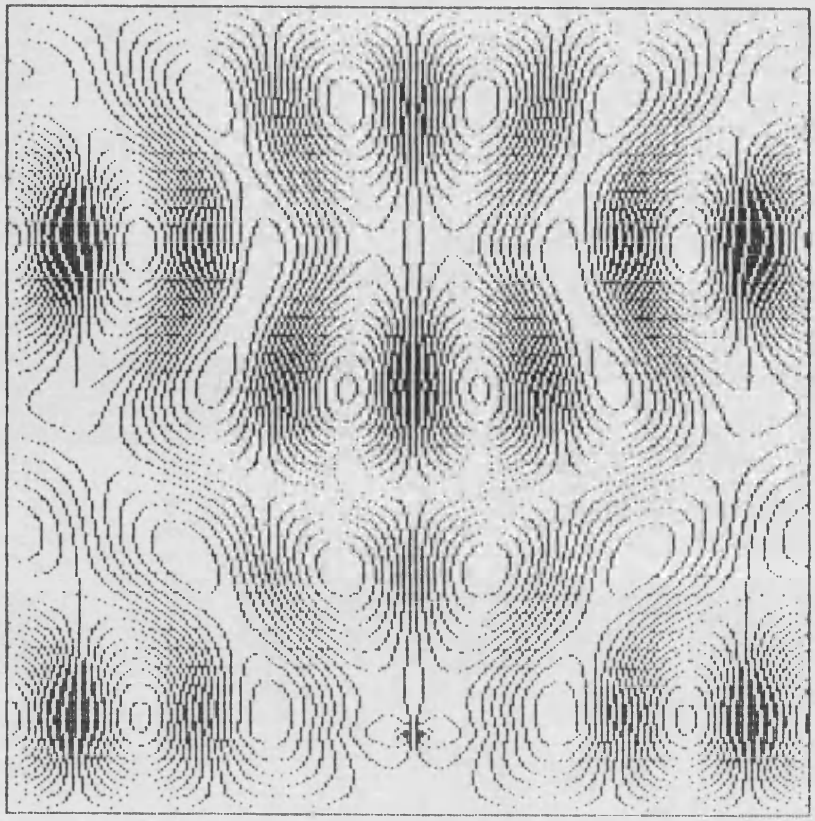

X directed E field
Frequency = 5.0 Strip width = 0.050 mm EpsEff = -278.233003

Fig 3.19 - Contour plot of E field in box cross-section

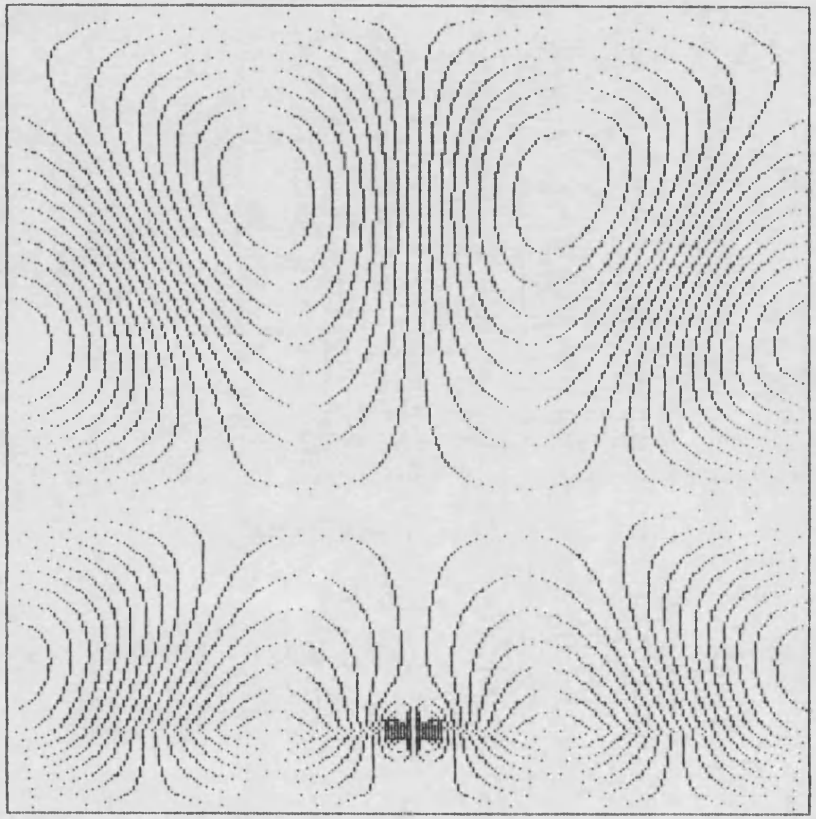

X directed E field
Frequency = 5.0 Strip width = 0.050 mm EpsEff = -55.808753

Fig 3.20 - Contour plot of E field in box cross-section

X directed E field
Frequency = 5.0 Strip width = 0.050 mm EpsEff = -54.557371

Fig 3.21 - Contour plot of E field in box cross-section

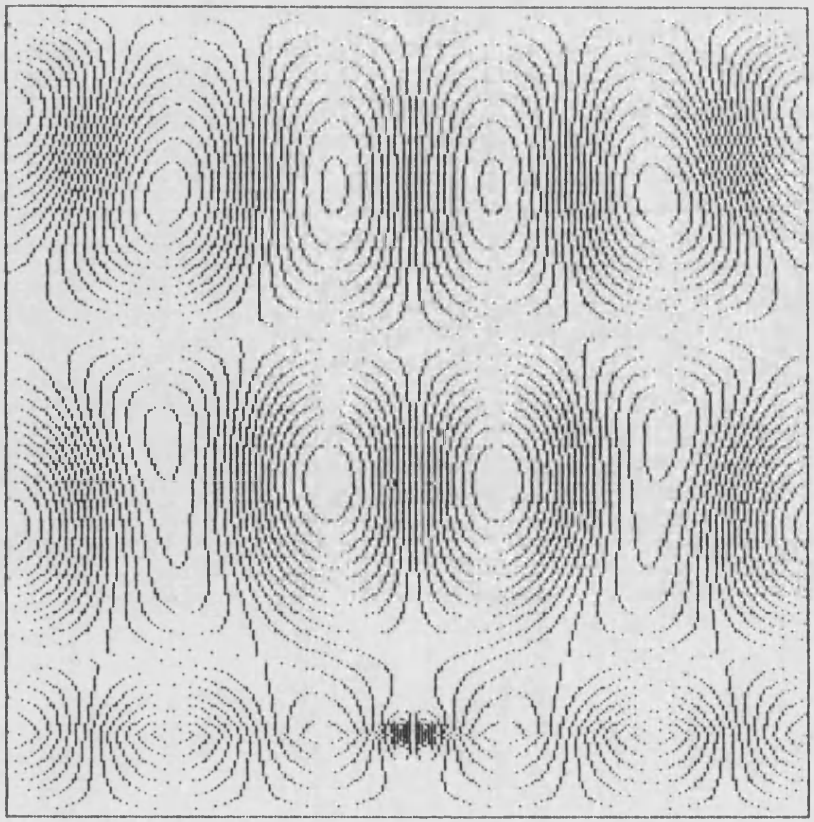

X directed E field
Frequency = 5.0 Strip width = 0.050 mm EpsEff = -165.229415

Fig 3.22 - Contour plot of E field in box cross-section

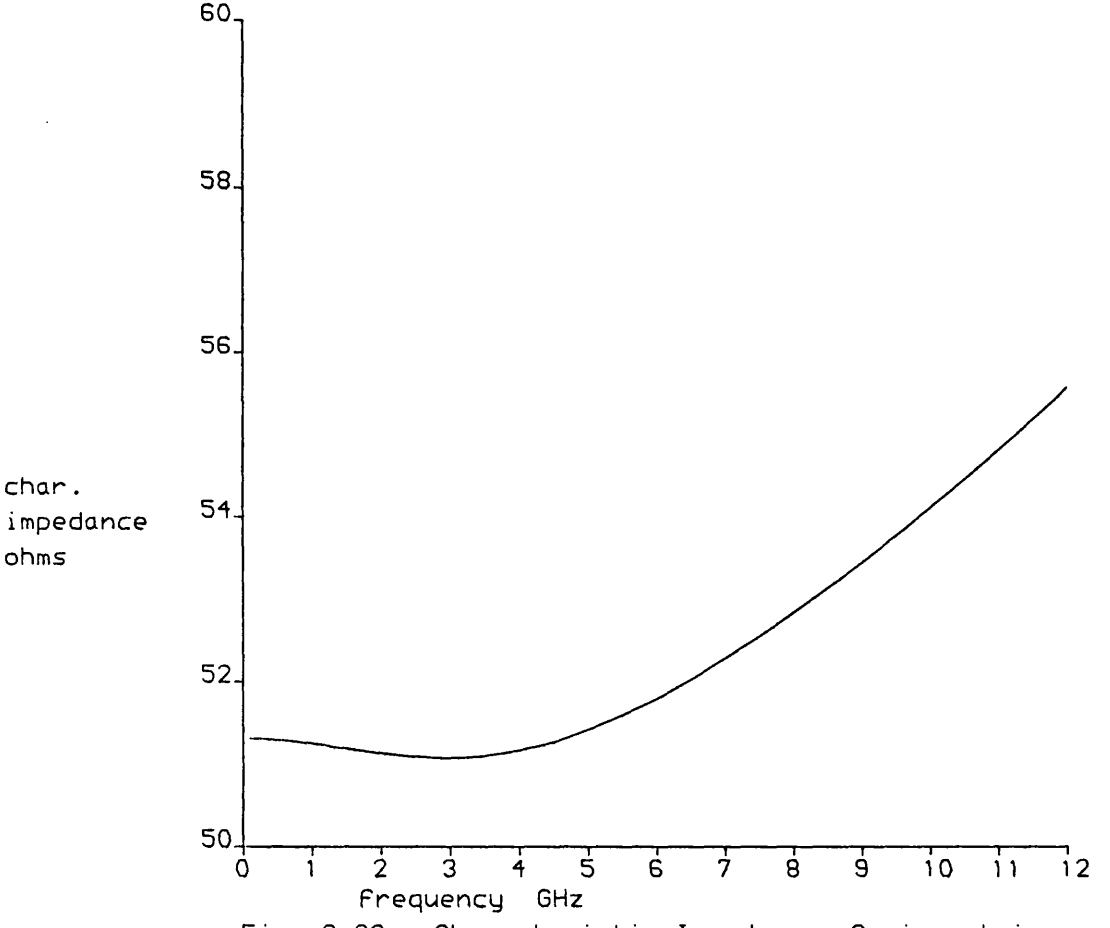

Fig. 3.23 - Characteristic Impedance of microstrip
a=12.7mm d=1.27mm h=10.43mm w=1.27mm eps=8.875

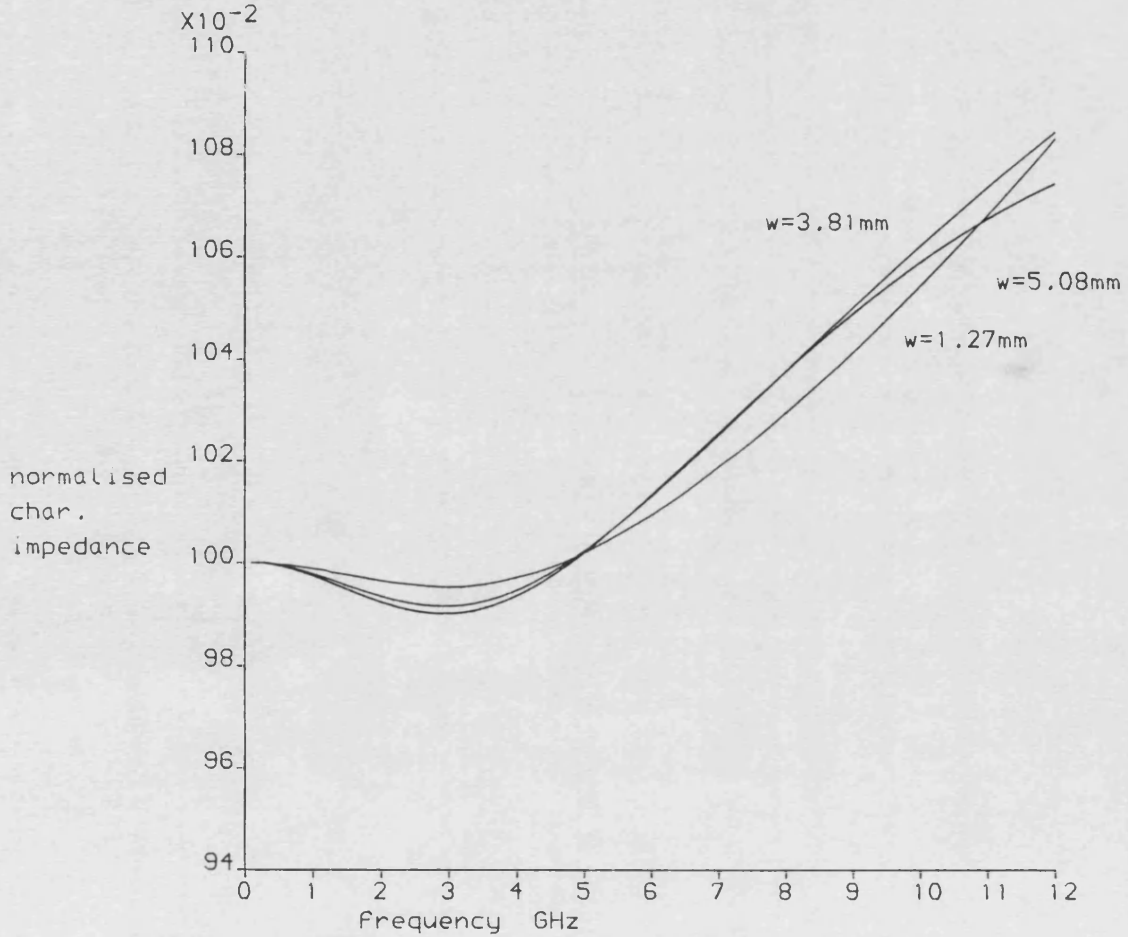

Fig 3.24 - Normalised char. imp. of microstrip
a=12.7mm d=1.27mm h=10.43mm eps=8.875

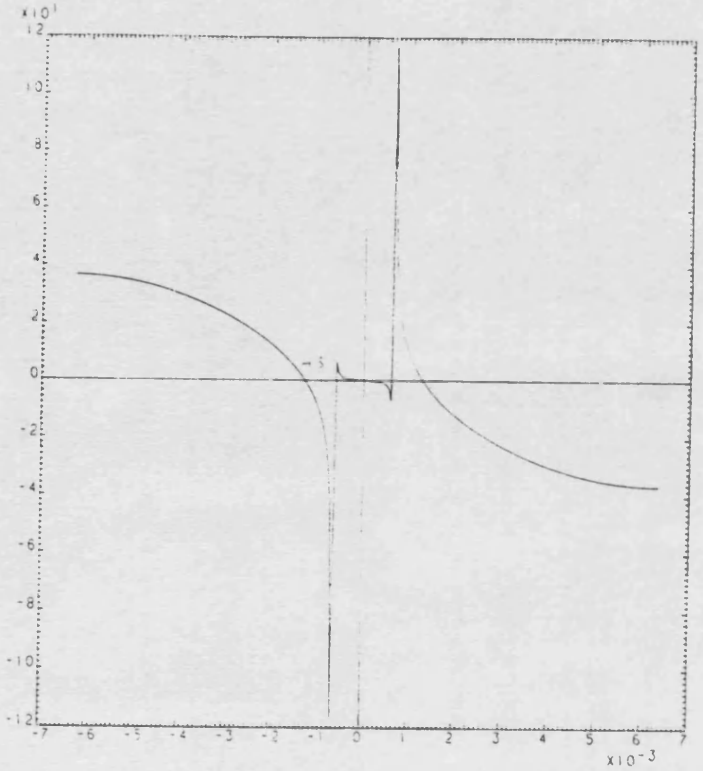

Fig 3.27 - Field pattern of mode 5 at 10 GHz

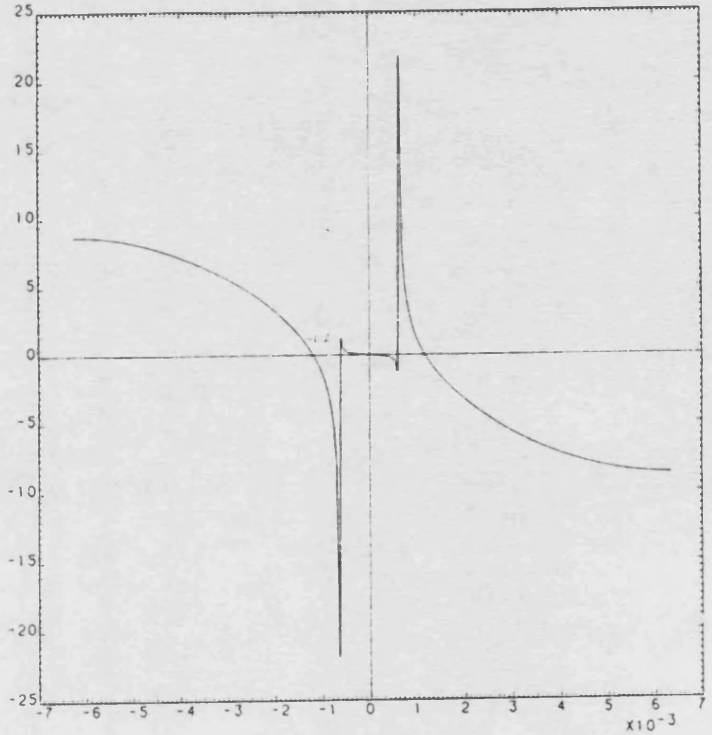

Fig 3.28 - Field pattern of mode 5 at 15 GHz

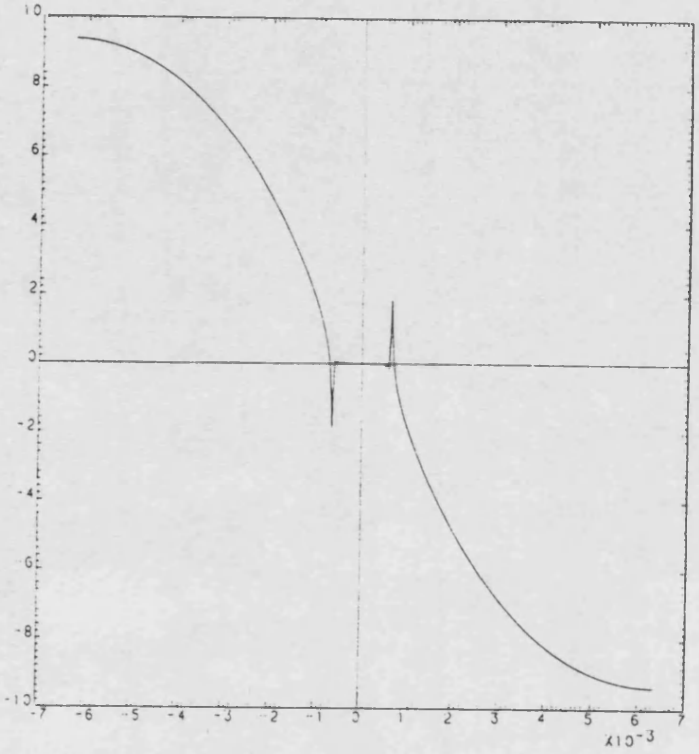

Fig 3.25 - Field pattern of mode 5 at 1 GHz

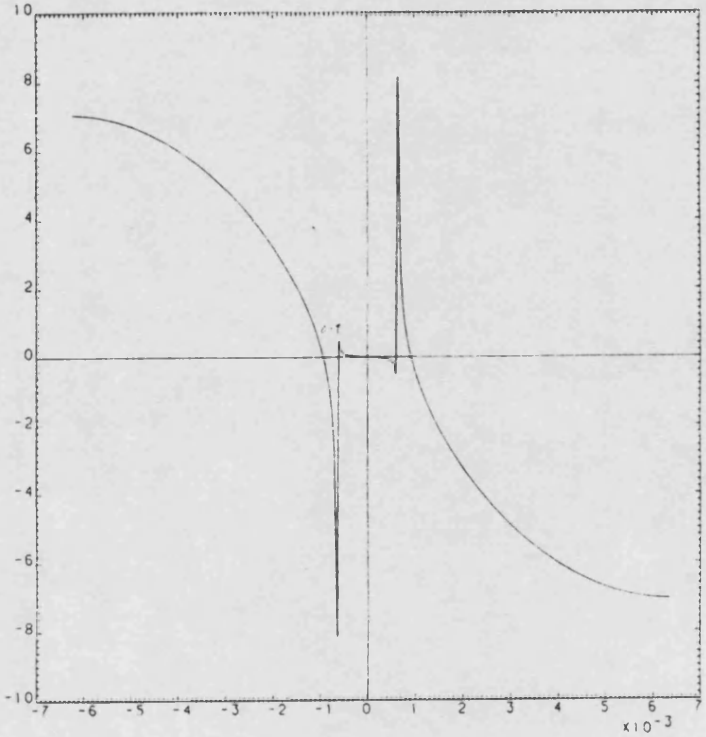

Fig 3.26 - Field pattern of mode 5 at 5 GHz

	1	2	3	4	5	6	7	8	9	10	11	12
1	1	4e-4	3e-4	6e-4	1e-4	5e-4	2e-4	4e-4	5e-4	1e-3	2e-4	1e-4
2	2e-4	1	2e-5	4e-5	7e-6	3e-5	1e-5	3e-5	3e-5	8e-5	1e-5	1e-5
3	2e-4	2e-5	1	3e-5	6e-6	2e-5	1e-5	2e-5	3e-5	6e-5	8e-6	8e-6
4	2e-3	2e-4	1e-4	1	5e-5	2e-4	9e-5	2e-4	2e-4	5e-4	7e-5	6e-5
5	2e-4	2e-5	2e-5	4e-5	1	3e-5	1e-5	3e-5	3e-5	7e-5	9e-6	9e-6
6	1e-4	1e-5	9e-6	2e-5	3e-6	1	7e-6	1e-5	2e-5	4e-5	5e-6	5e-6
7	5e-4	5e-5	4e-5	9e-5	2e-5	7e-5	1	7e-5	8e-5	2e-4	2e-5	2e-5
8	2e-5	2e-6	2e-6	4e-6	7e-7	3e-6	1e-6	1	4e-6	8e-6	1e-6	1e-6
9	2e-3	2e-4	2e-4	4e-4	7e-5	3e-4	1e-4	3e-4	1	8e-4	1e-4	1e-4
10	5e-5	5e-6	4e-6	8e-6	1e-6	7e-6	3e-6	6e-6	7e-6	1	2e-6	2e-6
11	3e-5	3e-6	2e-6	5e-6	9e-7	4e-6	2e-6	4e-6	4e-6	1e-5	1	1e-6
12	5e-4	5e-5	4e-5	9e-5	1e-5	7e-5	3e-5	6e-5	7e-5	2e-4	2e-5	1
13	1e-4	1e-5	1e-5	2e-5	4e-6	2e-5	8e-6	2e-5	2e-5	5e-5	6e-6	6e-6
14	2e-3	3e-4	2e-4	5e-4	8e-5	3e-4	1e-4	3e-4	4e-4	9e-4	1e-4	1e-4
15	1e-4	1e-5	9e-6	2e-5	3e-6	1e-5	7e-6	1e-5	2e-5	4e-5	5e-6	5e-6
16	7e-4	7e-5	5e-5	1e-4	2e-5	9e-5	4e-5	8e-5	1e-4	2e-4	3e-5	3e-5
17	2e-4	2e-5	2e-5	4e-5	7e-6	3e-5	1e-5	3e-5	4e-5	8e-5	1e-5	1e-5
18	5e-4	5e-5	4e-5	9e-5	2e-5	7e-5	3e-5	6e-5	7e-5	2e-4	2e-5	2e-5
19	9e-4	9e-5	7e-5	2e-4	3e-5	1e-4	5e-5	1e-4	1e-4	3e-4	4e-5	4e-5
20	7e-4	6e-5	5e-5	1e-4	2e-5	9e-5	4e-5	8e-5	9e-5	2e-4	3e-5	3e-5
21	5e-4	5e-5	4e-5	9e-5	1e-5	7e-5	3e-5	6e-5	7e-5	2e-4	2e-5	2e-5
22	2e-4	2e-5	2e-5	4e-5	7e-6	3e-5	1e-5	3e-5	3e-5	8e-5	1e-5	1e-5
23	4e-3	4e-5	3e-4	8e-4	1e-4	6e-4	2e-4	5e-4	6e-4	1e-3	2e-4	2e-4
24	5e-5	5e-6	4e-6	8e-6	1e-6	7e-6	3e-6	6e-6	7e-6	2e-5	2e-6	2e-6
25	5e-4	5e-5	4e-5	8e-5	1e-5	6e-5	3e-5	6e-5	7e-5	2e-4	2e-5	2e-5

Table 3.1. The modulus of the mode coupling integrals for the first 25 modes of microstrip. a = 34mm d=3.175mm b=34mm ϵ_r = 2.33 w = 4.2mm frequency = 3GHz.

	13	14	15	16	17	18	18	20	21	22	23	24	25
1	6e-4	4e-4	2e-3	5e-5	2e-3	2e-5	1e-4	3e-4	2e-5	2e-3	4e-4	5e-5	4e-3
2	4e-5	3e-5	1e-4	3e-6	1e-4	1e-6	9e-6	2e-5	1e-6	1e-6	2e-5	3e-6	2e-4
3	3e-5	2e-5	1e-4	2e-6	9e-5	1e-6	7e-6	1e-5	1e-6	8e-5	2e-5	3e-6	2e-4
4	3e-4	2e-4	8e-4	2e-5	7e-4	1e-5	6e-5	1e-4	8e-6	7e-4	2e-4	2e-5	2e-3
5	4e-5	3e-5	1e-4	3e-6	1e-4	1e-6	8e-6	2e-5	1e-6	1e-6	2e-5	3e-6	2e-4
6	2e-5	1e-5	6e-5	2e-6	6e-5	7e-7	4e-6	9e-6	6e-7	5e-5	1e-5	2e-6	1e-4
7	1e-4	7e-5	3e-4	7e-6	2e-4	3e-6	2e-5	4e-5	3e-6	2e-4	6e-5	8e-6	6e-4
8	4e-6	3e-6	1e-5	3e-7	1e-5	1e-7	9e-7	2e-6	1e-7	1e-5	2e-6	3e-7	3e-5
9	4e-4	3e-4	1e-3	3e-5	1e-3	1e-5	9e-5	2e-4	1e-5	1e-3	2e-4	3e-5	3e-3
10	9e-6	6e-6	3e-5	7e-7	2e-5	3e-7	2e-6	4e-6	3e-7	2e-5	5e-6	7e-7	5e-5
11	6e-6	4e-6	2e-5	4e-7	1e-5	2e-7	1e-6	2e-6	2e-7	1e-5	3e-6	4e-7	3e-5
12	9e-5	6e-5	3e-4	7e-6	2e-4	8e-4	3e-6	2e-5	4e-5	3e-6	2e-4	5e-5	5e-4
13	1	2e-5	7e-5	2e-6	6e-5	8e-7	5e-6	1e-5	7e-7	6e-5	1e-5	2e-6	1e-4
14	5e-4	1	1e-3	4e-5	1e-3	2e-5	1e-6	2e-4	1e-5	1e-3	3e-4	4e-5	3e-3
15	2e-5	1e-5	1	2e-6	6e-5	7e-7	4e-6	9e-6	6e-7	5e-5	1e-5	2e-6	1e-4
16	1e-4	8e-5	3e-4	1	3e-4	4e-6	2e-5	5e-5	3e-6	3e-4	7e-5	6e-6	7e-4
17	4e-5	3e-5	1e-4	3e-6	1	1e-6	9e-6	2e-5	1e-6	1e-4	2e-5	3e-6	3e-4
18	9e-5	6e-5	3e-4	7e-6	2e-4	1	2e-5	4e-5	3e-6	2e-4	5e-5	7e-6	5e-4
19	2e-4	1e-4	5e-4	1e-5	4e-4	6e-6	1	7e-5	5e-6	4e-4	9e-5	1e-5	1e-3
20	1e-4	8e-5	3e-4	8e-6	3e-4	4e-6	2e-5	1	3e-6	3e-4	7e-5	9e-6	7e-4
21	9e-5	6e-5	3e-4	6e-6	2e-4	3e-6	2e-5	4e-5	1	2e-4	5e-5	7e-6	5e-4
22	4e-5	3e-5	1e-4	3e-6	1e-4	1e-6	8e-6	2e-5	1e-6	1	2e-5	3e-6	2e-4
23	8e-4	5e-4	2e-3	6e-5	2e-3	3e-5	2e-4	3e-4	2e-5	2e-3	1	6e-5	4e-3
24	8e-6	6e-6	2e-5	6e-7	2e-5	3e-7	2e-6	4e-6	2e-7	2e-5	5e-6	1	5e-5
25	8e-5	6e-5	2e-4	6e-6	2e-4	3e-6	2e-5	4e-5	2e-6	2e-4	5e-5	7e-6	1

Table 3.1 continued. The modulus of the mode coupling integrals for the first 25 modes of microstrip. a = 34mm d=3.175mm b=34mm ϵ_r = 2.33 w = 4.2mm frequency = 3GHz.

Chapter 4

The Analysis of Microstrip Discontinuities

4.1. Introduction

In this chapter the results for the uniform microstrip, are used in a rigorous analysis of single step discontinuities and cascades of strongly coupled multiple step discontinuities in microstrip. Use is made of a variational formulation involving the expansion of the transverse E field at the step in terms of suitable basis functions. Strongly coupled steps are analysed making use of the concept of "localised" and "accessible" modes. Comparisons with other published formulations are made and the relative advantages and disadvantages of each are discussed.

4.2. Background

It is becoming increasingly important to be able to accurately predict the behaviour of microstrip circuits before manufacture. This is especially true in the design of microwave integrated circuits where adjustments after fabrication are very difficult or impossible to carry out.

The currently available methods for use in the computer aided design of microwave components, eg [1-2] rely heavily on quasi-static approximations which are only correct in the limit of low frequency and which suffer significant error as the frequency increases.

Cascades of step discontinuities constitute a basic configuration for the design of filters and impedance transformers, and it is to these in particular that this chapter is addressed. Methods by which a more accurate frequency dependent solution have previously been attempted includes the equivalent waveguide model eg. [3], the Transmission line matrix method eg [4], the Finite Element Method. The method of mode matching has been applied both directly to finline [5], microstrip [19] and also to the parallel plate waveguide model [6] although it is well known that this method may suffer from the "relative convergence" problem [7].

More recently a rigourous formulation of the single step discontinuity in microstrip, such as that shown in Figure 4.1, has been published [8] and a wide variety of results presented. In this method, the portion of microstrip including the step is enclosed by electric walls to form a resonant cavity. By varying the length of the cavity and evaluating the resonant frequencies, the S parameters of the step can be obtained.

While this method gives good results for the single step, it does not lend itself readily to the treatment of cascades of strongly coupled discontinuities. This is due to the fact that the amount of computation becomes very large when a complicated metallisation pattern is analysed.

The formulation presented in this chapter makes use of variational principles for the generalised S parameters of a single step discontinuity. This lends itself to the treatment of strongly interacting discontinuities by means of the concept of accessible and localised modes [9],[10],[11]. In this approach the higher order modes excited at the discontinuity are treated according to their effect at the neighbouring discontinuities. If they have a significant effect then they are deemed to be "accessible" otherwise they are deemed to be "localised". Since there is no localised mode incident at a discontinuity, these scattered modes are effectively terminated in their characteristic impedances. Each discontinuity is treated as a multiport device, each port corresponding to an accessible mode. Likewise the microstrip which connects neighbouring discontinuities is modelled as a set of transmission lines, each carrying one accessible mode. In this way the coupling between the discontinuities can be accurately accounted for.

The single step discontinuity is analysed using the Galerkin variational method. The E field at the discontinuity is expanded both in the set of microstrip modes each side of the step, and also in a suitable set of vector basis functions appropriate to the step itself.

In order to analyse a microstrip discontinuity in this way, it is necessary to calculate the field patterns of a large number of microstrip modes, typically 100. An efficient method for achieving this has been presented in the previous chapter.

4.3. General Theory of the Single Step Discontinuity

Most formulations of the microstrip step discontinuity make use of the equivalent circuit shown in Figure 4.2. This model, however, suffers from the disadvantages that it is only correct for microstrip in the limit of low frequency, and that as it stands it cannot be used to model strongly coupled steps.

The formulation presented here uses the model shown in Figure 4.3. The step is represented by a multi-port device with frequency dependent S parameters. Each port on the model corresponds to an accessible mode, that is a mode which does not decay to negligible levels by the time it reaches the next discontinuity. Combination of these S matrices, by standard network methods, makes possible the characterisation of cascades of strongly coupled discontinuities. In principle, the accuracy of the model can be systematically improved by increasing the number of modes which are treated as accessible. In practice, however, as the number of modes deemed to be accessible is increased, the increase in numerical error becomes greater than the improvement from the formally more accurate representation.

Referring to the plan of Figure 4.1 we start from the continuity equations for the E and H fields.

$$\sum_n \left(a_n^{\langle 1 \rangle} + b_n^{\langle 1 \rangle} \right) \underline{E}_n^{\langle 1 \rangle} = \sum_n \left(a_n^{\langle 2 \rangle} + b_n^{\langle 2 \rangle} \right) \underline{E}_n^{\langle 2 \rangle}$$

$$= \underline{f}(r) \qquad (4.1)$$

$$\sum_n \left(a_n^{\langle 1 \rangle} - b_n^{\langle 1 \rangle} \right) \underline{H}_n^{\langle 1 \rangle}$$

$$= \sum \left(a_n^{\langle 2 \rangle} - b_n^{\langle 2 \rangle} \right) \underline{H}_n^{\langle 2 \rangle} + \hat{\underline{z}} \times \underline{J} \qquad (4.2)$$

where:

the coefficients "a" represent the incident wave amplitudes

the coefficients "b" represent the scattered wave amplitudes

the superscripts (1) and (2) refer to the regions defined in Figure 4.1.

Note that it is necessary to specify the E field and the H field separately since it is not possible to define a unique wave impedance for microstrip.

We normalise the modes such that:

$$< \underline{E}_n \mid \underline{H}_m > = \delta_{mn} \qquad (4.3)$$

and the inner product is defined as:

$$\int \underline{E}_n \times \underline{H}_m \cdot \hat{\underline{z}} \, dS$$

with the integral taken over the box cross-section.

By taking the inner products of each side of equation 4.1 with each of the microstrip modes in turn we get:

$$a_n^{(1)} + b_n^{(1)} = \frac{\langle \underline{\mathcal{E}} \mid \underline{H}_n^{(1)} \rangle}{\langle \underline{E}_n^{(1)} \mid \underline{H}_n^{(1)} \rangle} \qquad (4.5)$$

$$a_n^{(2)} + b_n^{(2)} = \frac{\langle \underline{\mathcal{E}} \mid \underline{H}_n^{(2)} \rangle}{\langle \underline{E}_n^{(2)} \mid \underline{H}_n^{(2)} \rangle} \qquad (4.6)$$

To proceed we choose the inputs to the ports to satisfy the following conditions:

$$\begin{aligned} a_t^{(1)} &= 1 \\ a_p^{(1)} &= 0 \qquad p \neq t \\ a_p^{(2)} &= 0 \end{aligned} \qquad (4.7)$$

substituting into equations 4.5 and 4.6 gives:

$$1 + b_t^{(1)} = \frac{\langle \underline{\mathcal{E}} \mid \underline{H}_t^{(1)} \rangle}{\langle \underline{E}_t(1) \mid \underline{H}_t^{(1)} \rangle} = 1 + S_{tt} \qquad (4.8)$$

$$b_p^{(1)} = \frac{\langle \underline{\mathcal{E}} \mid \underline{H}_p^{(1)} \rangle}{\langle \underline{E}_p^{(1)} \mid \underline{H}_p^{(1)} \rangle} = S_{pt} \qquad (4.9)$$

$$b_p^{(2)} = \frac{\langle \underline{\mathcal{E}} \mid \underline{H}_p^{(2)} \rangle}{\langle \underline{E}_p^{(2)} \mid \underline{H}_p^{(2)} \rangle} = S_{qt} \qquad (4.10)$$

We now substitute these expressions into equation 4.2.

$$(1-b_t^{(1)})H_t^{(1)} - \sum_{n\neq t} \frac{< \underline{\xi} \mid H_n^{(1)} >}{< E_n^{(1)} \mid H_n^{(1)} >} H_n^{(1)}$$

$$= \sum \frac{< \underline{\xi}, H_n^{(2)} >}{< E_n^{(2)} \mid H_n^{(2)} >} H_n^{(2)} \qquad (4.11)$$

Therefore:

$$2 H_t^{(1)} = \sum_n \frac{< \underline{\xi} \mid H_n^{(1)} >}{< E_n^{(1)} \mid H_n^{(1)} >} H_n^{(1)}$$

$$+ \sum \frac{< \underline{\xi} \mid H_n^{(2)} >}{< E_n^{(2)} \mid H_n^{(2)} >} H_n^{(2)} \qquad (4.12)$$

We now take inner products of both sides of this equation with $\underline{\xi}$ yielding:

$$< \underline{\xi} \mid H_t^{(1)} > = < \underline{\xi} \mid \underline{\underline{G}} \mid \underline{\xi} > \qquad (4.13)$$

where the kernel $\underline{\underline{g}}$ of the integral operator $\underline{\underline{G}}$ is given by:

$$2\underline{\underline{g}}(r, r') = \sum_{n=1}^{\infty} \frac{H_n^{(1)}(r) \; H_n^{(1)}(r')}{< E_n^{(1)} \mid H_n^{(1)} >}$$

$$+ \frac{H_n^{(2)}(r) \; H_n^{(2)}(r')}{< E_n^{(2)} \mid H_n^{(2)} >} \qquad (4.14)$$

Making use of equations 4.8 to 4.10 and the normalisation given by equation 4.3 we get the following expressions for the elements of the S matrix.

$$\frac{\langle \underline{\mathcal{E}} \mid \underline{\underline{G}} \mid \underline{\mathcal{E}} \rangle}{\langle \underline{\mathcal{E}} \mid \underline{H}_p^{(2)} \rangle \langle \underline{\mathcal{E}} \mid \underline{H}_q^{(2)} \rangle} = R_{pq} \qquad (4.15)$$

where $R_{pq} = \dfrac{1}{S_{pq} - \delta_{pq}}$ $\qquad p <= \alpha$ $\qquad (4.16)$

$$R_{pq} = \frac{1}{S_{pq}} \qquad p > \alpha$$

α is the number of accessible modes in region 1.

We expand the unknown function for the electric field at the discontinuity in terms of a complete set of two dimensional vector basis functions which satisfy the boundary conditions.

$$\underline{\mathcal{E}} = \sum_{q=1}^{\infty} c_q \underline{\phi}_q (x,y) \qquad (4.17)$$

Substituting these expressions into equation 4.15 and taking partial derivatives of each side of the equation with respect to c_u we obtain the following:

$$< \underline{\xi} | H_p^{(1)} >< \underline{\xi} | H_\phi^{(1)} > \frac{\partial R_{p\phi}}{\partial c_u} + \sum_q c_q <\phi_u | H_\phi^{(1)} >< \phi_q | H_p^{(1)} > R_{p\phi}$$

$$= \sum_q^* c_q < \underline{\phi}_q \mid \underline{\underline{G}} \mid \underline{\phi}_u > \qquad (4.18)$$

substituting for $R_{p\phi}$ we get:

$$\left\{ < \underline{\phi}_u \mid \underline{H}_\phi^{(1)} > - \sum c_q < \underline{\phi}_\phi \mid \underline{\underline{G}} \mid \underline{\phi}_\phi > \right\}$$

$$+ < \underline{\xi}_\phi \mid \underline{H}_p^{(1)} > < \underline{\xi}_p \mid \underline{H}_\phi^{(1)} > \frac{\partial R_{p\phi}}{\partial c_q} = 0 \qquad (4.19)$$

from equation 4.12 we get:

$$< \underline{\phi}_u \mid \underline{H}_\phi^{(1)} > = < \underline{\phi}_u \mid \underline{\underline{G}} \mid \underline{\xi} > \qquad (4.20)$$

which if we substitute into equation 4.19 we get the results:

$$\frac{\partial R_{p\phi}}{\partial c_u} = 0 \qquad (4.21)$$

$$< \underline{\phi}_u \mid \underline{H}_\phi^{(1)} > = \sum_q c_q < \underline{\phi}_q \mid \underline{\underline{G}} \mid \underline{\phi}_u > \qquad (4.22)$$

The first result shows that the expressions for the elements of the S matrix are stationary with respect to small changes in the trial field function and hence we have a variational principle. The second result has the form of an infinite set of simultaneous equations from which the coefficients c_q may be calculated. Hence the field may be found from equation 4.17, and the left half of the S matrix can be found from equations 4.8-4.10. The other half of the S matrix is found by means of a similar analysis with inputs to the ports satisfying the conditions:

$$a_p^{\langle 1 \rangle} = 0$$

$$a_t^{\langle 2 \rangle} = 1$$

$$a_p^{\langle 2 \rangle} = 0 \qquad p \neq t$$

instead of those specified in equation 4.7.

We note that equation 4.22 is the same as would have been obtained if Galerkin's method had been applied to 4.12. This is a consequence of the fact that the operator G is self adjoint which in turn is a consequence of the law of conservation of energy.

In practice, of course, we approximate the field with a small number of basis functions, chosen to well approximate the actual field at the discontinuity. This leads to an efficient and accurate formulation. The form of the chosen basis functions is discussed later.

It is interesting to note that the function g can be split into two parts g_c and g_l where the sum in equation 4.14 is taken over the capacitive and inductive modes respectively. The corresponding operators G_c and G_l are negative and positive definite respectively. From the theory of operators this means that the calculated values of R_c and R_l will form an upper bound on the true value. Unfortunately because these quantities are summed, the stationary point in R will in general be neither a maximum or a minimum. This is in contrast to the simpler situation which would exist if there were only capacitive or only inductive modes excited. Then one could place bounds on the required functionals. Also, in the present case, the fact that equation 4.14 contains subtractions means that, to maintain accuracy in the solution, the field patterns must be calculated to a high degree of accuracy.

4. CHOICE OF BASIS FUNCTIONS FOR THE STEP

In equation 4.17 we made use of a set of basis functions in which to expand the transverse E field at the step. It is crucial that a good choice is made here. Otherwise the result will be inaccurate. It is this aspect of Galerkin's method, and other methods of a similar nature, which has attracted criticism [14]. Where it is possible, from physical considerations, to know a priori the important characteristics of the unknown function, then basis functions can be chosen which ensure fast convergence. Such a procedure has been used to good effect for the solution of the modes of continuous microstrip [12] and for finline [15] where the singularity of the fields at the edge of the infinitely thin strip or fin are known exactly.

Unfortunately, for the case of the step discontinuity, it is not obvious what the form of the field will be. There is no simply applicable condition corresponding to the edge condition at a wedge, which can be used. Possible ways of deriving a suitable set of basis functions would be using numerical methods to solve the static problem [16], or making the order of the singularity at the corner of the step a parameter in the variational formulation [17].

Various sets of basis functions which satisfy the boundary conditions, but which incorporate no beliefs concerning the form of the field at the step, have been tried. In most cases, however, the result has been a very ill conditioned set of equations (4.22) from which no satisfactory answer could be obtained.

A simple set of basis functions which can be used is the wave patterns of Ex and Ey of the modes of the microstrip containing the wider of the two strips. These functions meet the boundary conditions, but do not have the correct singularity at the corner. From physical considerations, however, it is likely that the field at the step will be similar to the field in the wider continuous microstrip. The ratio of Ex to Ey is left as a parameter to be found during the solution of the variational expression. If this were not done, then the higher order modes of the wider microstrip excited by the discontinuity, would be orthogonal to the basis functions and would not, therefore, contribute to the sum in equation 4.12. Figure 4.5 shows the results of calculating the phase of S12 for a step discontinuity using different numbers of basis functions at frequencies up to 12GHz. It can be seen that convergence is achieved at various frequencies when 9 basis functions are used and the ratio of the strip widths is 4:1. While not ideal, this result means that only a moderately small matrix need be handled.

This contrasts with the large matrices which result from employing mode matching methods such as [19].

In addition, numerical experiments have been carried out using the modes of the wider strip multiplied by an expression of the form:

$$\left\{ \left\{ \frac{a-w}{2} \right\}^2 - x^2 \right\}^{\mu}$$

where a is the box width, w is the wider strip width, and μ is a parameter which is chosen to achieve best convergence. The multiplication was carried out by taking the convolution of the Fourier transform of the above expression, expressed in terms of Bessel functions, with the previously calculated Fourier components of the modal fields. By this means it was hoped to improve on the results obtained by using the unchanged microstrip modes as basis functions by bringing the edge behaviour closer to what it really was. Results for various values of μ were obtained but the convergence showed no improvement over that achieved using the unmodified modes.

5. CONVERGENCE OF THE GREENS FUNCTION

The Green's function (equation 4.14) is built up as an infinite sum of the eigenmodes of the continuous microstrip. In practice, of course, it is necessary to truncate this sum after a finite number of terms. The effect of such a truncation on the calculated value of the equivalent circuit impedance Z11 is shown in Figure 6. It can be seen here that for accurate results it is necessary to take into account about one hundred eigenmodes each side of the step. Examination of the geometry shows that this should be expected. We are essentially dealing with three complete sets of functions. Any transverse electric field pattern which satisfies the boundary conditions may be expressed as a linear combination of any of these sets. These are the microstrip modes for the continuous microstrip each side of the step, and the basis functions chosen to express the field at the step itself. Each of these sets contain singular functions where the singularities may occur at different places and have different strengths in each set. Clearly if we are to express a singular function as a linear combination of a set of singular functions, when the singularities do not coincide, we need many terms in order to obtain an accurate representation. Thus in expressing the Greens function in terms of a summation of eigenmodes, many eigenmodes must be included.

It is interesting to compare the situation existing here, to that of the analysis of continuous microstrip [12]. In the latter case we also have a Green's function expressed as a sum of eigenmodes, in this case they are the eigenmodes of a slab loaded waveguide. Unlike the present case these functions are not singular, but the microstrip modes which are to be expressed as a linear combination of them do contain a singularity. In that form, it would also be necessary to take a large number of terms in order to achieve convergence. It was possible, however, in that case to find an asymptotic form of the expression to be summed, with a consequent decrease in computer time. In the present case, however, no such asymptotic form has so far been found.

6. RESULTS FOR THE SINGLE STEP DISCONTINUITY

The S parameters for a step discontinuity calculated using the formulation described above, are shown in Figures 4.7 and 4.8. These show the modulus and the phase respectively. Also shown are the rigourous results read from the graphs presented in [8] and results using published quasi-static approximations [1].

It can be seen that at low frequencies, the agreement between rigourous methods and the quasi-static approximation is good, especially for the transmission coefficient.

However as the frequency rises and we approach the cutoff frequency of the second mode, there is considerable deviation.

In Figure 4.9 we see the coupling between the dominant mode and the first two higher order modes at the step. It can be seen that the coupling increases almost linearly with frequency so long as we are well below the cut off of the higher order modes.

7. NETWORK FORMULATION OF MULTIPLE DISCONTINUITIES

In the conventional equivalent circuit model for a step discontinuity, the parasitic effects are represented by two series inductors and a shunt capacitor (see Fig 4.2). This model has the following limitations. First the validity of the equivalent circuit presupposes that a characteristic impedance can be defined for microstrip. Because of the hybrid nature of the microstrip modes, such a definition is unambiguous only at zero frequency. Secondly, the values of the components are frequency dependent. This fact limits the usefulness of a simple equivalent circuit. Thirdly no account is taken of the existence of higher order modes, excited by the discontinuity, other than as a means of energy storage. If we have closely spaced discontinuities, then the effect of these modes will be significant.

In order to overcome these limitations, it is possible to model the discontinuity as a multi-port device with inbuilt storage elements. Such a model has previously been used for cascades of interacting irises and steps in rectangular waveguide [9] [10],[11].

The basic model is shown in Figure 4.3. We split the mode spectrum of the microstrip into "accessible" and "localised" modes. The former are considered to have a significant amplitude at the next discontinuity. These include all the propagating modes and the first few evanescent modes. The localised modes are considered to have decayed to negligible amplitude at the next discontinuity. The distinction is obviously dependent on the geometry, frequency of operation and the accuracy required.

For each accessible mode there exists an input/output port. The microstrip which connects successive discontinuities is then modelled as a set of transmission lines, one for each accessible mode, each with its own propagation coefficient. The localised modes which are excited propagate outwards from the discontinuity and do not see any reflection, therefore they can be treated as being terminated with a matched termination.

The complete cascade can therefore be treated as a cascade of multi-port networks connected as shown in Figure 4. The first and last of these networks have all but the dominant modes terminated in their characteristic impedances. Once the S matrices for each discontinuity are known and the propagation coefficients of the intervening microstrip for each accessible mode is known, then the overall S matrix can be calculated using standard methods (eg. [1]).

8. RESULTS FOR THE DOUBLE STEP DISCONTINUITY

The above method has been applied to the double step discontinuity, the plan of which is shown in Figure 4.1. For given frequencies of 3GHz and 7GHz the input VSWR was calculated as a function of the length of the step. The results are shown in Figures 4.10 and 4.11. Here we have the results of taking just one accessible mode, ie. assuming the steps have neglegible coupling and the results of taking two accessible modes. In addition the results using quasi-static formulae are shown. It can be seen that at 7GHz the calculated resonant length is noticably changed when the second accessible mode is included, thus indicating a significant amount of coupling. At 3GHz the results are almost indistinguishable implying that there is no significant coupling. The quasi-static results are significantly different in both cases.

9. APPLICATION TO A LOW PASS FILTER

A five section low pass filter made up of a cascade of microstrip step discontinuities has been analysed using the rigorous method, in order to see the effect of including more than one accessible mode in the model. The geometry of the filter is shown in Figure 4.12. It has been designed using 50 ohm input and output lines, 25 ohm capacitive lines and 90 ohm inductive lines. The cut off frequency is 10GHz. In Figure 4.13 we see the calculated frequency response by means of taking one and two accessible modes into account. It can be seen that at high frequencies, the effect of the second accessible mode becomes noticeable, although not in fact significant.

To produce Figure 4.12, the steps were characterised at 1GHz frequency intervals and the parameters at intervening frequencies were calculated using interpolation. This produces accurate results except in the region of the cutoff of the higher order modes where the parameters and their derivatives vary rapidly.

It is noted that there are only two different step discontinuities contained in the filter, a step from 50 ohms to 25 ohms and a step from 25 ohms to 90 ohms. Once these steps have been characterised, optimisation of the filter consists of varying only the lengths of the lines between each step. Thus for each iteration of an optimisation procedure, the only calculations involved are those of the S parameters of the lines and the resulting network problem. The computationally more expensive rigorous analysis of the step need not be repeated.

CONCLUSION

In this chapter, a formulation for the solution of single and multiple strongly coupled step discontinuities has been developed. This network model used for the single step lends itself well to extension to cascades of discontinuities, while the use of previously computed microstrip modes leads to a reduction in computation. Results have been presented for the single step which show good agreement with other published results, and for the double step which shows the effect of coupling between the steps.

REFERENCES:

1. K.C. Gupta et al. "Computer Aided Design of Microwave Circuits"
Artech 1981

2. Hoffmann "Integrierte Mikrowellenschaltungen"
Springer-Verlag 1983

3. R. Mehren "Grundelemente des Rechnergestutzten Entwurfs von Microstreifleitungs-schaltungen"
Verlag H. Wolf f, Aachen

4. P.B. Johns "Use of Condensed and Symmetrical TLM nodes in Computer aided electromagnetic Design."
Proc IEE. Vol 133 part H No. 5 Oct. 1986 pp368-374

5. M. Helard et al. "Theoretical and Experimental Investigation of Finline Discontinuities."
IEEE Trans on MTT. Vol MTT-33 Oct. 1985 pp 994-1003.

6. T.S. Chu, T. Itoh and Y.C. Shih "Comparitive Study of Mode Matching Formulations for Microstrip Discontinuity Problems."
IEEE Trans on MTT. Vol MTT-33 Oct. 1985 pp 1018-1023

7. R. Mittra, T. Itoh, and T.S. Li. "Analytical and Numerical Studies of the Relative Convergence Phenomenon arising in the solution of an integral equation by the Moment Method."
IEEE Trans on MTT. Vol MTT-20 Feb 1972 pp 96-104

8. Koster and Jansen "The microstrip Discontinuity - A revised Description."
IEEE Trans on MTT. Vol MTT-34 No.2 Feb. 1986 pp213-223

9. T.E.Rozzi "Network Analysis of Strongly Coupled Transverse Apertures in Waveguide"
Circuit Theory and Applications Vol 1 1973 pp 161-178

10.T.E.Rozzi "The Variational Treatment of Thick Interacting Inductive Irises"
IEEE Trans on MTT Vol MTT- 21 pp82-88 1973

11.T.E.Rozzi "A New Approach to the Network Modelling of Capacitive Irises and Steps in Waveguide"
Circuit Theory and Applications Vol 3 pp 339-354 1979

12.C.J. Railton, T.E. Rozzi and J. Kot. "The Efficient calculation of high order Microstrip modes dor use in Discontinuity Problems."
Proc. 16th European Microwave Conference. 1986 pp 529-534

13.C.J. Railton and T.E. Rozzi. "Complex modes in Microstrip"
IEEE Trans on MTT.

14. F.S. Acton "Numerical Methods that Work"
Harper and Row 1970 pp 250-252

15.C.A. Olley and T.E.Rozzi. "Systematic Characterisation of the Spectrum of Unilateral Finline."
IEEE Trans on MTT. Vol MTT-34 Nov 1986 pp 1147-1156.

16.P. Benedek and P. Silvester "Capacitance of Parallel Rectangular Plates Separated by a Dielectric Sheet"
IEEE Trans on MTT. Vol MTT-20 Aug. 1972 pp 504-510

17.H. Shigesawa and M. Tsuji. "Mode Propagation through a Step Discontinuity in Dielectric Planar Waveguide"
IEEE Trans on MTT. Vol MTT-34. Feb 1986 pp 205-

18.Collin "Field Theory of Guided Waves"
McGraw-Hill 1960

List of Figures

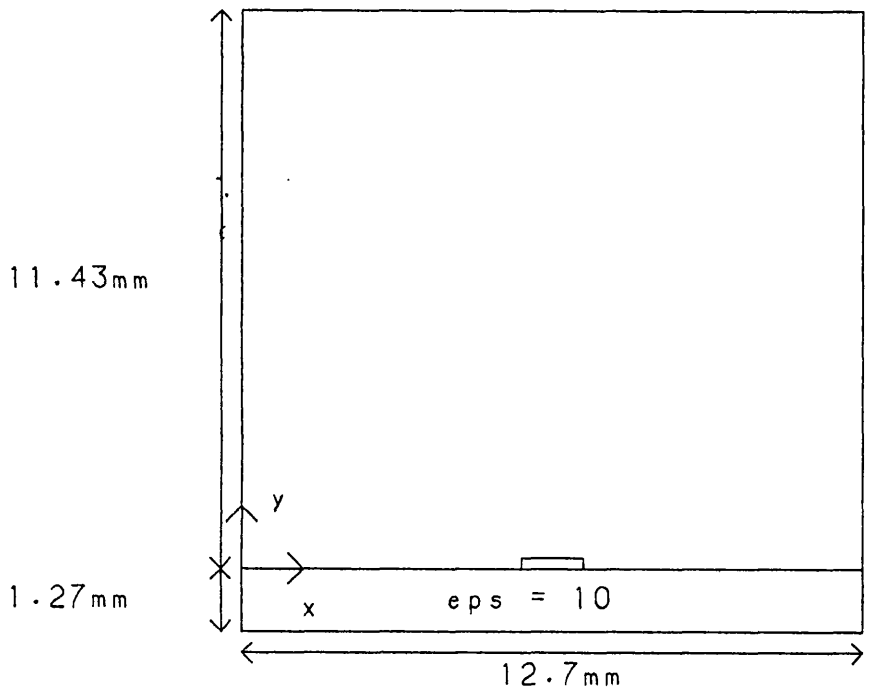

Fig. 4.1a - Microstrip cross section

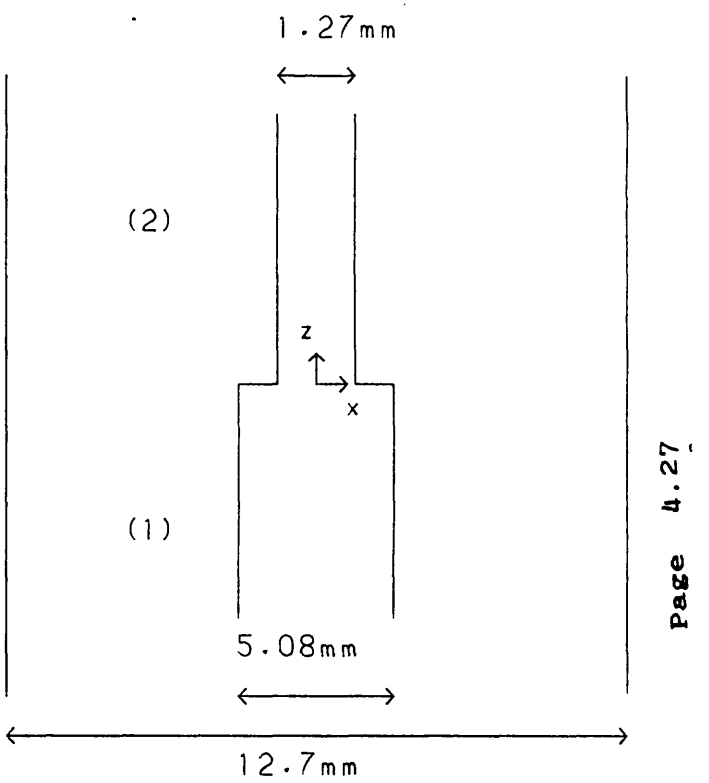

Fig. 4.1b - Plan of step discontinuity

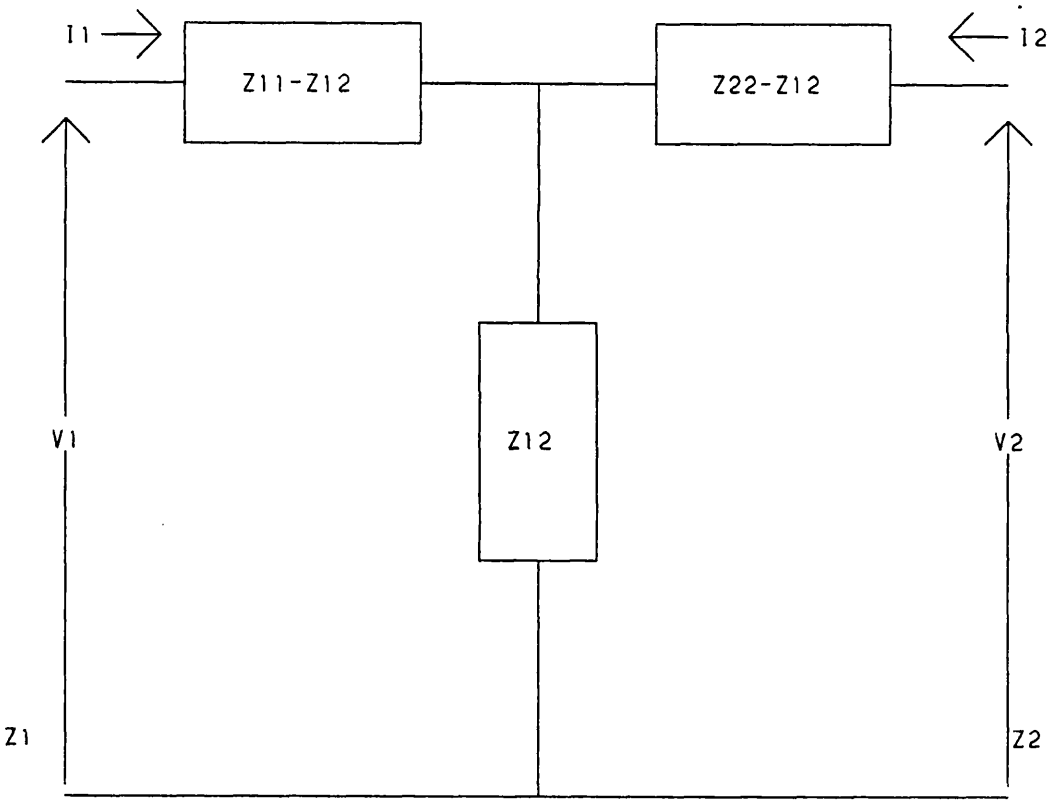

Fig. 4.2 - Quasi static equivalent circuit of step

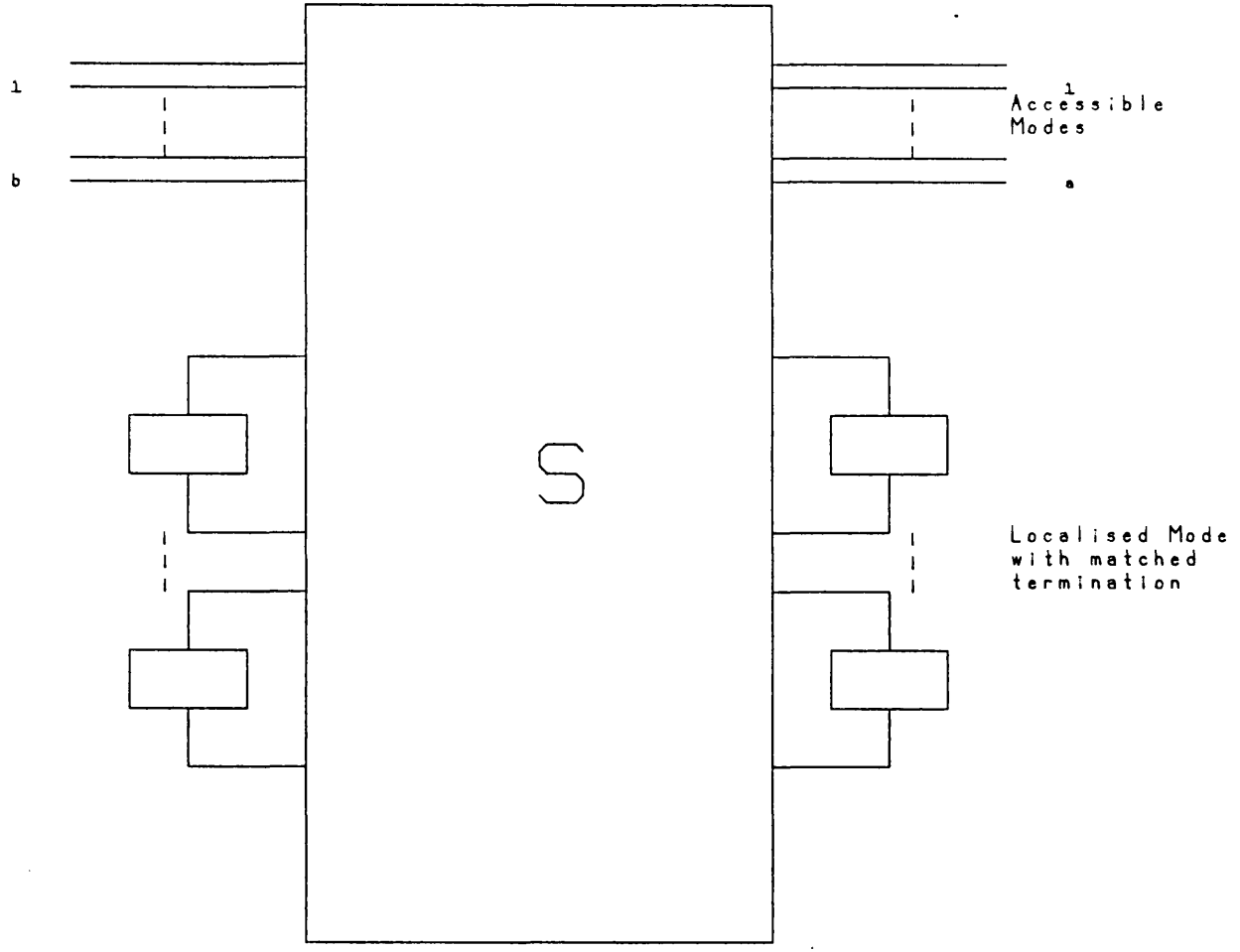

Fig. 4.3 - Network model of single discontinuity

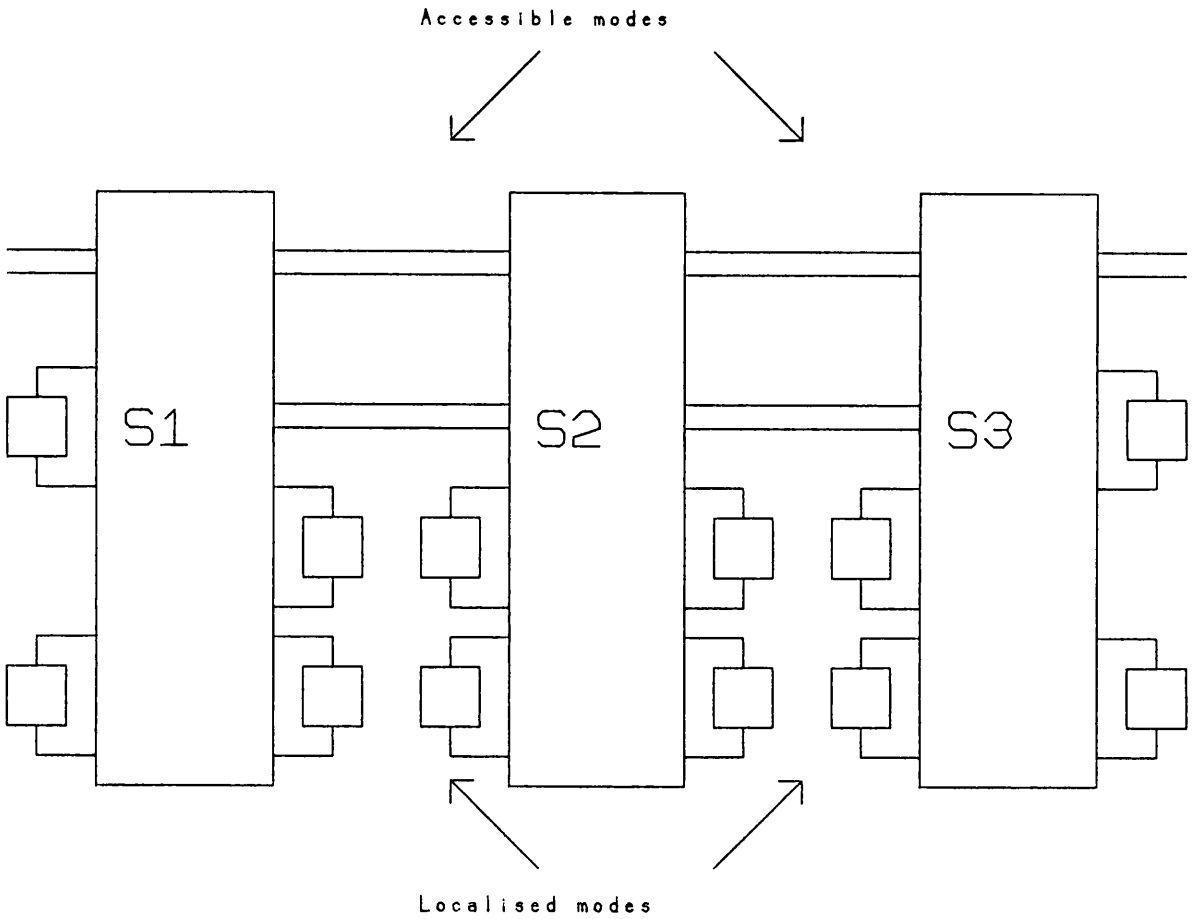

Fig. 4.4 - Network model of cascaded discontinuities

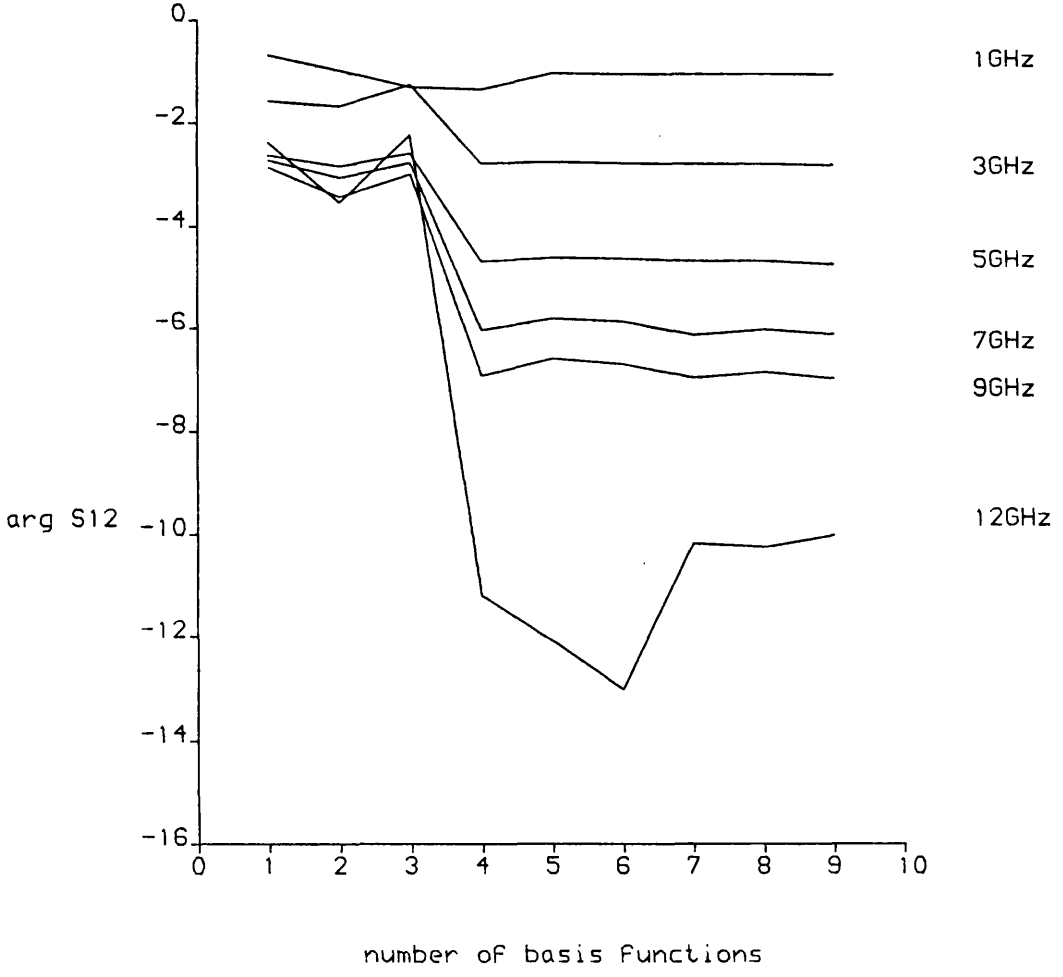

Fig 4.5 - Convergence of S12 as basis functions increased

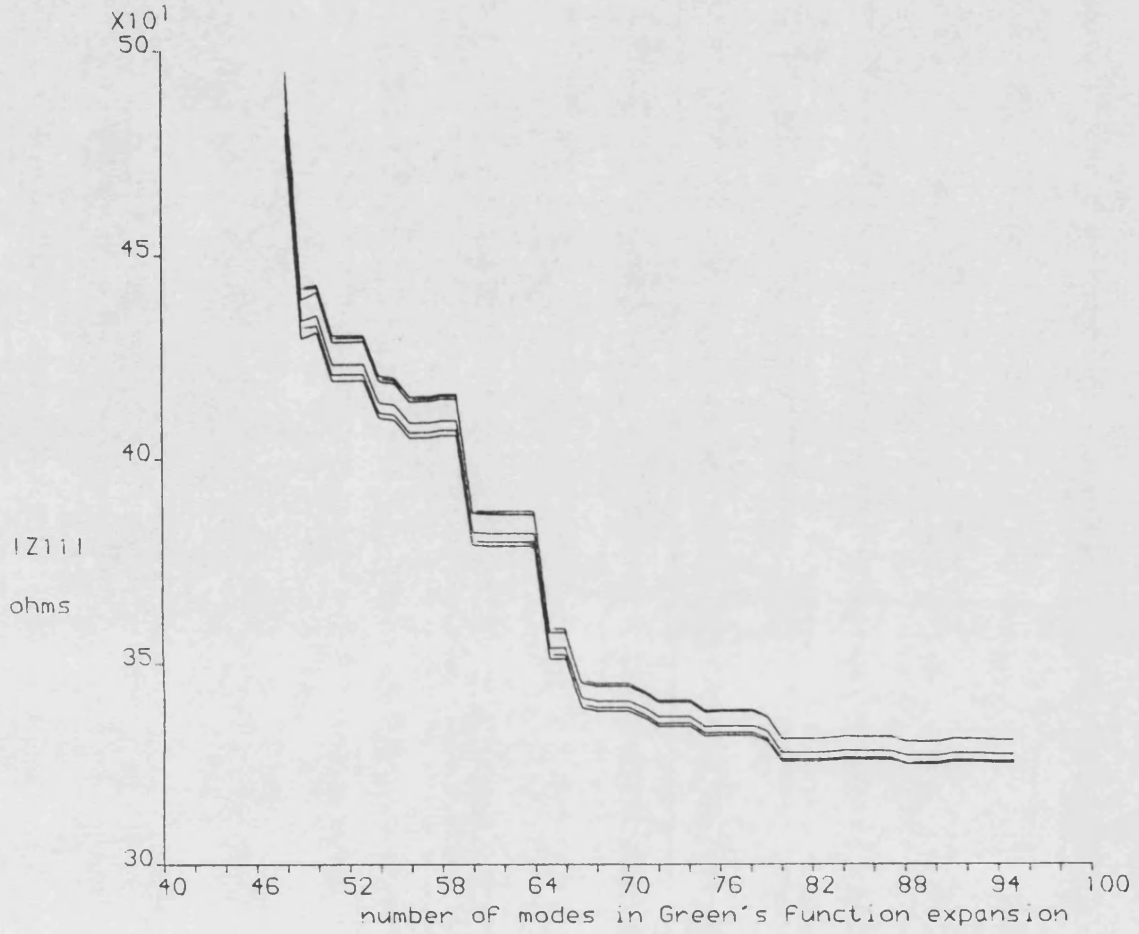

Fig 4.6 - Convergence of |Z11| with number of modes for different numbers of basis functions.

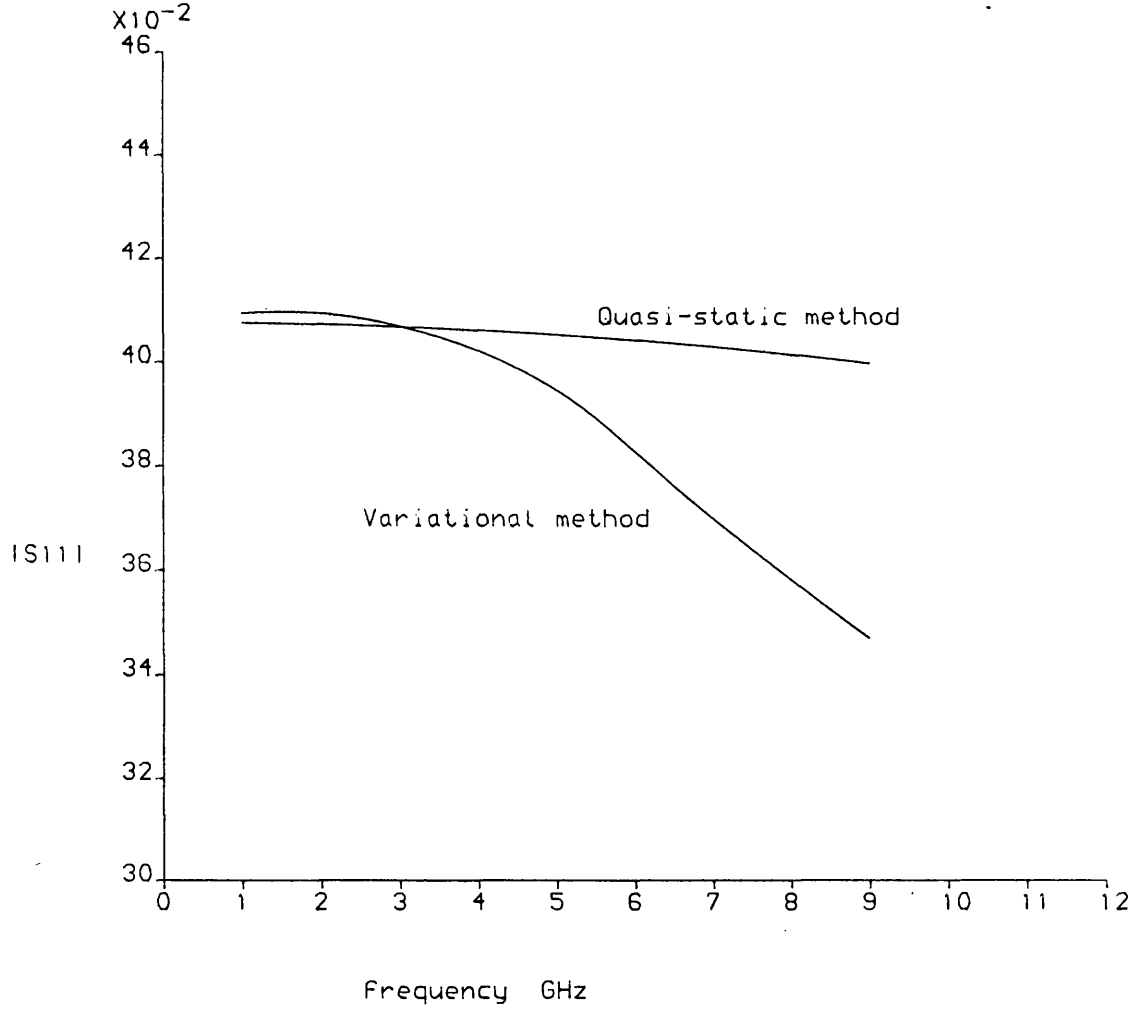

Fig. 4.7a - S11 modulus versus frequency

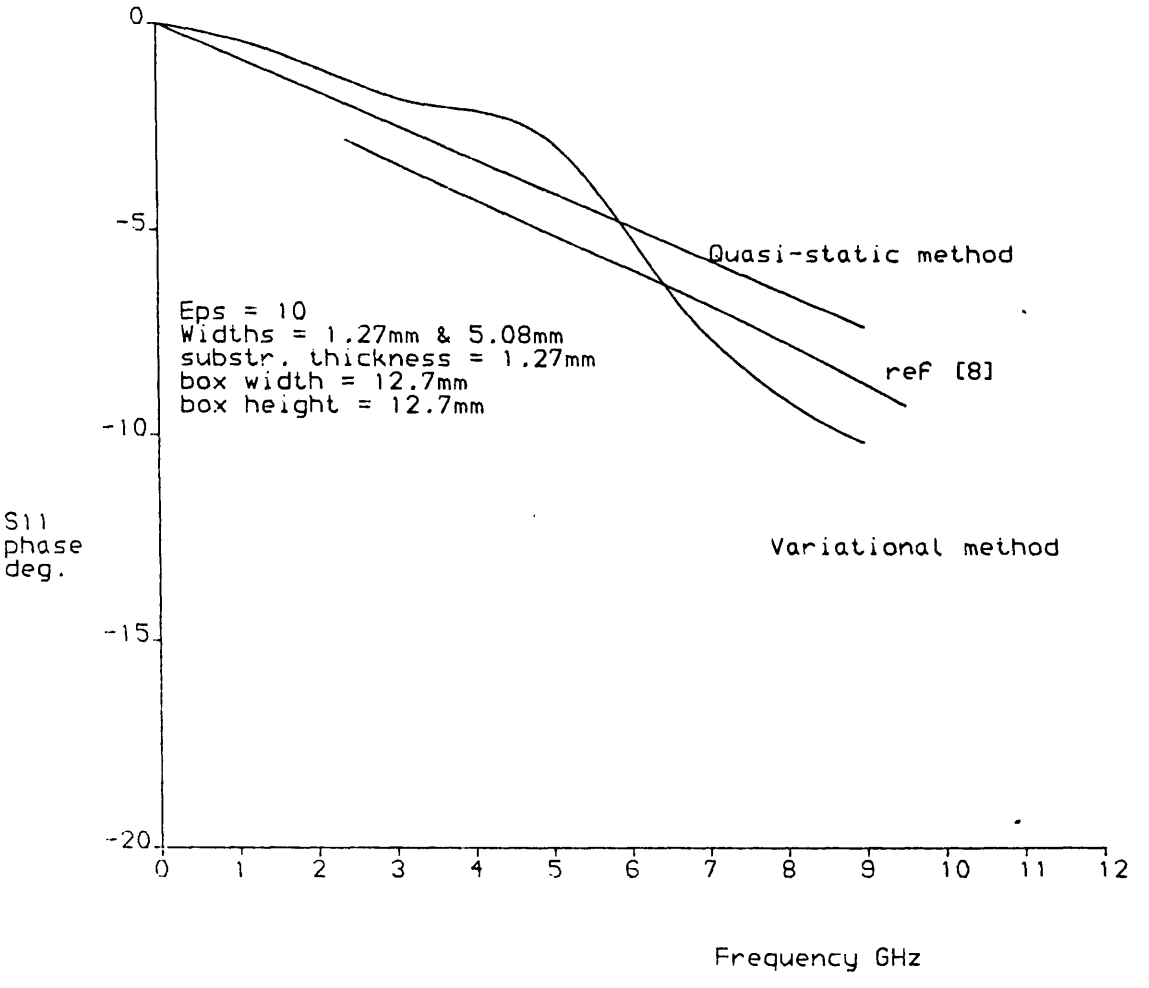

Fig 4.7b - S11 phase versus frequency

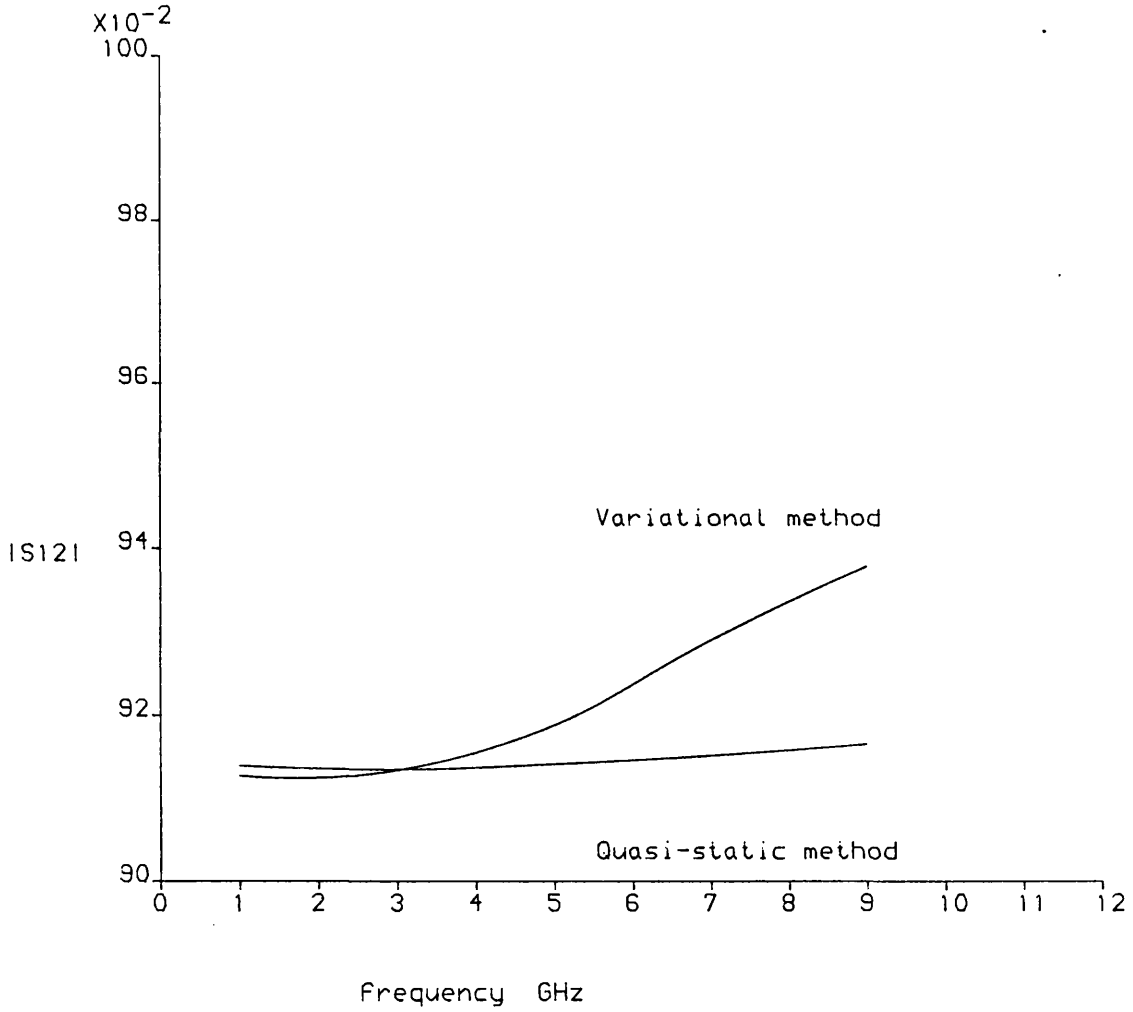

Fig 4.8a - S12 modulus versus frequency

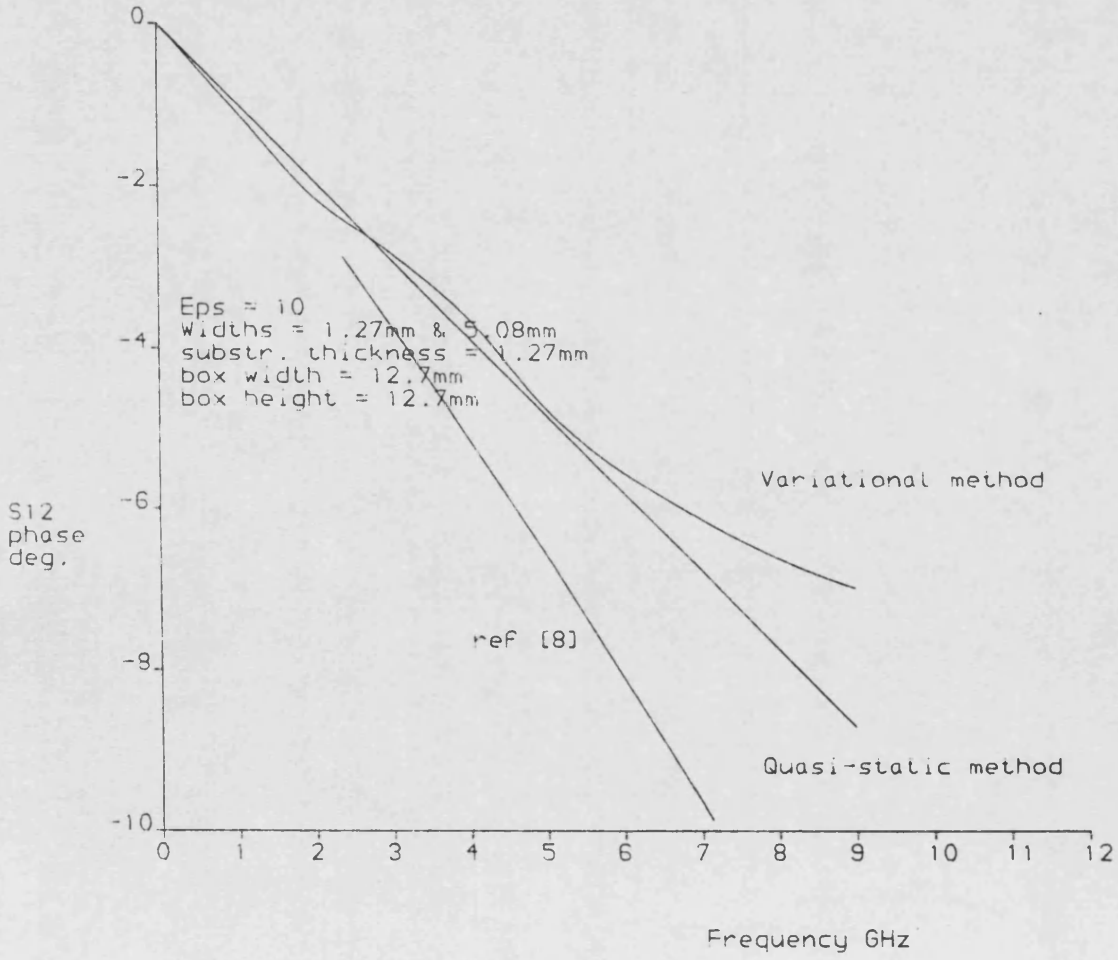

Fig 4.8b - S12 phase versus frequency

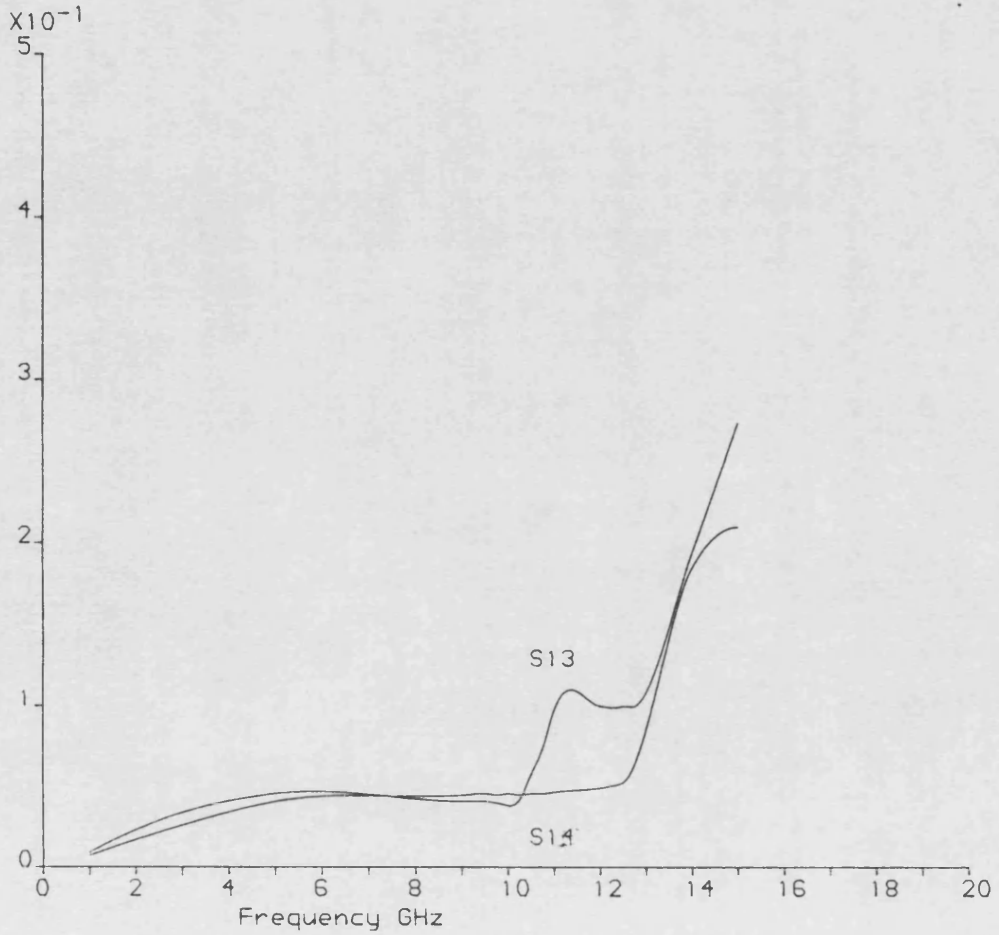

Fig 4.9 - Coupling to first and second higher order modes

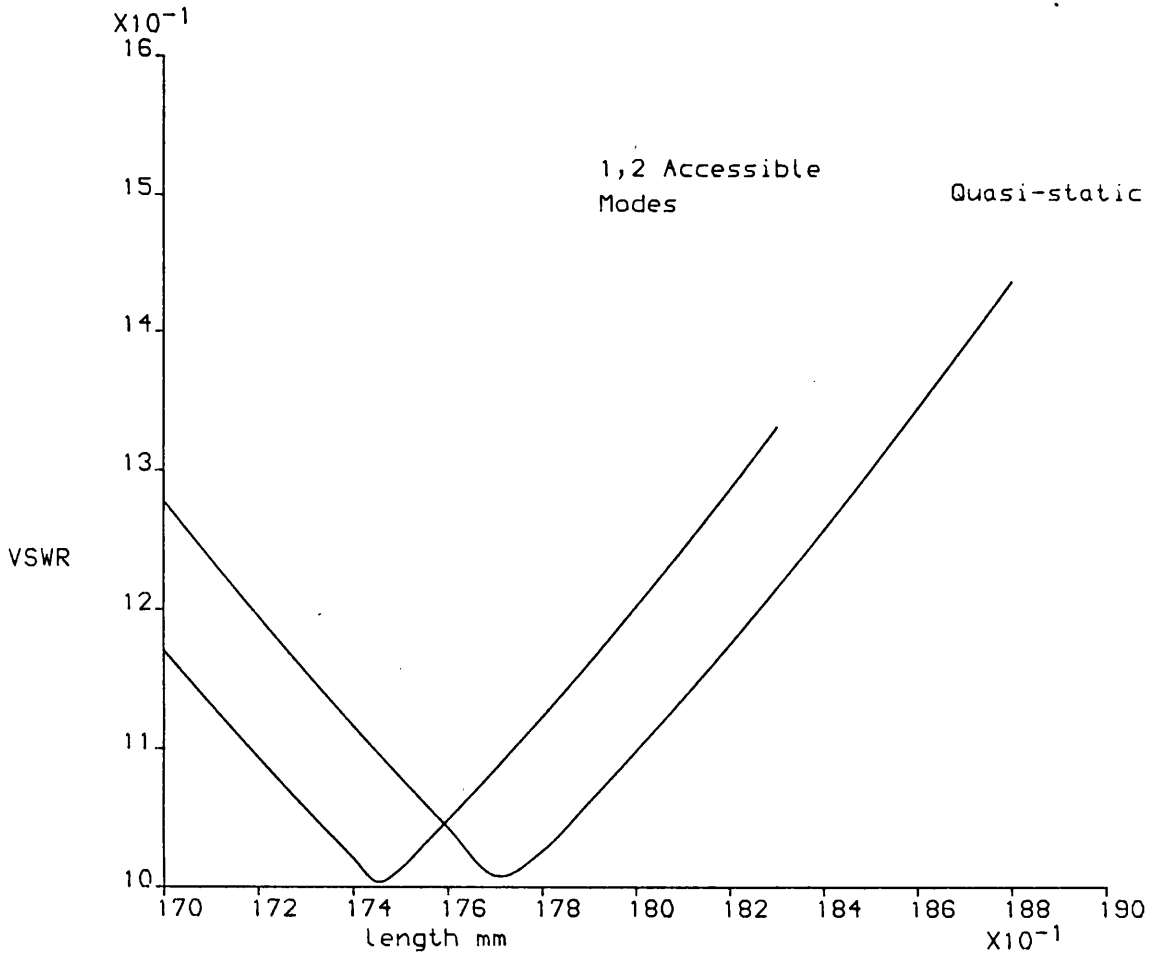

Fig. 4.10 - VSWR of a double step discontinuity 3GHz
a=12.7mm d=1.27mm h=10.43mm eps=10 w1=w3=1.27mm w2=5.08mm

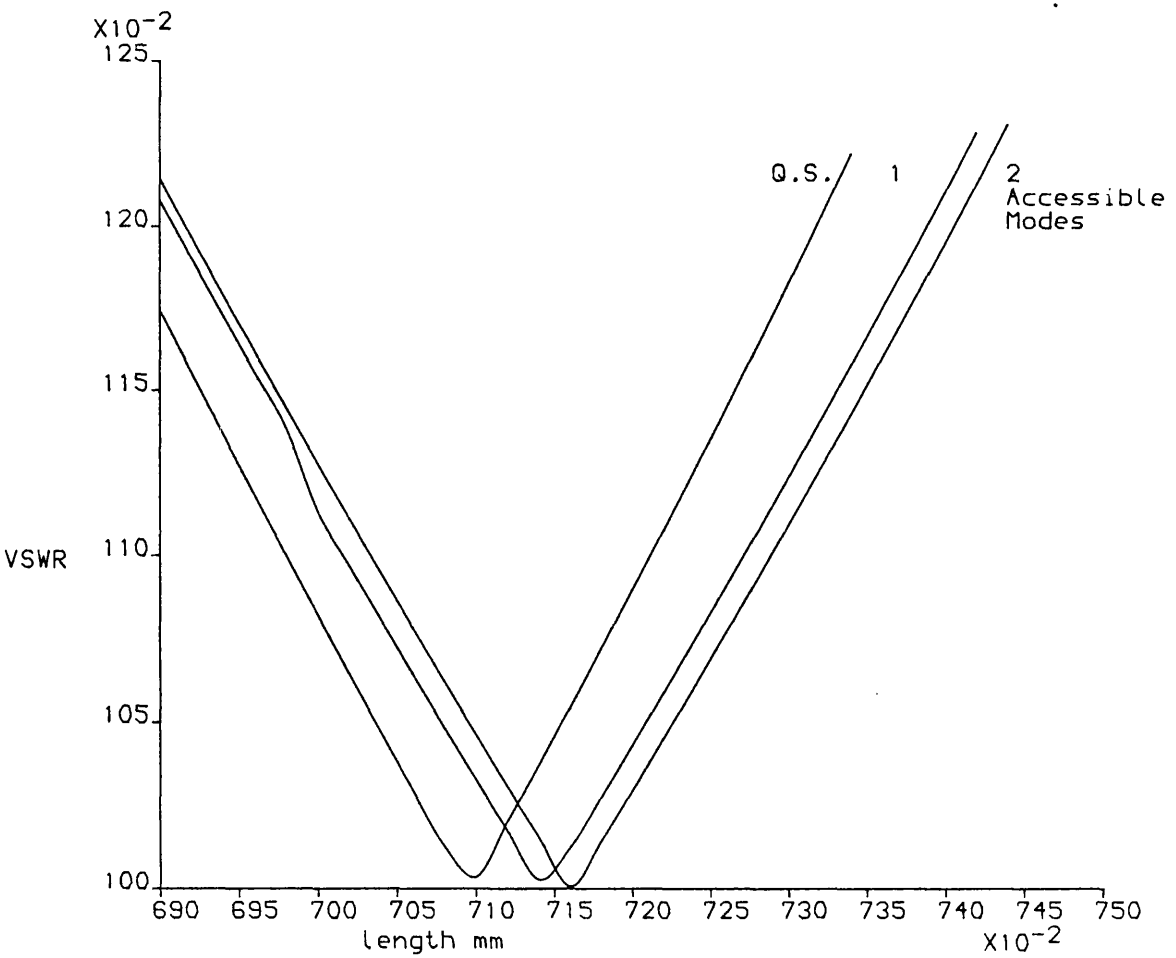

Fig. 4.11 - VSWR of a double step discontinuity 7GHz
a=12.7mm d=1.27mm h=10.43mm eps=10 w1=w3=1.27mm w2=5.08mm

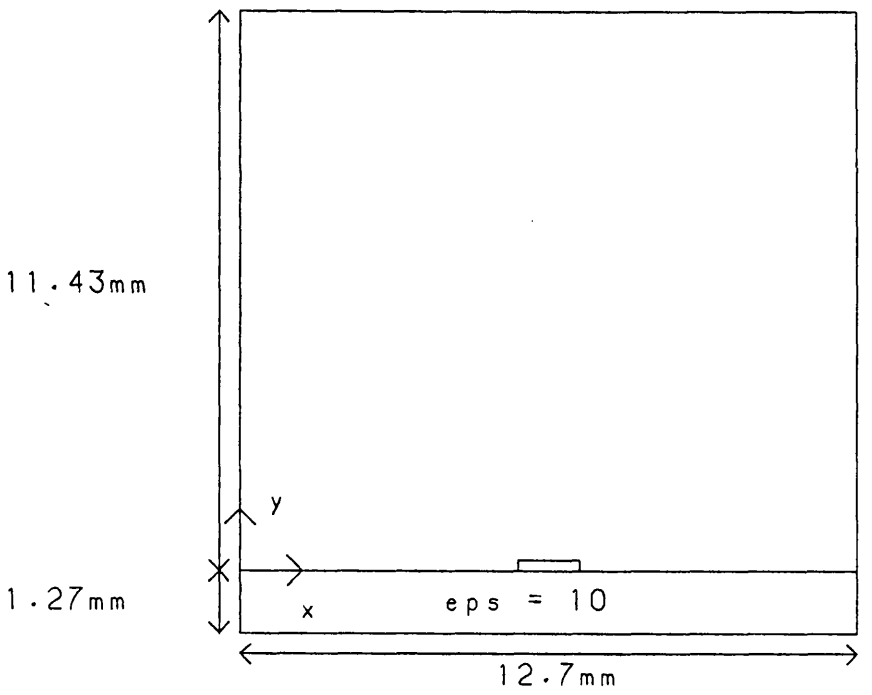

Fig. 4.12a - Filter cross section

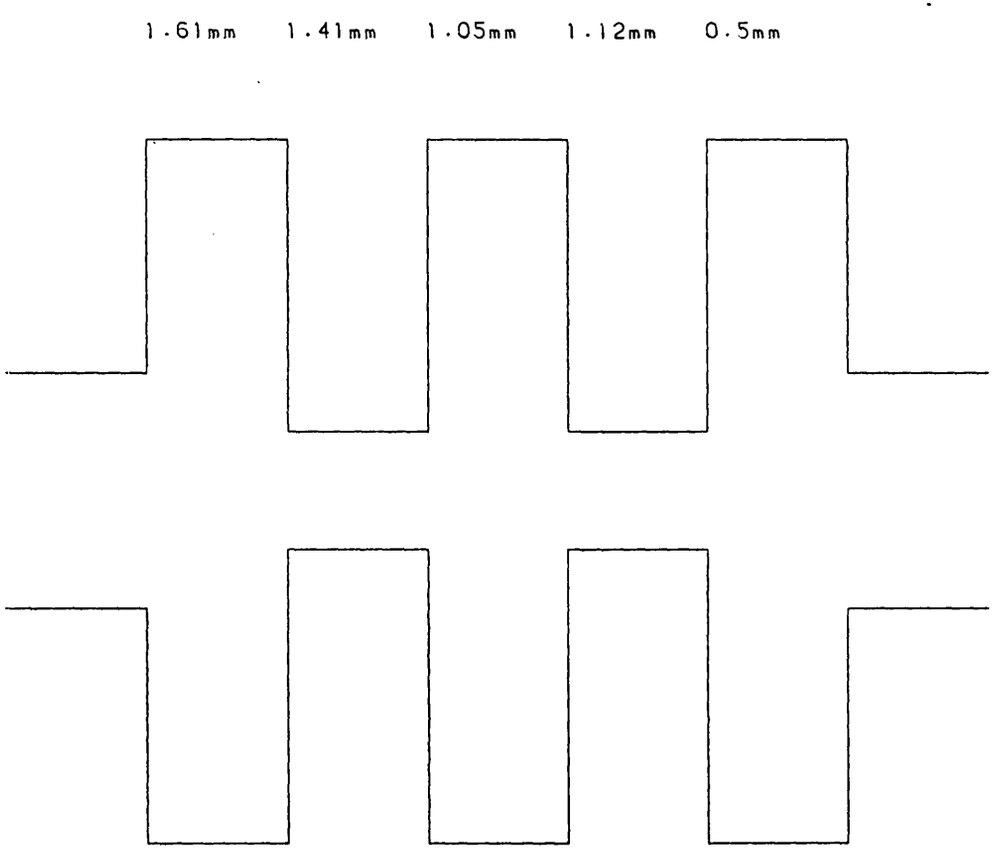

Fig 4.12b - Plan of Low Pass Filter

Strip widths are 1.25mm, 5.9mm and 1.92mm

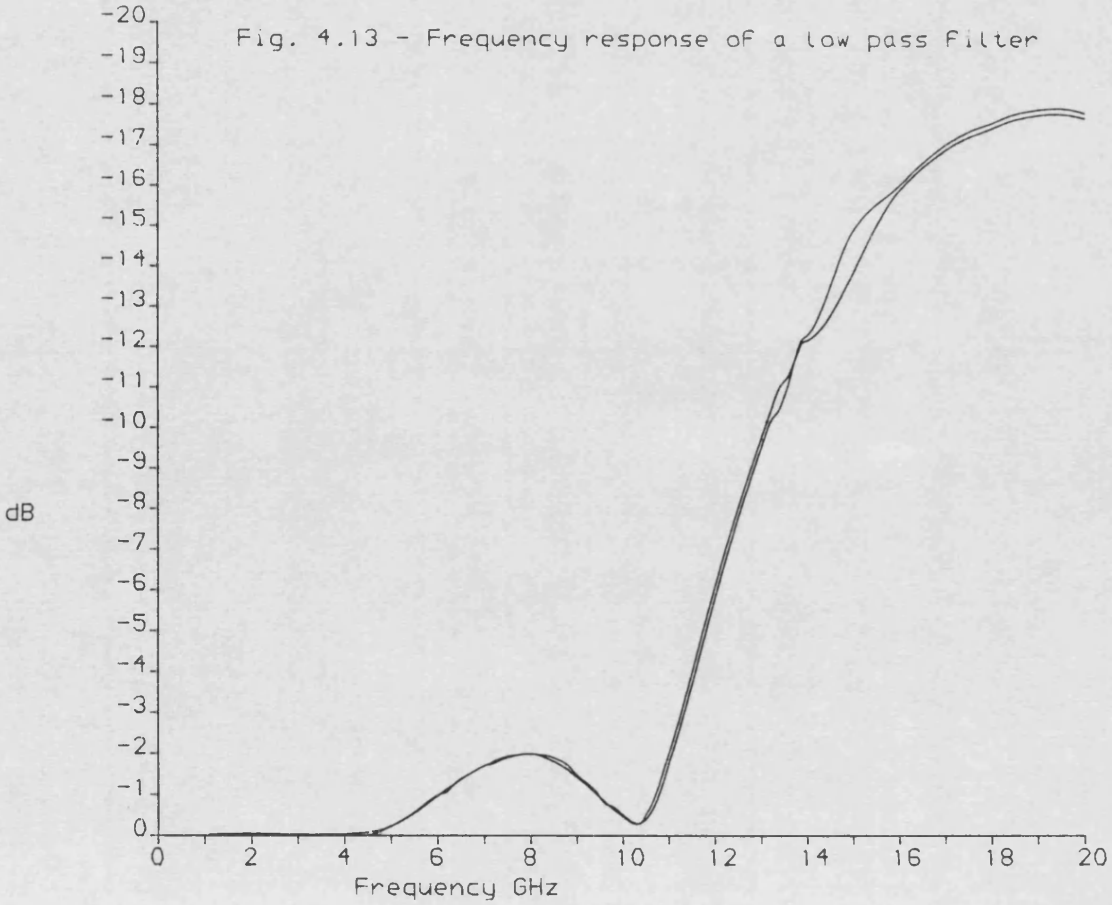

Fig. 4.13 - Frequency response of a low pass filter

CHAPTER 5

ANALYSIS OF BOXED MICROSTRIP RESONATORS

5.1 Introduction

In this chapter the general methods of chapter 2 are applied to the analysis of a boxed microstrip resonator. The resonator consists of a box bounded by perfect conductors and containing a number of rectangular metal patches on the interface between air and substrate. The usefulness of this analysis is not only the calculation of the resonant frequencies for such structures, but also because it leads to methods of characterising microstrip discontinuities [1], [2]. Of the other published rigorous formulations of the step discontinuity, the method described in [1] and [2] with their many accompanying results appeared to be the best formulation alternative and is the current state-of-the-art. The method which is used in the above references is essentially to apply Galerkin's method to equation 2.16. The basis functions are chosen such that, away from the discontinuity the current is that of a standing wave as would be found in continuous microstrip.

Close to the discontinuity, where the currents are perturbed, a separate set of basis functions are used. This is explained for the case of an abrupt microstrip termination in [1].

Unfortunately, neither [1] or [2] state what basis functions have been used, thus making it impossible to duplicate the method. In [3] a similar technique is used for the open structure. Here the basis functions used are the incident and reflected dominant microstrip modes plus a set of piecewise sinusoidal functions near the discontinuity.

In order to get a feel for this method the abrupt termination was analysed using the geometry of Figure 5.1. The basis functions chosen were the same as those used for the continuous microstrip having the correct edge singularity. The singularity at the corners is not exactly represented, although, as the results show, convergence is achieved using just two basis functions for each current component in each direction (a total of 8 scalar functions). Apart from the basis functions chosen, the method is the same as [2]. It is also similar to [4] and [5] except that there the open structure is treated.

In the following, the formulation is developed and some calculated results for a microstrip resonator are presented. Since the purpose of the work described in this chapter was to compare this method with that developed in chapter 4 for the analysis of the step discontinuity, no attempt was made to produce extensive numerical results.

5.2 The formulation

We start with equation 2.16, which as can be seen, is a two dimensional version of equation 2.14 which has already been examined in detail in chapter 3. It is possible to extend the derivation in that chapter to make it applicable to the resonator case.

We use the Green's function in the form given in equation 2.30, and the Fourier transforms of the currents, the appropriate forms of which are:

$$\tilde{I}_x(\alpha_n, \beta_m) = \int\int I_x(x,z)\,\mathrm{Cos}\,\alpha_n(x+a/2)\,\mathrm{Sin}\,\beta_m(z+l/2) \quad (5.1)$$

$$\tilde{I}_z(\alpha_n, \beta_m) = \int\int I_z(x,z)\,\mathrm{Sin}\,\alpha_n(x+a/2)\,\mathrm{Cos}\,\beta_m(z+l/2) \quad (5.2)$$

where l is the length and a is the width of the cavity.

These equations, which correspond to 2.53 and 2.54, are valid for metallisation of any shape placed on the air-dielectric interface. For the case of rectangular patches which are not in contact with the cavity walls, the transformed current is given as:

$$\tilde{I}_x = \sum_r \int\int I_x(x_r, z_r) \text{Sin } \alpha_n(x_r + xo_r) \text{Cos } \beta_m(z_r + zo_r)\, dx_r dz_r \tag{5.3}$$

$$\tilde{I}_z = \sum_r \int\int I_z(x_r, z_r) \text{Cos } \alpha_n(x_r + xo_r) \text{Sin } \beta_m(z_r + zo_r)\, dx_r dz_r \tag{5.4}$$

where:

$$xo_r = \frac{c_r + d_r + a}{2}$$

$$zo_r = \frac{e_r + f_r + l}{2}$$

c_r and d_r are the x coordinates of the edges of the r^{th} strip

e_r and f_r are the z coordinates of the edges of the r^{th} strip

By algebraic manipulation of these equations we can express the transformed currents in terms of the partial derivatives $\partial \bar{I}_z / \partial z$ and $\partial \bar{I}_x / \partial x$. This manipulation is described in appendix 5.1.

We substitute these values into the field equations and get:

$$E_z(x,z) = \sum_{n,m} \sum_{r} \left(\frac{\xi_{zz}}{\beta_m} \bar{I}_{zr}' + \frac{\xi_{zx}}{\alpha_n} \bar{I}_{xr}' \right) \text{Sin } \alpha_n(x+a/2) \text{Cos } \beta_m(z+1/2) \qquad (5.5)$$

$$E_x(x,z) = \sum_{n} \sum_{m} \left(\frac{\xi_{xz}}{\beta_m} \bar{I}_{zr}' + \frac{\xi_{xx}}{\alpha_n} \bar{I}_{xr}' \right) \text{Cos } \alpha_n(x+a/2) \text{Sin } \beta_m(z+1/2) \qquad (5.6)$$

where the boundary conditions at z = +/- 1/2 have been imposed, and the primes indicate partial differentiation.

The Greens functions g_{ij} are given by equations 2.43 etc.

We expand the currents in a set of basis functions as follows:

$$I_{zr}\ (\ x_r\ ,\ z_r\ ) = \sum_p Z_{pr}\ I_{zpr}(x_r, z_r) \qquad (5.7)$$

$$I_{xr}\ (\ x_r\ ,\ z_r\ ) = \sum_p X_{pr}\ I_{xpr}(x_r, z_r) \qquad (5.8)$$

Now take the two dimensional inner products of the above equations with I_{zqt} and I_{xqt} respectively for all q and t yielding.

$$\sum_{n,m} \frac{\mathcal{E}_{zz}}{\beta_m^2} \sum_{p,r} Z_{pr} I_{zpr} I_{zqt} + \frac{\mathcal{E}_{zx}}{\alpha_n \beta_m} \sum_{p,r} X_{pr} I_{xpr} I_{zqt} = 0 \qquad (5.9)$$

$$\sum_{n,m} \frac{\mathcal{E}_{xz}}{\alpha_n \beta_m} \sum_{p,r} Z_{pr} I_{zpr} I_{xqt} + \frac{\mathcal{E}_{xx}}{\alpha_n^2} \sum_{p,r} X_{pr} I_{xpr} I_{xqt} = 0 \qquad (5.10)$$

where I_{ipr} is the p^{th} basis function of the i directed current on the r^{th} patch.

If we use separable basis functions of the form:

$$I_{zpr}(\alpha_n, \beta_m) = I_{zxpr}(\alpha_n) I_{zzpr}(\beta_m) \qquad (5.11)$$

$$I_{xpr}(\alpha_n, \beta_m) = I_{xxpr}(\alpha_n) I_{xzpr}(\beta_m)$$

then the left hand sides of the above equations become:

$$\sum_{n,m} \frac{\varepsilon_{zz}}{\beta_m^2} \sum_{p,r} Z_{pr} I_{zxpr} I_{zxpr} I_{zxqt} I_{zzqt} \qquad (5.12)$$

$$+ \sum_{n,m} \frac{\varepsilon_{xx}}{\alpha_n \beta_m} \sum_{p,r} X_{pr} I_{xxpr} I_{xzpr} I_{zxqt} J_{zzqt}$$

and

$$\sum_{n,m} \frac{\varepsilon_{xz}}{\alpha_n \beta_m} \sum_{p,r} Z_{pr} I_{zxpr} I_{zzpr} I_{xxqt} I_{xzqt} \qquad (5.13)$$

$$+ \sum_{n,m} \frac{\varepsilon_{xx}}{\alpha_n^2} \sum_{p,r} X_{pr} I_{xxpr} I_{xzpr} I_{xxqt} I_{xzqt}$$

The solutions of this set of homogeneous equation are given by setting:

$$\det \begin{pmatrix} A^{xx} & A^{xz} \\ A^{zx} & A^{zz} \end{pmatrix} = 0 \qquad (5.14)$$

where the matrices A^{ij}_{pq} are given by:

$$\sum_{n}\sum_{m} B^{ip}\,\tilde{g}_{ij}\,B^{jq}$$

and the column vector B^{ip} is given by:

$$B^{ip}_{r} = \tilde{I}_{ixpr}\,\tilde{I}_{izpr}$$

There is a direct analogy with equations 3.1 and 3.2 for the case of boxed microstrip. In this case the computation is greatly increased due to the double sum occuring in the Green's function and the requirement for a two dimensional set of basis functions.

If we use basis functions of the same form as for boxed microstrip (equation 2.62) we get corresponding to equation 2.64:

$$\tilde{I}_{z}(n) = \sum_{p}\sum_{r} Z_{zpr}Q_{zprn} + Z_{(zp+1)r}R_{(zp+1)rn} \qquad (5.15)$$

And:

$$\tilde{I}^{*}_{x}(n) = \sum_{p}\sum_{r} X_{zpr}Q_{zprn} + X_{(zp+1)r}R_{(zp+1)rn} \qquad (5.16)$$

$$n > 0$$

$$= \sum_{r} w_r/4 \qquad p = 1 \ , \ n = 0$$

$$= 0 \qquad \text{otherwise}$$

where:

$$Q_{rn} = \text{Sin}\ \alpha_n \left\{ \frac{c_r + d_r + a}{2} \right\} J_{zp}(\alpha_n w/2)$$

$$R_{rn} = \text{Cos}\ \alpha_n \left\{ \frac{c_r + d_r + a}{2} \right\} J_{zp+1}(\alpha_n w/2)$$

$$\tilde{I}_{x}(m) = \sum_{p}\sum_{r} X_{zpr}Q_{zprm} + X_{(zp+1)r}R_{(zp+1)rm} \qquad (5.17)$$

And:

$$\bar{I}^{*}_{z}(m) = \sum_{p} \sum_{r} Z_{zpr} Q_{zprm} + Z_{(zp+1)r} R_{(zp+1)rm} \qquad n > 0$$

$$= \sum_{r} l_r/4 \qquad p = 1 \ , \ n = 0$$

$$= 0 \qquad \text{otherwise}$$

where:

$$Q_{rm} = \text{Sin}\ \beta_m \left\{ \frac{e_r + f_r + a}{2} \right\} J_{zp}(\beta_m l/2)$$

$$R_{rm} = \text{Cos}\ \beta_m \left\{ \frac{e_r + f_r + a}{2} \right\} J_{zp+1}(\beta_m l/2)$$

We can now search for a solution of the characteristic equation to find the resonant frequency. Once we have obtained this result, and have also calculated the propagation coefficient of the uniform microstrip, we can immediately calculate the effective length of the open circuited microstrip [1].

5.3 Results for a microstrip resonator

The resonant frequency for a microstrip resonator with the geometry shown in Fig. 5.1 was calculated using various numbers of basis functions. The convergence is shown in Fig. 5.2 and can be seen to be very fast.

5.4 Computational Considerations

In order to evaluate the determinant in equation 5.20 accurately a large number of terms must be taken in the double sum.

In addition as the number of basis functions increase, the number of matrix elements increases as the fourth power of the number of basis functions taken. In order to find the zero of the determinant, these functions must be calculated many times. It is thus essential that this calculation be done as efficiently as possible.

The assymptotic forms of the Green's function can be used in a similar manner to the way described in section 3.5 for uniform microstrip. In this case, however, the assymptotic limit is valid when $\alpha^2 + \beta^2$ is large.

We express each of the elements of the characteristic determinant as follows:

$$\sum_{n}\sum_{m} B^{ip}\left\{\tilde{g}_{ij}-\tilde{g}'_{ij}\right\}B^{jq}+\sum_{n}\sum_{m} B^{ip}\,\bar{g}'_{ij}\,B^{jq}$$

The second term has the following form:

$$g'_{ij}\sum_{n}\sum_{m}\frac{I_p(n,m)\;I_q(n,m)}{\sqrt{(\alpha_n^2+\beta_m^2)}}$$

and is independent of frequency.

The first term converges much more rapidly than the unmodified expression so the summation can be truncated much sooner. The second term need be calculated only once for each geometry. Thus the total amount of computation is greatly reduced.

Since, in practice, we must truncate all the summations at finite n and m, care must be taken that in so doing, we maintain numerical stability and avoid the possibility of convergence to an incorrect answer. This is achieved by using the values of n and m contained by the curve shown in Fig 5.3. The constant k is chosen to achieve the desired degree of convergence. Here we maintain approximately equal spatial resolution in the X and Z directions and we recognise the fact that convergence is of the order $(n^2 + m^2)^{-1/2}$ $(nm)^{-1}$.

5.5 Comparison with the formulation of Chapter 4

Although the method described in 5.4 is capable of producing accurate, numerically stable, results, the amount of computation required is large.

This is mainly due to the large number of terms required in the summation of equation (5.14) for convergence to take place. Even using the assymptotic forms of the Green's and basis functions, the amount of computer time required was very large. Moreover the amount of computation increases as the fourth power of the number of basis functions used for each current component. This appears to make analysis of a more complicated structure, such as the strongly coupled step, prohibitively expensive.

The method described in chapter 4, by making use of the microstrip eigenmodes, can relatively quickly produce results in a form especially suitable for use in a network model of a microstrip circuit of high complexity, and therefore has advantages as a basis for providing results for use in CAD.

Mainly for simplicity, the basis functions used here are the same as those used in the analysis of uniform microstrip in chapter 3. In practice, excellent convergence was obtained using these functions and it is doubtful whether a different choice of basis would lead to a significant improvement in this.

5.6 Conclusion

In this chapter microstrip resonators have been analysed using the method of Chapter 2. The advantages and disadvantages of applying the results of this analysis to the problem of microstrip discontinuities is discussed. This is currently the state-of-the-art method of treating such problems. It is shown that the method is capable of producing accurate and stable results but at the cost of much greater computational effort than the method of Chapter 4. This is especially true when strongly coupled discontinuities are analysed.

REFERENCES

1. L. P. Schmidt "Rigorous computation of the frequency dependent properties of filters and coupled resonators composed from transverse microstrip discontinuities"
Proc 8th EuMC Warsaw pp436-440

2. R.H. Jansen "Hybrid mode Analysis of End Effects of Planar Microwave and Millimetrewave Transmission Lines"
Proc IEE Vol 128 Part H No.2 April 1981 pp77-86

3. R. Jackson and D. Pozar "Full-Wave analysis of Microstrip Open-End and Gap Discontinuities"
IEEE Trans MTT-33 1985 pp 1036-1042

4. T. Itoh "Analysis of Microstrip Resonators"
IEEE Trans on MTT. Vol MTT-22 No. 11 Nov. 1974 pp946-952

5. J. S. Hornsby "Full-Wave Analysis of Microstrip Resonator and Open-Circuit End Effect"
Proc. IEE Vol. 129 Pt. H No. 6. Dec 1982 pp 338-341

Appendix 5.1

Transformation of the Basis Functions

We express the transformed currents as follows:

$$\bar{I}_{xm} = \sum_r \text{Sin}(\alpha_n x o_r)\text{Cos}(\beta_m z o_r) I_{xcc} \qquad \text{(A51.1)}$$

$$- \sum_r \text{Sin}(\alpha_n x o_r)\text{Sin}(\beta_m z o_r) I_{xcs}$$

$$+ \sum_r \text{Cos}(\alpha_n x o_r)\text{Cos}(\beta_m z o_r) I_{xsc}$$

$$- \sum_r \text{Cos}(\alpha_n x o_r)\text{Sin}(\beta_m z o_r) I_{xss}$$

where:

$$I_{xcc} = \int\int I_x(x_r, z_r)\ \text{Cos}(\alpha_n x_r)\text{Cos}(\beta_m z_r)\,dx_r\,dz_r \qquad \text{(A51.2)}$$

$$I_{mcs} = \int\int I_m(x_r, z_r)\ \mathrm{Cos}(\alpha_n x_r)\mathrm{Sin}(\beta_m z_r)dx_r dz_r$$

$$I_{msc} = \int\int I_m(x_r, z_r)\ \mathrm{Sin}(\alpha_n x_r)\mathrm{Cos}(\beta_m z_r)dx_r dz_r$$

$$I_{mcs} = \int\int I_m(x_r, z_r)\ \mathrm{Cos}(\alpha_n x_r)\mathrm{Sin}(\beta_m z_r)dx_r dz_r$$

We perform the integration of I_{mij} with respect to z and the integration of I_{mij} with respect to x by parts, making use of the fact that the current normal to the edge of a strip is zero at that edge. We get:

If m > 0

$$I_{mcc} = -\int\int \frac{\partial I_m}{\partial z}\ \frac{\mathrm{Cos}(\alpha_n x_r)\mathrm{Sin}(\beta_m z_r)dx_r dz_r}{\beta_m} \qquad \text{(A51.3)}$$

$$I_{mcs} = \int\int \frac{\partial I_m}{\partial z}\ \frac{\mathrm{Cos}(\alpha_n x_r)\mathrm{Cos}(\beta_m z_r)dx_r dz_r}{\beta_m}$$

$$I_{msc} = -\int\int \frac{\partial I_m}{\partial z}\ \frac{\mathrm{Sin}(\alpha_n x_r)\mathrm{Sin}(\beta_m z_r)dx_r dz_r}{\beta_m}$$

$$I_{mss} = -\int\int \frac{\partial I_m}{\partial z}\ \frac{\mathrm{Sin}(\alpha_n x_r)\mathrm{Cos}(\beta_m z_r)dx_r dz_r}{\beta_m} \qquad \text{(A51.4)}$$

if n > 0

$$I_{ncc} = -\int\int \frac{\partial I_n}{\partial x}\ \frac{\mathrm{Sin}(\alpha_n x_r)\mathrm{Cos}(\beta_m z_r)dx_r dz_r}{\alpha_n}$$

$$I_{ncs} = -\int\int \frac{\partial I_n}{\partial x}\ \frac{\mathrm{Sin}(\alpha_n x_r)\mathrm{Sin}(\beta_m z_r)dx_r dz_r}{\alpha_n}$$

$$I_{nsc} = \int\int \frac{\partial I_n}{\partial x}\ \frac{\mathrm{Cos}(\alpha_n x_r)\mathrm{Cos}(\beta_m z_r)dx_r dz_r}{\alpha_n}$$

$$I_{nss} = \int\int \frac{\partial I_n}{\partial x} \frac{\cos(\alpha_n x_r)\sin(\beta_m z_r)dx_r dz_r}{\alpha_n}$$

When n = 0 we get

$$I_{ncc} = -\int\int x_r \frac{\partial I_n}{\partial x} \cos(\beta_m z_r)dz_r dx_r \qquad \text{(A51.5)}$$

$$I_{nsc} = -\int\int x_r \frac{\partial I_n}{\partial x} \sin(\beta_m z_r)dz_r dx_r$$

$$I_{ncs} = 0$$

$$I_{nss} = 0$$

When m = 0 we get

$$I_{mcc} = -\int\int z_r \frac{\partial I_m}{\partial z} \cos(\alpha_n x_r)dz_r dx_r \qquad \text{(A51.6)}$$

$$I_{msc} = -\int\int z_r \frac{\partial I_m}{\partial z} \sin(\alpha_n x_r)dz_r dx_r$$

$$I_{mcs} = 0$$

$$I_{mss} = 0$$

List of Figures

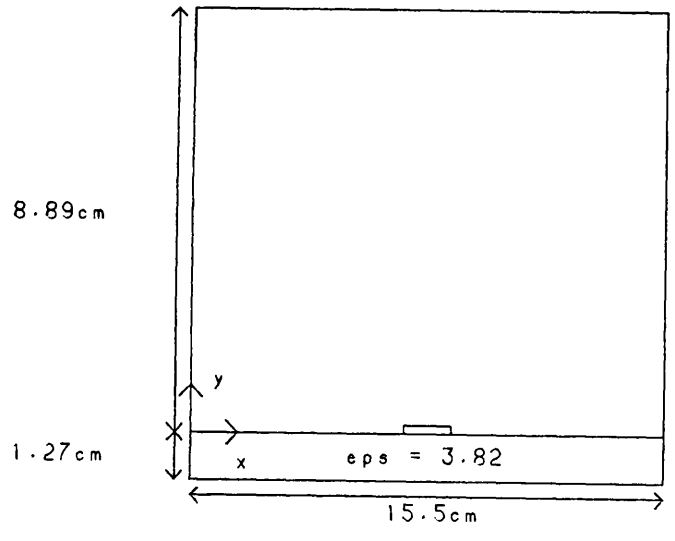

Fig. 5.1a - Resonator cross section

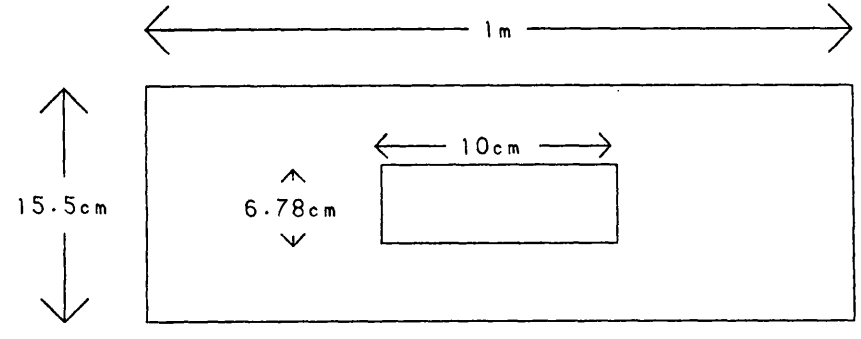

Fig 5.1b - Plan of a Microstrip Resonator

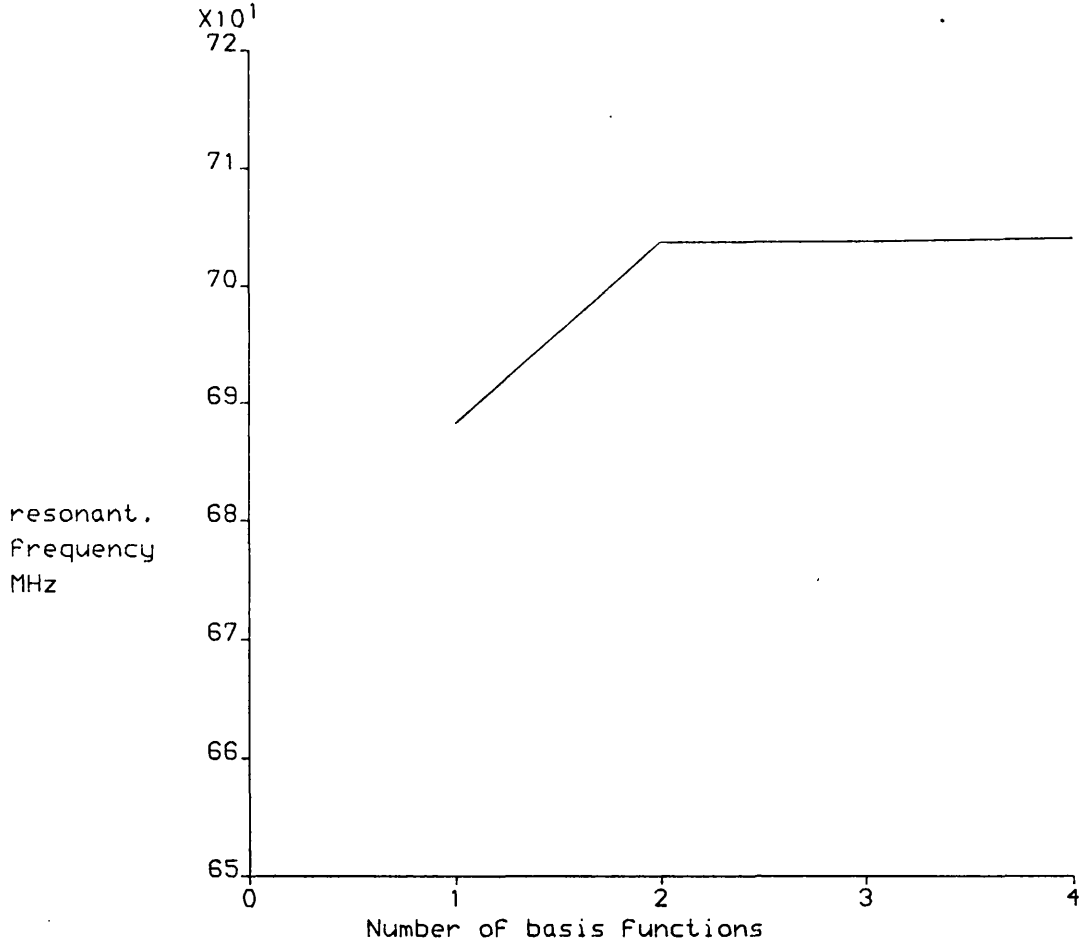

Fig 5.2 - Convergence of resonant frequency

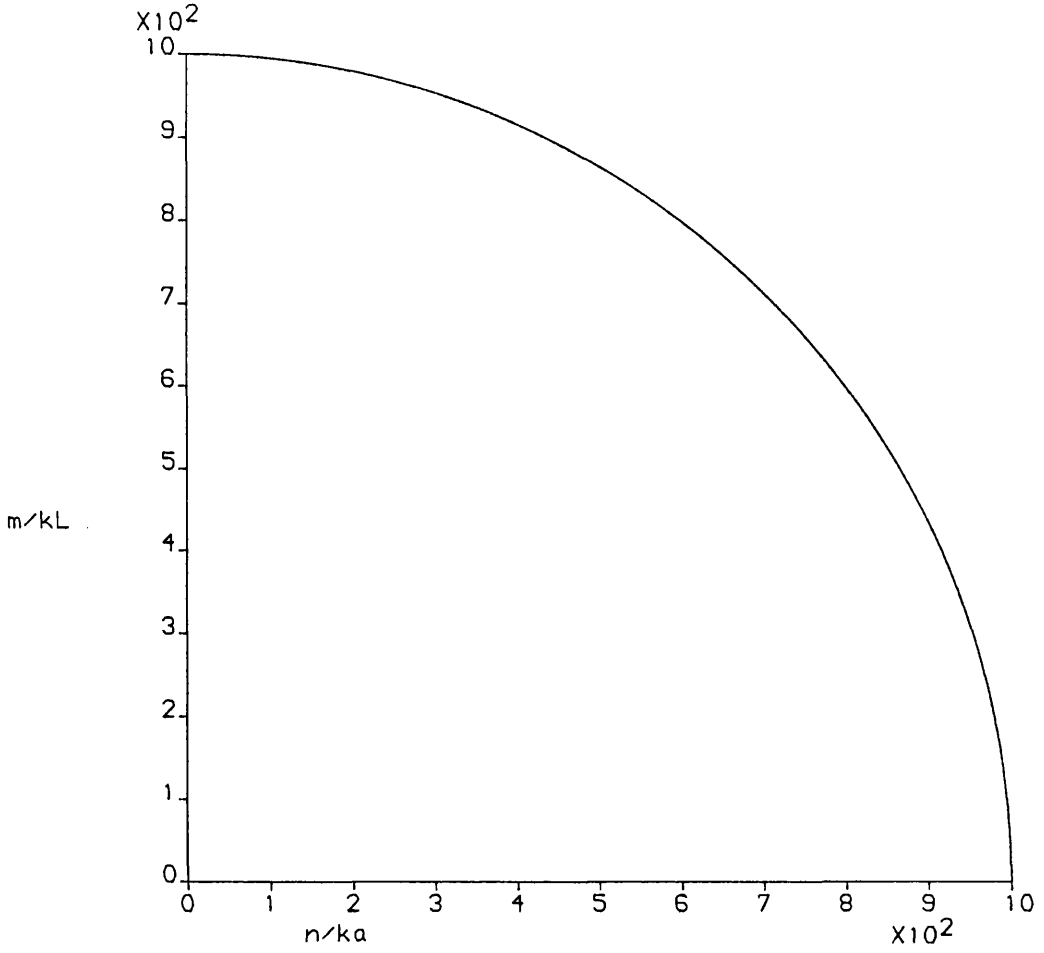

Fig 5.3 - Values of n and m to include in the sum
k is a freely chosen constant

CHAPTER 6

Computer Programs for Microstrip Analysis

6.1 Introduction

For the purpose of gaining understanding of planar structures and the analysis techniques and for the purpose of efficiently calculating the parameters of uniform microstrip and microstrip step discontinuities, several computer programs were written. Versions of these programs will run on almost any computer with a PASCAL compiler, including the Sinclair Spectrum, IBM PC compatibles, Honeywell Multics and others. Throughout the development of these programs, the basic philosophy has been to make them general, expandable and readable. In addition, where a much used option in the programs could be made more efficient by using a special purpose routine, this has been included. This design philosophy has been facilitated by using the PASCAL programming language in all but one of the programs. Use of the PASCAL programming language has meant that the programs are portable, structured for ease of modification and readability and less prone to programming error than if they had been written in some of the more popular languages. The programs will perform the following tasks:

1. Find the modes of a slab loaded waveguide.

2. Find the modes of microstrip using the methods of Chapter 2.

3. Find the modes of Finline using the methods of Chapter 2.

4. Calculate and display graphically in 2 or 3 dimensions the field patterns associated with any of the above modes.

5. Calculate the S parameters of a single step discontinuity in Microstrip using the methods of Chapter 4.

6. Calculate the S parameters of a cascade of step discontinuities.

7. Calculate the resonant modes of a boxed microstrip resonator, and the end effect of a boxed microstrip open circuit.

6.2 The Programs

For convenience, and in order to keep the size of the programs reasonably small, the above tasks are shared among several programs in the following manner:

EGUIDE Calculates the modes for a slab loaded waveguide with no strips. Since these modes coincide with the poles in the Green's function this information enables MSTRIP to function faster. See sections 2.6 and 3.2.
Written in Pascal.

Inputs: The slab loaded guide geometry.

Outputs: A list of the slab loaded guide modes:

MSTRIP Solves the chacteristic equation of a general planar structure, in particular microstrip and finline, to find the mode parameters and to calculate the field patterns for each mode. "Complex modes" are not calculated here.
Written in Pascal.

Inputs: The geometry of the structure. Optionally a file of data from EGUIDE containing the poles of the Green's function.

Outputs: A list of the modes of the structure.

A file containing field information.

MSTRIPC Calculates the "complex modes" of microstrip. Written in PASCAL.

Inputs: The microstrip geometry.
Optionally a file from MSTRIP containing the non-complex modes of the microstrip and a file from EGUIDE containing the modes of the slab guide.

Output: A list of the complex modes of the microstrip.

MDISC Calculates the generalised S or Z matrix for a single step microstrip discontinuity.
Written in PASCAL

Inputs: Two files from MSTRIP containing the field patterns for the microstrip each side of the. step.
Optionally a file containing a set of basis functions for the field at the discontinuity.

Output: A file containg the generalised S matrix of the step.

MNET Calculates the S matrix for a cascade of microstrip step discontinuities.
Written in PASCAL.

Inputs: Files from MDISC containing the S matrices for each single step in the cascade. A text file specifying the geometry of the cascade.

Output: The S matrix of the cascade.

RESON Calculates the resonant frequency of an enclosed microstrip structure. Makes use of this information to calculate the parameters of microstrip open circuits and gaps.

Input: The resonator geometry.

Output: The resonant frequency of the structure. Discontinuity parameters which can be derived therefrom.

FFT Sums the field components for a given value of *y*. and produces a GINO plot of the results Written in FORTRAN.

Inputs: A file produced by MSTRIP. The value(s) of *y* at which the fields are to be calculated.

Output A GINO plot to screen or plotter.

This program allows plots of the E field versus x for a given value of *y*. Also it is possible to produce a contour plot of the E field versus x and *y*.

The use of each of these programs will now be described in more detail.

6.3 EGUIDE

Upon being run this program will ask for the microstrip geometry, this may either be a "standard" geometry or all the dimensions may be entered.

The program then asks whether to calculate ALL modes or just EVEN or ODD modes (in Ez).

The program then asks whether the slab loaded guide modes are required (which can be used with MSTRIP when using a current expansion) or whether output is required which is suitable for MSTRIP when using E field expansion.

Next the program asks whether to list the modes as: 1. Effective Permittivities at a specified frequency or 2. Frequencies at a specified Effective Permittivity.

Finally the number of modes which it is required to locate is entered.

EGUIDE produces a text file called "emptyroots" which contains the specified geometry, the specified frequency or effective permittivity, and a list of effective permittivities or frequencies. This file can be printed or used as input to MSTRIP.

6.4 MSTRIP

The program MSTRIP has the dual purpose of investigating the methods for analysing a general planar structure and of calculating, in an efficient manner, the characteristics of the microstrip modes. The latter include field patterns, characteristic impedances and propagation constants. The output of MSTRIP is suitable for use in programs to solve the microstrip discontinuity problem.

The higher order modes of Microstrip, Unilateral and Bi-lateral Finline of any specified geometry can be calculated. More general structures such as multi-layer and multi strip transmission lines can also be analysed.

The program is written in PASCAL in a modular form so that, if required, it would be a simple matter to produce a smaller program with fewer options. Indeed most of the functions of the program have been implemented on the Sinclair Spectrum using the HiSoft pascal compiler with little change to the Pascal code.

MSTRIP can either be used as a stand alone program or in conjunction with the programs EGUIDE, FFT, and MDISC. These provide information to enable microstrip modes to be found more quickly, provide a means to produce graphical output of field patterns, and perform calculations on microstrip discontinuities respectively.

6.4.1 General MSTRIP options

The following general options are available within MSTRIP

a. Find Accurate Root

This option will calculate the value of effective permittivity for a mode to a specified accuracy, given a pair of values within which a root can be found.

b. Evaluate characteristic Determinant

Simply prints the value of the characteristic determinant, this option is used to get a feel for the behaviour of the characteristic equation.

c. Find roots of characteristic equation

Finds all the roots and poles of the caracteristic equation within a specified range of frequency and effective permittivity using the "naive" method ie. searching step by step. This is a very slow method and will not normally be used. For microstrip this option has been superceeded by option "e". For other lines, however, option "e" has not yet been implemented. There is, however, no conceptual difficulty in doing so should it be required.

d. Find root and calculate fields

As "a" but also calculates the field patterns and produces an output file for input to MDISC.

e. Produce a list of accurate roots.

This is the means of efficiently producing a list of microstrip modes. It requires, as input, a file from EGUIDE, and produces a text file which contains optionally a list of effective permitivities for a given frequency or a list of frequencies for a given effective permittivity. This text file can be used as input for option f.

f. Produce field files

This option takes two files produced by option "e" and produces two binary files containing the field patterns for each mode. These files are used by MDISC for calculating discontinuity parameters.

6.4.2 Computation options

The program uses the methods described in chapter 2. Either strip currents or aperture fields can be used as the unknown quantity. A choice of basis functions in which to expand the unknown is given. This includes Schwinger's functions [1], the weighted Tchebychev functions of equation 2.62 and weighted Gegenbaur polynomials with any desired built-in singularity. See equation 2.70. Normally the Tchebychev functions of equation 2.62 are selected, the others being for investigating the convergence rate of different basis functions.

The number of functions in which the unknowns are approximated is selectable.

Depending on which of the options are selected some or all of the following information will be prompted for when the program is run.

1. Geometry information: Either a "standard" geometry can be selected, or the physical dimensions of the structure to be analysed can be entered. One can select Microstrip, Unilateral finline or Bilateral finline or a General planar structure as the structure to be analysed.

2. Basis information: The program gives the option of which set of basis functions is to be used. The normal choice is the Tchebychev functions. Also available are the Schwinger functions [1] and weighted Gegenbaur functions. In the latter case the required singularity is prompted for. It is to be noted that the Schwinger functions are only available if just the EVEN modes are to be calculated using a current expansion or the ODD modes using a field expansion. This corresponds to the dominant mode in Microstrip and Finline respectively.

The program then asks whether a current expansion or a field expansion is required. Usually a current expansion is used for microstrip and a field expansion for finline although this is not necessary. The number of functions to use is then prompted for. Each component of the basis vector can be separately specified. Finally the parity of the modes under consideration is requested. Note that for an unsymmetrical structure, ALL modes must be specified.

The number of terms to take in the Green's function summation (See equation 2.30) before using the assymptotic form (See section 2.5) is optionally entered. If zero is entered then the default is taken. This is a satisfactory compromise between accuracy and computer time.

6.5 MSTRIPC

The program MSTRIPC has been developed from the program MSTRIP by making the following changes.

1. The program only considers microstrip, the facilities for finline are not implemented. This is not, however, a fundamental limitation and if required, the appropriate facilities for locating the complex modes of finline could be added.

2. The evaluation of the characteristic equation is done using complex arithmetic. Unlike in MSTRIP no attempt is made to speed up the program by assuming pure real or pure imaginary propagation coefficients.

3. In place of the bisection algorithm for locating the roots of the characteristic equation on the real axis, a "quad search" algorithm has been included for searching the complex plane.

MSTRIPC can be used as a stand alone program, or in conjunction with EGUIDE and MSTRIP. These provide information from which the complex modes can be more quickly found.

The following general options are available within MSTRIPC.

6.5.1 Find Accurate Root.

This option will calculate the (complex) value of effective permittivity for a mode to a specified accuracy, given a pair of complex numbers specifying a rectangle on the complex plane within which roots can be found.

6.5.2 Evaluate Characteristic Determinant

Simply prints the complex value of the characteristic equation. This option is used to get a feel for the behaviour of the characteristic equation in the complex plane.

6.5.3 Produce list of Complex Roots.

This option takes as input a file produced from EGUIDE containg the poles of the characteristic equation and a file produced by MSTRIP containg the "real" roots of the characterictic equation. MSTRIPC will compare the two, find the areas where complex modes are expected and locate them as in section 3.2. Also produced is a list of current vectors for use in the discontinuity programs.

As in MSTRIP a choice of basis functions is offered, but only current expansions are allowed. In addition if option 6.5.3 is selected the basis used is automatically the same as that selected when MSTRIP was run.

6.6 MDISC

The program MDISC has been written to implement the formulation described in chapter 4, and to produce thereby the S or Z matrix of the single step discontinuity.

Provision is made to try various trial field basis functions. The following options are available:

1. The modal fields for the wider strip modified as described in section 4.4.

2. Weighted Gegenbauer polynomials with a specified corner singularity.

3. The convolution of the first modal function of the wider strip with weighted Gegenbaur polynomials of specified singularity. See section 4.4.

In addition the number of basis functions used can be specified. Details of basis functions and their effects are discussed in chapter 4.

MDISC uses files of field patterns taken from MSTRIP. These consist of the Fourier transforms of Ex and Ez for each mode. The other field components are calculated from these. This means that the files are large even though they need only exist in workspace for the duration of the job.

An alternative version of MDISC has been written which accepts files from MSTRIP containing the current vectors for each mode and the basis functions used in MSTRIP. These files are much smaller and the possibility of using assymptotic forms of the field expansions is available. The disadvantage is that this version takes longer to run due to the extra arithmetic which is performed. The results, of course, are identical from each version.

6.6.1 Options within MDISC

a. Calculate discontinuity S matrix using mode matching:

This option uses the mode matching formulation to characterise the step discontinuity. It was included for experimental reasons but is not as good a method as the variational methods of chapter 4.

b. S Matrix formulation using combined basis

The variational method of chapter 4 is used together with the basis functions consisting of the modal functions of the microstrip with the wider strip. The ratio of Ex to Ey is fixed.

c. Calculate overlap integrals

The overlap integrals of all combinations of the modes of two microstrips is calculated. If the input files are the same this gives a measure of the orthogonality in the calculated field patterns. This option was used to produce table 3.1.

d. Variational method using S parameter formulation

Calculates the S matrix of the single step using the methods of chapter 4.

e. Variational method using Z parameter formulation

Calculates the Z matrix of the single step using the methods of chapter 4.

f. Dump field files.

Takes a file of field patterns from MSTRIP and produces a file in a form suitable for input to the display program FFT. In addition, for propagating modes, the characteristic impedance of the mode is calculated using the three definitions of characteristic impedance. viz: Power-current, power-voltage, voltage-current.

With the exception of option "f" the following information is prompted for:

1. Number of modes: This is the number of terms to be taken in the summation in the Green's function for the discontinuity (See equation 4.14). This assumes that the specified number of modes is available in the input field files from MSTRIP. If not then the summation will be truncated when an end of the input file is reached.

2. Basis information: Three options are given, a. The modal functions of the wider strip with the ratio of Ex to Ey being left as a free parameter in the variational formulation. b. Calculated functions consisting of weighted Gegenbaur polynomials, of any desired singularity. c. As "a" but with each function multiplied by a weighting function. A discussion of these basis functions and their properties is given in chapter 4.

6.7 MNET.

This program takes a set of S parameters for single step discontinuities produced by MDISC and the lengths of the interconnecting transmission lines and produces the overall S matrix. The method used follows that used in the MCAP program described in [2]. Each step discontinuity is treated as a (N+M)-port where N and M are the numbers of accessible modes each side of the discontinuity. The transmission lines are treated as N or M separate transmission lines independently connecting the discontinuities. See chapter 4. Once the lengths are specified, the electrical length is available from the effective permittivities of the first few modes produced by MSTRIP.

As the single step S parameters from MDISC will be available only at spot frequencies, MNET uses linear interpolation in order to produce a result for the overall S matrix at any frequency.

6.8 RESON

This program makes use of the methods of Chapter 2 to calculate the resonant frequency of an enclosed microstrip structure. Any number of strips may be specified (up to the value of MAXSTRIP set within the program) and they may be of any size and placed anywhere on the air-dielectric interface. The same choice of basis functions is provided as in MSTRIP but two sets are required, one for the x direction and one for the z direction.

With this program the microstrip open circuit and microstrip gap may be investigated using the methods in [3]. The basis functions in RESON are, however, different from those used in the above references.

Due to the large amount of computation required to produce the basis functions and their assymptotic sums (See chapter 5), these results are dumped to a file BDATA from which they may subsequently be read.

6.9 FFT

This program takes a file produced by MDISC containing the Fourier transforms of all the field components, and plots them either as a graph of amplitude versus position, or as a three dimensional contour or isometric projection of the transverse field intensity over the box cross-section.

When the 2 dimensional plot is selected, the results can be plotted on a linear scale or on a dB scale. The field pattern is plotted versus x for any specified value of y within the box. If y=0 is specified then 9 graphs are produced.

1. E field x component
2. E field y component above the interface
3. E field y component below the interface
4. H field x component above the interface
5. H field x component below the interface
6. H field y component
7. E field z component
8. The difference between Dy above the interface and Dy below
9. The difference between Hx above the interface and Hx below

The last two graphs, which should be zero in the aperture region, are included in order to gain confidence that the fields are being calculated accurately.

If any other value of y is specified then graphs 2 or 3, 4 or 5 and 8 and 9 are not plotted since they are not applicable.

6.10 Conclusion

In this cahpter, a suite of computer programs for the analysis of microstrip and other planar transmission lines has been described. In addition, programs for the analysis of step discontinuities in microstrip and for the display of field patterns presented. These programs are portable, flexible and are applicable to a large number of problems.

References

1. Boxed Microstrip Circuits - Annual Report 1983-1984
University of Bath

2. K.C. Gupta et. al. "Computer aided design of Microstrip Circuits"
Dedham MA. Artech House 1981.

3. R.H. Jansen "Hybrid mode analysis of end effects of planar microwave and millimetre wave transmission lines"
Proc IEE Vol 128 H 1981 pp 77-86

CHAPTER 7

CONCLUSIONS AND SUGGESTIONS FOR FURTHER WORK

7.1 CONCLUSION

The work described in this thesis was undertaken for the purpose of investigating boxed microstrip and characterising discontinuities therein with the aim of providing improved techniques and more accurate results for use in the computer aided design of boxed microstrip circuits. The culmination of the work so far is contained in Chapter 4 where a new technique for the analysis of cascades of multiply coupled step discontinuities in boxed microstrip is presented. In the course of developing this technique several other useful results and techniques have emerged.

1. The Green's function for a general multilayer dielectric structure was derived together with assymptotic limits and a quick method of locating the poles thereof in Chapter 2. From these are recovered the Green's functions appropriate to the boxed microstrip. These are a pre-requisite to finding the mode spectrum of the structure. Because the derivation of the Green's functions is general, however, the complete mode spectrum of other structures such as finline and coplanar transmission line follow immediately.

2. During the calculation of the mode spectrum it was realised that the quadratic nature of the characteristic equation made possible the existence of "complex modes". Such modes were indeed found and reported at the 1986 European Microwave Conference. This was the first time that complex modes had been reported in microstrip.

3. By making use of an efficient method of normalising the modes, and of calculating the overlap between them (Section 3.3), it was possible to prove that the calculated modes were orthogonal as theory requires. In addition the characteristic impedance could be calculated using the widely accepted power/current definition. The results were at variance with the quasi-static predictions and in agreement with other published rigorous results.

4. Results were obtained for the single step discontinuity in microstrip using the variational method described in Chapter 4. These results were in agreement with quasi-static results in the limit of low frequency.

5. Computer programs of general utility have written. These are described in detail in Chapter 6. They enable the calculation of the modes of general transmission lines, and the graphical display of the field patterns thereof. Also they enable the characterisation of step discontinuities in microstrip and allow the use of different basis functions in order to get the best result.

7.2 Further Work

The work described herein can be usefully continued in the following ways.

1. The derivation of basis functions for the vector E field at the step discontinuity which more precisely incorporats the characteristics of the field near the 90 degree corner in the strip.

2. Extension of the technique to other discontinuities such as the open end and the gap. This should present little problem and may be only a matter of using one set of empty guide fields and one set of microstrip fields in the Green's function for the discontinuity instead of two sets of microstrip fields. The basis functions could be those described in section 4.4. The microstrip gap would then be modelled as a cascade of two "open end" discontinuities.

3. Extension of the technique to other waveguiding structures. This would require consideration of the appropriate basis functions for the fields at the step. The modal functions for building the Green's function are available from the existing computer programs.